

American University in Cairo

AUC Knowledge Fountain

Theses and Dissertations

6-1-2015

Integrated life-cycle cost & risk optimization framework for coastal protection structures

Ayman Hassan Abdel-Wahab El Hakea

Follow this and additional works at: <https://fount.aucegypt.edu/etds>

Recommended Citation

APA Citation

El Hakea, A. (2015). *Integrated life-cycle cost & risk optimization framework for coastal protection structures* [Master's thesis, the American University in Cairo]. AUC Knowledge Fountain.

<https://fount.aucegypt.edu/etds/1221>

MLA Citation

El Hakea, Ayman Hassan Abdel-Wahab. *Integrated life-cycle cost & risk optimization framework for coastal protection structures*. 2015. American University in Cairo, Master's thesis. *AUC Knowledge Fountain*.

<https://fount.aucegypt.edu/etds/1221>

This Thesis is brought to you for free and open access by AUC Knowledge Fountain. It has been accepted for inclusion in Theses and Dissertations by an authorized administrator of AUC Knowledge Fountain. For more information, please contact mark.muehlhaeusler@aucegypt.edu.

The American University in Cairo
School of Science and Engineering

**INTEGRATED LIFE-CYCLE COST & RISK OPTIMIZATION
FRAMEWORK FOR COASTAL PROTECTION STRUCTURES**

A Thesis Submitted To
Department of Construction and Architectural Engineering
In partial fulfillment of the requirements for the degree of

Master of Science
in
Construction Management

By
Ayman Hassan Abdel-Wahab El Hakea

Under the Supervision of

Dr. Ossama Hosny

Professor, the Construction and
Architectural Engineering
Department,
The American University in
Cairo, Egypt

Dr. Hesham Osman

Associate Professor, Department of
Structural Engineering,
Cairo University, Egypt

Dr. Moheb Iskander

Associate Professor and Head of the
Hydrodynamics Department,
Coastal Research Institute,
Alexandria, Egypt

February 2015

DEDICATIONS

This work is dedicated to the people of Alexandria, my hometown, and the place that will always reserve the most special place in my heart. This work is intended to be nothing but a step towards attaining a better future for this unique city and its people.

This work is equally the least dedication I can offer to my beloved daughter and son, Alya and Moez, Allah's most gracious gift to me, who have been always in the center of my mind and thoughts while doing this work. I dedicate this work to my mother Dr. Emtiaz Hassoon, who provided an invaluable support to me during my course of masters studies whether emotionally or physically, and to my Father Admiral Engineer Hassan El Hakeh, the former Chief Engineer of the Egyptian Naval Forces, for his immense support to me whether by technical guidance or by providing contacts, which made data acquisition doors wide open. I offer this research to my sister researcher and Engineer Amira El Hakeh, for her crucial persuasion of me to embrace the academic career; and equally to my grandfather Mr. Counselor Khalid Hassoon, my grandmother Mrs. Fatima El Hakeh, my aunt Mrs. Layla Hassoon and her husband Mr. Engineer Mahmoud Hegazy, for the generous support they all gave me during my sojourn in Cairo over the course of my study.

I also dedicate this work to the soul of my great grandfather Aly Bek El Hakeh, the former Chief of Education of Al-Dakahliya Province, and the prominent education pioneer; and also to the soul of Prof. Dr. Mahmoud Fayed Zaki, Professor of Coastal Engineering and Harbor Design at Alexandria University; the dear family friend who introduced me to the world of coastal engineering and management.

ACKNOWLEDGEMENTS

My sincere acknowledgement to Prof. Dr. Ossama Hosny, of the Construction and Architectural Engineering Department at the AUC, not only for his generous physical and psychological support throughout my thesis work, but also for his invaluable encouragement to myself to get involved in Academic research, writing, and publishing. I equally thank Prof. Dr. Hesham Osman of the Civil Engineering Department, Cairo University; for his patience, diligence, and attention to detail which he expressed in reviewing my thesis work, and in providing extremely thorough guidance as to infrastructure asset management methods and tools. My deep appreciation to Prof. Dr. Moheb Mina Iskander, Head of the Hydrodynamics Department at CoRI, Alexandria, not only for his generous provision of historical design, environmental, and cost data regarding the study area, but also for his continuous follow-up and support during the write-up and the review of the thesis.

Special thanks to my fellow colleague Engineer Soliman Amr Abu-Samra of the Construction and Architectural Engineering Department at the AUC, for the joint work we published together in the field of deterioration and optimization with regard to coastal infrastructure. Such works laid the base towards establishing and enhancing the modeling tools utilized in this research. Special acknowledgement to Prof. Dr. Alfy Morcos Fanous, former Chairman of CoRI; Prof. Dr. Mohamed El-Raey, Higher Research Institute (HRI), Alexandria; Mr. Engineer Walid Khalil, Syndicate of Egyptians Engineers and former Technical Manager at Dr. Mahmoud Fayed Zaki (FZ) Consulting Co., Alexandria; Mr. Engineer Mohamed El Dakkak, the Head of the Engineering Division at the Port of Alexandria Authority, PhD Candidate at the Arab Academy for Science and Technology, Alexandria, Egypt; Mr. Engineer Medhat Khalifa and Mr. Engineer Yasser Samak of the Arab Contractors Co., Alexandria Branch; Mr. Engineer Abdessalam El-Fiky, Chairman of the Abdessalam El-Fiky Construction Co. (AF Co.); Mr. Engineer Mohamed Said Farahat, Head of Execution Department, Suez Canal Co. for Port Works and Mega Projects, Alexandria Area; and Mr. Engineer Ahmed Neamatallah of the Engineering Department of Talaat Mostafa Holding Group. All of you have significantly contributed towards this research by either provision of design data for structures within the scope of the study, or by providing expert opinion whenever the research required, and by also verifying and validating the findings of this research.

Data acquisition was not an easy task. The first part was to collect the data pertaining to the design attributes, construction and repair history, bathymetry, and wave data for all structures within the study area. Data regarding the cost of construction and repair were also collected by the author. The author first approached the CoRI Hydrodynamics Department. The guidance received from CoRI was invaluable in terms of the environmental data. In the zone extending between Al-Saraya Beach and Al-Mandara, an old bathymetric map produced by CoRI was utilized although dating back to year 2002 (i.e. before the launch of the Cornice widening works), given that the study area did not witness any works that affected its seabed bathymetry. Furthermore, CoRI provided the author with copies of two editions of the Shore Protection Master Plan of the Northern Nile Delta Coast, developed by Tetra Tech Inc. in 1985 and 1986. Tetra Tech (1985:1986) included all design attributes of the Eastern Harbor breakwaters, as well as their condition, cost of repair, maintenance, and replacement. It also included a study on the old Eastern Harbor seawall attributes, condition, repair, maintenance and replacement policies as well as their associated costs. CoRI also provided essential guidance as to the wave data of the study area, and suggested the cited literature in this research.

Among the approached marine works contractors in Alexandria was Abdessalam El-Fiky (AF Co.). AF Co. provided the author with a photographic progress report they produced, documenting their Qaytbey Fort marine protection works in 1994. The report includes valuable information of the problems that culminated into the need for marine protection works for the historic fort, the obstacles faced, and the works that were accomplished for the new revetment and seawall. The report also report displays design plans, cross-sections of the Qaytbey Fort marine protection works, bills of quantities, and bathymetry of the area immediately facing the fort. Other design information for the Police Club breakwaters and Al-Kihrbay were obtained from data provided by their designer, Professor Dr. Mahmoud Fayez Zaki Consulting Office (FZ Co.). As for San Stefano area, specifications, design and as-built drawings for the breakwaters, piers, and groins; were acquired from Egyco, the project's main contractor. Egyco's documents also include a bathymetric survey post the construction of the San Stefano breakwaters and piers.

Arab Contractors Co. were kind enough to provide a copy of a report produced by his company in 2007. The report includes extensive data on a variety of

projects executed by Arab Contractors in Alexandria between 2000 and 2007. Such works include the Pharos Promenade widening project, the Cornice Widening works in Al-Chatby, Cleopatra, Camp Cesare, Al-Ibrahimiya, Sporting, Sidi Gaber, Stanley, and Sidi Bishr. The report, written in Arabic, includes also detailed information on breakwaters, revetments, and groins constructed by Arab Contractors Co. in the Mustapha Kamel Armed Forces Club, Teachers Club, Professional Clubs area, Glim Bay, Bir Masoud, Miami, and Al-Mandara. The report contains typical cross-sections and includes data regarding durations of execution, equipment used, and total costs of the works. Other historical data on Alexandria including Admiralty Maps and marine works in Alexandria prior to the Cornice Widening works were acquired from the design office TELCONSULT Co. In light of the data availability, the final study area was decided to comprise the region between the Pharos peninsula and the western boundary of Al-Montaza headland. This is the area where all sorts of data were acquired by the author between December 2012 and July 2013.

**INTEGRATED LIFE-CYCLE COST & RISK OPTIMIZATION FRAMEWORK
FOR COASTAL PROTECTION STRUCTURES**

By:

Ayman Hassan Abdel-Wahab El Hakea

Thesis Advisors:

Dr. Ossama Hosny

Dr. Hesham Osman

Dr. Moheb Iskander

ABSTRACT

While extensive research has been carried out on the management of various types of infrastructure assets, limited research has been carried out for coastal structures. The rapid growth of the world population living in low-lying areas within close range to the shoreline over the past century compounded by the impact of global climate change on shoreline hydrodynamics; have increased the importance of coastal infrastructure management. Climate change has recently increased storm intensities in addition to decreasing storm return periods; imposing greater risks to life and property. The aim of this research is to provide an artificial-intelligence-based framework for coastal protection structures, which is capable of predicting structural deterioration patterns, and accordingly offers the end user the capability of optimization of repair, maintenance, and rehabilitation costs, in addition to the optimization of risk exposure limits under pre-defined budgetary constraints. For this purpose, an Asset Inventory Database (AID) for coastal assets is developed, comprising the design, environmental, and historical data pertaining to coastal assets. Established visual inspection and condition rating procedures are followed to obtain the values for the Structural Condition Index (SI) and a Structural Condition Matrix (SCM) for individual structures, considering a single inspection point. This takes into account cases where no previous inspection and condition rating records are

available. SI's are in their turns classified into severity ranges. Functional Condition Indices (FI's) are also calculated for submerged structures that could not be visually inspected and taken as the equivalent to the Condition Index (CI). Deterioration Transition Matrices (DTM's), including transition probabilities between each of the deterioration severity ranges are next calculated using backward Markov-Chain (MC) analysis. Such probabilities are then utilized to formulate the Markovian Deterioration Transition Matrix (DTM) for each individual sub-reach and hence each individual structure; enabling the prediction of future deterioration. The trends obtained from this forward Markovian deterioration modeling are approximated by mathematical functions using best-fit regression. The single-time deterioration effect of design and intermediate storms is also considered by virtue of the Storm Simulator feature. By calculating the average maintenance and repair per meter run of every coastal structure, corresponding to the condition of the structure, a Genetic-Algorithm (GA) – based Life-Cycle Cost (LCC) optimization modeling is then developed with the aim to minimize the total LCC for the entire coastal assets up to year 2050, while achieving the minimum reliability of structures, expressed as a Priority Index (PI). PI's are numerical values that are factors in the condition state of the structure and its criticality with respect to risk to life and property upon failure. In parallel, another optimization module aims at minimizing the total risk exposure level under various budget scenarios. Both the LCC and risk optimization modules were run for various scenarios of storm occurrences to account for the effect of global climate change. The considered case study in this research is a group of 43 different structures in Alexandria, Egypt. It was found that under stringent climatic conditions, the required LCC to maintain coastal structures at the desired level of reliability increases dramatically as opposed to normal climatic conditions. In addition, it was observed that the risk to life and property decreases with the increase of available budget for maintenance and repair. Further, the suggested framework was observed to be more cost-efficient than the common maintenance and repair strategies, in terms of keeping the maximum acceptable PI threshold.

TABLE OF CONTENTS

GLOSSARY OF SYMBOLS.....	X
GLOSSARY OF TERMS AND ABBREVIATIONS	XII
LIST OF FIGURES.....	XX
LIST OF TABLES	XXVIII
LIST OF EQUATIONS	XXVIII
CHAPTER I – INTRODUCTION	1
1-1. Significance of Coastal Infrastructure Worldwide and Locally	1
1-2. Problem Statement.....	3
1-2.1. Climate Change and Eustatic SLR	4
1-2.2. Seismic and Geological Subsidence and its effect on RSLR	6
1-2.3. Flooding Risk Areas.....	7
1-2.4. Need for Effective and Collective Coastal IAM	8
1-2.5. Need for Optimization.....	10
1-3. Research Scope and Objectives	10
1-4. Research Motivation	12
1-5. Research Methodology	13
1-6. Thesis Organization	14
CHAPTER II - LITERATURE REVIEW	15
2-1. Introduction.....	15
2-2. Coastal Structure Inspection Methods and Technologies.....	15
2-2.1. Subdivision of Structures into Reaches and Sub-Reaches	15
2-2.2. Coastal Structures Distress Types and Mechanisms	19
2-2.3. Inspection Methods and Technologies	25
2-3. Condition Assessment and Rating	30
2-3.1. General Condition Index	30
2-3.2. Structural Condition Index	32
2-3.3. Functional Condition Index.....	37
2-4. Prediction of Deterioration and Damage Progression	41
2-4.1. Empirical Relationships based on Laboratory Testing.....	41
2-4.2. New Trends in Deterioration Modeling for Coastal Structures	44

2-5. Maintenance and Repair Methods and Equipment for Coastal Structures	48
2-5.1. General Overview.....	48
2-5.2. Common Construction and Repair Methods	50
2-5.3. Integrated Inventory, Condition Rating, Maintenance and Repair Models	56
 CHAPTER III – RESEARCH METHODOLOGY FRAMEWORK.....	63
3-1. Introduction.....	63
3-2. Methodology Development	63
3-3. Methodology Framework Outline	64
3-4. Asset Inventory Database (AID).....	66
3-4.1. Purpose	66
3-4.2. Zoning and Nomenclature of Assets	66
3-4.3. Logging of Design, Historical, and Environmental Attributes	67
3-5. Visual Inspection and Condition Assessment.....	71
3-5.1. Structural Condition Assessment	71
3-5.2. Functional Condition Assessment.....	75
3-6. Deterioration Module.....	76
3-6.1. General Overview.....	76
3-6.2. Development of SCM's for Reaches and Sub-Reaches.....	76
3-6.3. Backward MC Deterioration Module.....	78
3-6.4. Forward MC Deterioration Module	79
3-6.5. Intermediate and Design Storm Simulator	79
3-7. Optimization Modules	82
3-7.1. General Overview.....	82
3-7.2. Initial Condition Index Calculation.....	82
3-7.3. Calculation of Storm Effect on Initial Condition Index	83
3-7.4. Calculation of Intervention Policy Effect on Condition Index.....	83
3-7.5. Calculation of Priority Index	86
3-7.6. LCC Optimization Module.....	87
3-7.7. Risk Optimization Module	89

CHAPTER IV – CASE STUDY, DISCUSSION, & ANALYSIS OF RESULTS	90
4-1. General Overview of the Case Study	90
4-2. AID Analysis	94
4-3. Visual Inspection and Condition Rating	99
4-3.1. Inspection Records	99
4-3.2. Structural Condition Rating	101
4-3.3. Functional Condition Rating	104
4-4. Deterioration Module	106
4-5. LCC Optimization Scenarios and Results	107
4-6. Risk Optimization Scenarios and Results	115
4-7. Verification and Validation	118
4-7.1. Verification of AID Data Sufficiency and Accuracy	118
4-7.2. Condition Rating Procedures and Results	119
4-7.3. Deterioration Modules	120
4-7.4. LCC and Risk Optimization Modules	121
4-7.5. Summary of Consulted and Interviewed Experts	122
 CHAPTER V – CONCLUSION AND RECOMMENDATIONS FOR FUTURE WORK.....	 125
5-1. Research Summary	125
5-2. Research Findings	126
5-3. Contribution to the Body of Knowledge.....	128
5-4. Research Limitations	128
5-5. Recommendations for Future Work	129
 REFERENCES.....	 131
APPENDIX 1 – Common Coastal Structure Concrete Armor Units.....	139
APPENDIX 2 – AID Summary	141
APPENDIX 3 – Sample Structural Inspection Sheet.....	150
APPENDIX 4 – Sample Functional Inspection Sheet	154
APPENDIX 5 – Historical Overview of Alexandria’s Marine Protection Works....	157
APPENDIX 6 – Summary of Intervention Policy Unit Cost Database for the Study Area in 2013	172

GLOSSARY OF SYMBOLS

- α :** Structure front-face angle with the horizontal.
- CI_c:** Cross-section component Index used for coastal structure reach/sub-reach structural condition rating.
- CH:** Channel or harbor or leeside cross-section structural component index for any reach/sub-reach.
- CI:** Condition Index, or General Condition Index, which is a numerical value between 0 and 100, reflecting the overall condition of the coastal structure. In this thesis is taken as the equivalent of the “Structural Index” or “SI”.
- CR:** Crest or Cap cross-section structural component index for any reach/sub-reach.
- DR:** Structural distress rating for coastal structure sub-reach component indices.
- D_n:** Nominal diameter of armor stone or natural rock.
- DTM:** Markov-Chain Deterioration Transition Matrix for coastal structures
- FI:** Functional Index of the entire structure, which is a numerical value between 0 and 100, reflecting the extent to which the coastal structure is fulfilling its function.
- FI_R:** Functional Index for the reach or sub-reach.
- H_s:** Significant wave height on the coastal structure; which is the average height of the highest of one third of the waves in a given sea state.
- K_D:** Shape coefficient in the Hudson formula for armor stability calculation, unique for every type of natural stone or concrete armor stone.
- M:** Refers generally to intervention policies for maintenance, repair and rehabilitation of coastal structures.
- M_U:** Unit cost of intervention policy “M”.
- N_s:** Stability number in various armor stone stability equations.
- P_i:** Transition probability between two consecutive structural condition states for coastal structures. In this research P1 through P7 are used.
- PI:** Priority Index for coastal structures, considered as the product of the probability of failure by the risk factor “RF”.
- PI_T:** Total Priority Index for a group of coastal structures located within one area or geographic zone.
- PI_w:** Weighted Priority Index of any particular structure, equal to the maximum **PI** over a certain study period multiplied by the structure’s seaside length.

- R:** Coastal structure Reach Functional Condition Index.
- RF:** Risk Factor representing the impact of coastal structure failure, taken in this research as an integer value 0, 1, 2, 3 and 4 ordered from lowest to highest impact.
- RI:** Reach and Sub-Reach Structural Condition Index, used interchangeably.
- S:** Dimensionless damage parameter in rock armor layer for rubble-mound structures. In this thesis it refers to the storm single-time impact on the structure's Condition Index.
- SCM:** Markov-Chain Structural Condition Matrix for coastal structures.
- SE:** Seaside cross-section structural component index for any reach/sub-reach.
- SI:** Structural Index, which is a numerical value between 0 and 100, reflecting the structural condition of the coastal structure.
- t:** Period of time between year of forecasting the structural Condition Index and year of construction or latest maintenance and repair, in the Markov-Chain deterioration model.
- T_m:** Significant wave period; which is a period taken arbitrarily as that of one of the highest waves within a given sea state.

GLOSSARY OF TERMS AND ABBREVIATIONS

Accretion: Build-up of sediment material which is only caused by natural forces by the deposition of water.

Accropode: Type of concrete armor stone with special shape, see Appendix 1 entitled, “*Overview of the History of Concrete Armor Units*”.

Admiralty Chart: Chart produced by the British Navy for the shores of Alexandria, Egypt, in the early 20th Century.

AID: Stands for “Asset Inventory Database” comprising the design and historical records of all **coastal structures** within the study area.

Antifer: Type of concrete armor stone with special shape, see Appendix 1 entitled, “*Overview of the History of Concrete Armor Units*”.

Armor Layer: Protective layer for rubble-mound coastal structures consisting of armor stones or units.

Armor Stones (units): Large quarry stones or special concrete shapes used.

Artificial Nourishment: Supplementation of the natural supply of beach material to a beach, using imported material.

Barge: A long, large, typically flat-top boat for transporting of materials used in the construction of coastal structures. It is generally unpowered and towed or pushed by other craft.

Bathymetry: Seabed topography.

Beach: The zone of beach material, which extends leeward from the lowest water line to the zone beyond the high water line, where there is a distinct change in the material form.

Beaufort Scale: An empirical scale from 1 to 12 measuring wind speeds. 1 being the calm condition, and 12 corresponding to the intensity of a hurricane.

Breaking Waves: Are shallow-water waves occurring in water having a depth less than one-half the wave length. The influence of the sea bottom changes the form of orbital motion to elliptical or near-elliptical. Waves break when the forward velocity of the wave crest particles exceeds the wave’s propagation velocity.

CAPMAS: Stands for the Egyptian “Central Agency for Public Mobilization and Statistics”.

CAS: Cassette Acquisition System, used for recording of wave heights and periods.

Climate Change: A change in global climate patterns apparent from the mid to late 20th century onwards, attributed largely to the increased levels of atmospheric carbon dioxide produced by the use of fossil fuels.

Coastal Infrastructure Asset Management: The efficient, life-cycle management of coastal infrastructure assets which aims to optimize their performance from engineering, economic, and environmental angles. It is the process of designing, operating and maintaining assets/facilities effectively and sustainably. It provides a decision-making tool throughout the life cycle of the structure, which can help provide the best reliability with the optimum cost.

Coastal Structures, Coastal protection works, and Shore protection works: Collective terms covering protection provided to the coastline.

Core Stone: Stone comprising the core of rubble-mound coastal structures, typical range of weight is between 10 and 300 kg, either basalt or dolomite.

CoRI: Stands for the “Coastal Research Institute”, an Egyptian government body based in Alexandria, Egypt, whose mission is centered around research work involving the protection of Egyptian coasts.

CoSCA: Coastal Structure Condition Assessment and Standardized Reporting Application scheme, launched by the US Army Corps of Engineers.

Crest: Highest part of breakwater or other coastal structures if applicable.

Cross-shore: Perpendicular to the shore.

CSARS: Stands for Coastal Structure Acoustic Raster Scanner, a modern device for coastal structure underwater scanning and inspection.

Cube: Type of concrete armor stone with special shape; see Appendix 1 entitled, “*Overview of the History of Concrete Armor Units*”.

Deep-Water Waves: Also known as “Oscillating waves”; are waves which occur in water having a depth greater than one-half the wave length, at which depth the sea bottom does not have any significant influence on the motion of the water particles. They are distinguished from Translation Wave, which are also known as the “Solitary waves”; and consist of a single wave crest, above the still-water level, traveling without change of form at a constant speed. This behavior takes place when deep-water waves break for the first time when reaching shallow water without being able to re-form.

Design Storm: Coastal structures are typically design to endure wave attack by the extreme design storm. The severity of the storm (i.e. return period) is chosen in light of the acceptable extent of damage or failure.

Detached Breakwater: Also known as “Offshore breakwater”, is a structure that is not connected to the shoreline, and is designed to protect an area from wave action. It may either serve as an aid to navigation, a shore-protection structure, a trap for littoral drift, or a combined purpose.

Deterministic: Model whose resulting behavior is entirely determined by its initial state and inputs, and which is not random or stochastic. Processes or projects having only a single outcome are said to be deterministic and their outcome is “pre-determined”. A deterministic model, if given the same input information, will always yield the same output information.

Diurnal Tides: The case when only one high tide a day occurs. They differ from semi-diurnal tides, which occur twice each lunar day (50 minutes longer than the solar days), meaning that the high tide occurs 50 minutes later on successive days.

Dolosse: Type of concrete armor stone with special shape; see Appendix 1 entitled, “*Overview of the History of Concrete Armor Units*”.

Dredge: Any of various machines equipped with scooping or suction devices and used to deepen harbors and waterways and in underwater mining.

Erosion: Wearing-away of material under the action of natural forces.

Eustatic Sea-Level Rise: Global sea level rise caused by the melting of polar ice caps as a result of global climate change.

Filter Layer: Also known as “Under-layer”; in rubble-mound structures, this stone layer covers the core stone either from the seaside or from both sides to prevent it being washed-away by wave attack. Its size is typically larger than that of the core stones, with stone weights ranging between 300 and 800 kg.

Floating Derrick: General terms used to describe any derrick used on water. Derricks are hoisting devices used to raise, lower, and laterally move loads using a rope-based hoisting mechanism. Floating derricks are typically used to salvage sunken vessels, dredging, and construction of coastal structures.

Flume: Also known as “Testing Flume” and “Prototype”; the actual structure or condition being simulated in a laboratory miniature model.

Freeboard: The structure’s height above still-water level.

Genetic Algorithms (GA's): The most extended group of modeling methods best representing the applications of Evolutionary Algorithms. The solution to a given problem is represented by string given the name “chromosome”, consisting of a set of elements called “genes”, which hold a set of values for the optimization variables. The fitness of each chromosome is compared against the requirement of an objective function.

Geotextile: Synthetic fabric which may be woven or non-woven used a filter between various stone sizes of a coastal structure.

Groin: A structure typically perpendicular to the shoreline, which is designed to control the movement of beach material by trapping the littoral drift.

Harbor: Area of the sea at the lee of a coastal structure or a natural headland where ships and vessels can moor and maneuver without any impedance caused by excessive wave energy, in average weather conditions.

Head: Also known as “Rounded Head”; is the extreme end of a breakwater or groin.

Headland: Geological land protrusion into the sea, usually rocky.

Higher High Water: The higher of the two high waters in any given diurnal tidal day.

Highest High Water: The highest high water of the spring tides of record.

HRI: Stands for the “Higher Research Institute” in Alexandria, Egypt.

Hydraulics: Science of water motion, flow, and mass behavior. Not to be confused with "hydrology", which is the science of the hydrological cycle, i.e. involving precipitation, runoff, and seasonal flooding.

IAM: Stands for “Infrastructure Asset Management”, which is as the coordinated activity of an organization to realize value from assets; which are infrastructure assets in this case.

LANDSAT: An Earth satellite imaging program launched by the United States government in 1999 with the aim of depicting land use patterns worldwide.

Leaside: Opposite to the seaside.

Life-Cycle Cost (LCC): The sum of all recurring and one-time (non-recurring) costs over the lifetime of the structure. It includes the costs of construction, inspection, maintenance, repair, rehabilitation, and remaining value of the asset at the end of its lifetime.

Littoral Drift: Also known as “Littoral Transport”; it is the movement of beach material in the littoral zone by waves and currents. Includes movement parallel

(longshore transport) and perpendicular (onshore-offshore transport) to the shore.

Littoral Zone: Consists of the beach and the surf zone.

Longshore: Along the shore.

Lower Low Water: The lower of the two low waters of any diurnal tidal day.

Lowest Low Water: The lowest low water of the spring tides of record.

Maintenance: Repair or replacement of components of a structure whose life is less than that of the overall structure, or of a localized area that has failed.

Markov Chains (MC's): Special method of stochastic modeling. Markov Chains have the special property that probabilities involving how the process will evolve in the future depend solely on the present state of the process, meaning they are independent of past events.

Mean High Water: The average of the high water over a 19-year period.

Mean Higher High Water: The average of the height of the higher high waters over a 19-year period.

Mean Low Water: The average of the low water over a 19-year period.

Mean Lower Low Water: The average of the height of the lower low waters over a 19-year period.

Mean Sea Level (MSL): The mean height of mean high water above mean low water.

Modified Cube: Type of concrete armor stone with special shape; see Appendix 1 entitled, "*Overview of the History of Concrete Armor Units*".

Morphology: Seabed form and its change over time.

Non-Rayleigh Sea States: Sea states in shallow water, where the wave height distribution at the structure's toe is not Rayleigh-distributed statistically.

OSPOS: Offshore Pressure-Operated Suspended Wave Recorder device.

Overtopping: Water passing over the top of a coastal structure.

Parapet: Solid wall at the crest of the structure projecting above deck level.

Pell-Mell: Random-placed armor stones.

Perched Beach: Beach that is formed by the accumulation of beach sediment material on the shore at the leeward side of a rocky outcrop.

Pocket Beach: Beach that is formed by the accumulation of beach sediment material on the shore between two headlands.

Pontoon: Large flat-bottomed barge or lighter equipped with cranes and tackle for offshore coastal construction.

Porosity: Capability of armor stone or natural rock to retain the incoming water waves. The more porous is the armor the more it dissipates the kinetic energy of the incoming wave.

Quarry: Site where natural rock stone is mined.

Quaywall: Vertical harbor structure used for mooring of ships, as well as loading and unloading of cargo and goods.

Rayleigh Sea States: Sea states in deep water, where the wave height distribution at the structure's toe is Rayleigh-distributed statistically.

Rehabilitation (Repair): Renovation or upgrading of coastal structures.

Relative Sea-Level Rise (RSLR): Specifically to the coastal region of Alexandria Egypt, this term describes the relative rise of the mean sea level caused by the combined effect of global climate change in addition to seismic and geological subsidence.

REMR: Stands for the “Repair, Evaluation, Maintenance, and Rehabilitation” Program, developed and conducted by the US Army Corps of Engineers for navigational and coastal structures.

Replacement: The action of demolishing a coastal structure and then its reconstruction.

Return Period: For a certain sea storm, designates the number of years when the occurrence of a single storm of equal intensity, on average, is likely to be exceeded only once.

Revetment: A cladding of stone, concrete or other material used to protect the shoreline surface of an embankment, natural coast or shoreline against erosion.

Rip-rap: Wide-graded quarry stone, typically used as a protective layer to prevent shoreline erosion.

Rocky Outcrop: Part of a seabed rocky formation that appears above the surface of the surrounding seabed.

Root: The first leeward reach of a semi-detached breakwater or groin.

Rubble-Mound Structure: A mound of random-placed and random-shaped stones.

Run-up: The rush of water up a structure or a beach resulting from wave incidence.

Salient Beach: Beach that is formed by the accumulation of beach sediment material on the shore at the leeside of a shore-parallel breakwater or an islet.

Seawall: Vertical **coastal structure** built to protect the shore from erosion or to act as a breakwater.

Seaward Seismic Subsidence: The tilting of a tectonic plate in such a way that reduces the level of the beach and surf zone seabed relative to MSL, as a result of seismic activity, hence exposing coastal zones to RSLR.

Semi-Detached Breakwater: A breakwater connected at only one end to the shoreline.

SCA: Stands for “Supreme Council of Antiquities”.

Shallow Water: Water whose depth cause surface waves to be affected by the seabed bathymetry. Such waters are typically located whenever the water depth is less than half the wave length.

SPA: Stands for the Egyptian “Shore Protection Authority”, the government agency reporting to the Egyptian Ministry of Irrigation and Water Resources, which is in charge of construction, maintenance, and repair of coastal protection structures across the Arab Republic of Egypt.

Spring Tides: It is the highest tides which occur at intervals of half a lunar month. They occur at or near the time when the moon is new or full, i.e. when the sun, moon, and earth fall in line, and the tide-generating forces of the moon and sun are additive.

Still-Water Level: Water level that would have been observed absent any waves.

Stochastic: A process or model that is statistically based upon random variation.

Storm Surge: The rise in water level induced by wind stress and atmospheric pressure on the sea surface during storms.

Submerged Breakwater: A rubble-mound breakwater whose crest is at or below the still-water level. Commonly known as “reef breakwater” and “low-crest breakwater”.

Surf Zone: The area located between the outermost breaker and the maximum reach of the wave run-up.

Tetrapods: Type of concrete armor stone with special shape; see Appendix 1 entitled, “*Overview of the History of Concrete Armor Units*”.

Toe: Lowest part of a coastal structure’s side slope, forming the transition to the seabed, and providing design protection for the structure against shear failure. Typically consists of natural stone of the same size and weight as the filter layer.

Trunk: The reach of a semi-detached breakwater or groin located between the root and the head of the structure, and also the part of a detached breakwater located between both heads.

Under-layer: See “**Filter Layer**”.

Wave Rose: A four-quadrant diagram representing the distribution of the directions where waves at certain point (the origin) on the sea come from, and indicates the heights of such waves. Similarly, a "Wind Rose" is a four-quadrant diagram representing the distribution of the directions where winds at certain point (the origin) blow, and indicates the speeds of such winds in the Beaufort scale.

LIST OF FIGURES

Figure	Page
1-1: Sea-level rise data in Alexandria (Frihy, 2003).....	4
1-2: Vulnerable areas to RSLR in the Nile Delta (Hassaan & Abdrabo, 2012).....	5
1-3: Storm surge in Al-Mandara area in 2003 (Courtesy of Arab Contractors).	6
1-4: Impact of the December 2010 storm in Alexandria.....	6
1-5: Land subsidence along Nile Delta coast (Frihy, 2003).....	7
1-6: Flooding risk areas in Alexandria, Egypt (Frihy et al., 2010).	8
2-1: Design concept of rubble-mound coastal structures (Oliver et al., 1998).	16
2-2: Sample non-rubble monolithic concrete structure (Pirie et al., 2005).	16
2-3: Division of coastal structures into reaches and sub-reaches (Hughes, 2003).....	18
2-4: Structural breach in a rubble-mound breakwater (Oliver et al., 1998).....	22
2-5: Core exposure resulting from armor loss (Oliver et al., 1998).....	23
2-6: Armor loss after initial settlement (Oliver et al., 1998).....	23
2-7: Armor quality degradation and loss of armor contact (Oliver et al., 1998).....	24
2-8: Slope defects and toe erosion impact on armor layer (Oliver et al., 1998).	25
2-9: Aerial photo of a breakwater's head under wave attack (Prickett, 1998).....	27
2-10: CSARS system set-up and mode of operation (Prickett, 1998).....	28

Figure	Page
2-11: SeaBat™ sonar device fan pattern (Prickett, 1998).....	29
2-12: Underwater survey for a marine wharf (Teledyne Reson, 2010).	29
2-13: Structural rating form for a rubble-mound jetty (Oliver et al., 1998).....	36
2-14: Functional rating form for a jetty (Pirie et al., 2005).....	40
2-15: Failure modes for a rubble-mound earth dike (Vrijling, 2001).	41
2-16: Various methods of damage evaluation (Kamali & Hashim, 2009).....	44
2-17: MC-based transition probabilities for structural deterioration.	46
2-18: Eastern Harbor Middle Breakwater deterioration (El Hakea et al., 2014).	48
2-19: Land-based construction schematic (Breakwaters, 2000).	51
2-20: Space requirements for construction equipment access (CIRIA, 2007).....	52
2-21: Combining land-based and waterborne equipment (Courtesy of AF Co.).	55
2-22: Breakwater™ software SI and FI report (Aguirre & Plotkin, 1998).....	57
2-23: CI of a rubble-mound breakwater against time (Oliver, et al., 1998).....	58
2-24: CoSCA™ software screenshot (US Army Corps of Engineers, 2008).	59
2-25: CoSCA™ 3D representation (US Army Corps of Engineers, 2008).	60
2-26: Optimizing armor LCC and weight (Sorensen & Burcharth, 2004).....	61
2-27: Maintenance strategy for a rubble-mound structure (Nguyen et al., 2010).....	62

Figure	Page
3-1: Research general outline.....	63
3-2: Outline of the research methodology framework.	65
3-3: ID number configuration for a typical sub-reach.	66
3-4: Subdivision of the Pharos Promenade breakwater (El Hakea et al., 2014).	68
3-5: Functional inspection by the author in Alexandria, Egypt, 2013.	76
4-1: Geographic location of Alexandria (El Hakea et al., 2014).	90
4-2: Scope of the case study area and its zoning layout.....	91
4-3: Map modified by author after Frihy et al. (2004) for the study area.	93
4-4: Structure's length per zone in the study area in year 2013.....	95
4-5: Length of each structure type per zone in year 2013.....	95
4-6: Length of each structural design concept per zone in year 2013.....	96
4-7: Length occupied by each type of armor per zone in year 2013.....	97
4-8: Length occupied by armor types and weights per zone in year 2013.....	97
4-9: Armor shapes and weights length distribution in year 2013.	98
4-10: Armor shapes and weights distribution in the study area in year 2013	98
4-11: Armor stone weight distribution over the total length of the study area.	99
4-12: Structural inspection for rubble-mound structures in year 2013.	100

Figure	Page
4-13: Structural inspection of non-rubble and composite structures in year 2013. ..	101
4-14: SI values for the study area’s structures in year 2013.	102
4-15: SI results by type of structure in year 2013.	102
4-16: Overall SI values per each type of structures in 2013.	103
4-17: SI distribution against armor stone shapes and weights in year 2013.	104
4-18: Length distribution of FI ranges in year 2013 per type of structure.	105
4-19: FI percentage distribution per structure type in year 2013.	105
4-20: FI values per structure type in year 2013.	106
4-21: Storm simulator demonstration on Al-Chatby to Sidi Gaber Revetment.	107
4-22: LCC Optimization Module’s output formulation.	109
4-23: Cumulative LCC for all coastal structures within the study area.	110
Figure 4-24: PI versus time for the study area against the PI threshold.	111
4-25: LCC per meter run per structure type between year 2013 and 2050.	112
4-26: Cross-section of the Eastern Harbor Breakwaters, (Tetra Tech, 1986).	113
4-27: Risk Optimization Module results for the six scenarios.	117

LIST OF TABLES

Table	Page
1-1: Coastal structures in Alexandria and their owning entities.	9
2-1: Condition rating guidelines for rubble-mound structures (Oliver et al., 1997).....	31
2-2: General CI scale for rubble-mound structures after Oliver et al. (1997).....	31
2-3: General CI scale for non-rubble coastal structures after Pirie et al. (2005).....	32
2-4: SI rating scale based upon Oliver et al. (1998) and Pirie et al. (2005).....	33
2-5: Structural rating sequence for rubble-mound structures (Plotkin et al., 1991)....	33
2-6: Typical frequencies of visual inspection (Hughes, 2003).	36
2-7: Primary and secondary coastal project purposes (Plotkin et al., 1991).	37
2-8: Suggested intervention actions against FI ranges (Plotkin et al., 1991).....	39
2-9: Limiting wave conditions for waterborne equipment (CIRIA, 2007).	54
2-10: Combinations of waterborne equipment sizes (CIRIA, 2007).	54
3-1: Structure general data as logged in the AID.	68
3-2: Core stone and filter layer attributes for a typical breakwater.....	69
3-3: Armor stone attributes for a typical breakwater.	70
3-4: Armor stone attributes for a typical breakwater.	70

Table	Page
3-5: Design and environmental attributes for a typical breakwater in year 2013.	71
3-6: CIC values for reaches of the Glim Bay East Groin in year 2013.....	72
3-7: Extract of the Inspection and Condition Rating Module.	73
3-8: CIC values for the Eastern Harbor Seawall in year 2013.....	74
3-9: Seaside armor structural ratings for the Eastern Harbor Seawall in year 2013. ..	74
3-10: FI values for Glim Bay East Groin in year 2013.	75
3-11: Average CI drop for Alexandria’s coastal structures due to storms.....	81
3-12: Intervention policies and their effect on CI values.	84
3-13: PI risk ranges as per expert consultation in year 2014.	87
4-1: Summary of threats surrounding the study area.	94
4-2: SI values for the study area and its zones in year 2013.	104
4-3: FI’s of the study area and its zones in year 2013.....	106
4-4: LCC Optimization Module scenarios.	108
4-5: Risk Optimization Module scenarios.....	116
4-6: List of experts consulted for the data and framework verification.....	123
4-7: List of experts consulted for the validation of the module outputs.	124

LIST OF EQUATIONS

Equation	Page
2-1: Cross-section component index (Oliver et al., 1998).	34
2-2: Reach / sub-reach structural index (Oliver et al., 1998).	34
2-3: Structural index for the entire structure (Oliver et al., 1998).	35
2-4: Reach functional index (Oliver et al., 1998).	39
2-5: Functional index for the entire structure (Oliver et al., 1998).	40
2-6: Backward MC formulation (El Hakea et al., 2014).	47
3-1: SCM at the year of construction or last major repair.	77
3-2: Expression of RI by a single-liner matrix.	77
3-3: Obtained regression equation for the Eastern Harbor West Breakwater.	82
3-4: Developed equation of the adjusted CI value after storm occurrence.	83
3-5: Adjusted CI value to account for intervention policy effect.	85
3-6: Priority Index calculation for structures, after Nugyen et al. (2010).	86
3-7: Total LCC formulation for the study area.	88
3-8: weighted PI formulation for individual structures.	89
3-9: Total PI formulation for the study area.	89

CHAPTER I – INTRODUCTION

1-1. Significance of Coastal Infrastructure Worldwide and Locally

The new ISO 55000 standard simply defines Asset Management (AM) as the coordinated activity of an organization to realize value from assets. As such, it could be stated that the aim of Infrastructure Asset Management (IAM) is to provide decision-makers with the tools and techniques that enable them to maintain the asset's minimum reliability while keeping a near optimal Life-Cycle Cost (LCC), over the life time of the asset. While extensive research has typically dealt with various fields of infrastructure assets such as roads, bridges, pipelines, airports, buildings, and power-plants, very limited research discussed coastal protection structures. Statistics reveal that almost 23% of the world population resided within 100 km from the coastline in the year 2003, accounting for approximately 1.2 billion people. This figure is expected to reach 50% by the year 2030. In light of these demographic realities and as a result of global climate change, almost 80 million people are expected to be exposed to coastal flooding resulting from seasonal storm surges by 2080 (Small & Nichols, 2003). The most dramatic examples of coastal storm flooding occurred in Bangladesh in 1992, where 100,000 deaths were recorded in addition to millions who were displaced (Adger et al., 2005). Effective coastal protection and flood defense structures are thus essential in terms of preserving life as well as public and private property. The failure of the flood defense system in New Orleans in 2005, for instance, had catastrophic consequences on life and property. The development of a LCC and risk optimization methodology based upon both the structural deterioration patterns and functional reliability for coastal structures is hence the core objective of this study.

From a historical perspective, the Nile Valley and its Delta have been the center of demographic concentration. Prior to the construction of the Aswan High Dam, the annual Nile flood used to transport sediments to the Nile promontories, which kept the Nile Delta under continuous seaward expansion. This has changed however when the dam has prevented the supply of sediments to the Nile promontories, and has been even compounded by global climate change, Relative Sea Level Rise (RSLR), and human activities near the coastal areas. Climate change has from one part contributed to the decreased return period of record seasonal storms, induced by increased SLR resulting from the melting down of the polar caps. The

RSLR is a further particular problem to the Nile Delta, caused by the presence of a Holocene mud layer underneath the entire delta, that has become prone to excessive compaction due to underground seawater percolation. Nevertheless, the entire northern part of the Nile Delta, including the largest populated city of that region, Alexandria, were identified among the areas that are subject to seaward seismic subsidence. Furthermore, some other areas of the northern Nile Delta coast, such as Al-Burullus, Baltim, Gamassa, and Al-Gamil were historically characterized by the presence of coastal sand dunes, which constitute a natural reliable defense against SLR risks. These coastal sand dunes have been systematically decaying under aggressive human consumption for construction and infrastructure works. The above risks were addressed in works by Farouk (1985), Tetra Tech (1985:1986) Fanos & Sharaf El Din, (2008), El-Sharnouby et al. (2010), and Hassaan & Abdrabo (2012).

In 1995, the International Protocol on Climate Change (IPCC) identified the low-lying Egyptian Nile Delta among the world's most high-risk under the threat of global eustatic Sea Level Rise (SLR), which is expected to be in the range of 0.18 to 0.59 cm by the end of the twenty-first century. Under various scenarios of SLR, the expected amount of lost area due to sea inundation in the northern Nile Delta governorates, namely Alexandria, Al-Beheira, Kafr Al-Sheikh, Damietta, and Port Said, is between 22.49% and 49.22% (Hassaan & Abdrabo, 2012). Nevertheless, Hassaan & Abdrabo (2012) suggest that 15.56% of the total areas of the Nile Delta are under inundation risk only due to land subsidence, even absent any SLR scenario caused by climate change. This poses devastating threats to the Egyptian population and the economy, given that the Nile Delta's demographic density is approximately 1600 inhabitants / km², and that the region contributes with 30-40% of the national agricultural output, in addition to 60% of fish catch (Frihy, 2003). Nevertheless, the Nile Delta and Alexandria altogether are home to more than half of the national manufacturing industrial infrastructure (Hassaan & Abdrabo, 2012).

The significance of coastal protection structures in Egypt became evident with the development of the Shore Protection Master Plan of the Northern Nile Delta Coasts in 1985-1986 by Tetra Tech Inc. and under the supervision of the Shore Protection Authority (SPA). In the Master Plan, several areas in Alexandria, Abu Qir Bay, Rosetta, Baltim, Ra's Al-Bar, and Al-Gamil area of Port Said were identified as high-risk areas, and recommendations were made to construct a group of coastal protection structures in these regions.

1-2. Problem Statement

The construction of the necessary coastal structures or the upgrading of existing structures is indispensable in order to minimize the risk to life and property. Such interventions need to be performed with the available budgets while keeping both the condition of the structure and the risk exposure limits within the safe region. Nevertheless, the coordination of such intervention policies between the various owning entities within a certain geographical region, and the need to consider the versatility of design and environmental attributes surrounding coastal structures are further challenges to a collective coastal IAM plan. Summarizing the problems that are facing coastal areas, the following issues could be identified as the center of attention:

- First, the impact of climate change and other seismic activities in coastal regions worldwide and locally directly affects the hydrodynamic properties of coastal waters, and accelerates the deterioration of coastal protection structures, posing further risks to life and property, especially in high-risk areas that are more prone to flooding risk areas during seasonal storms.
- Second, a significant portion of coastal structures are out of lifetime, and are subject to deterioration due to regular wave attack and storm conditions. They require significant intervention cost to be maintained at a safe level of service.
- Third, the presence of various stakeholders responsible for ownership, decision-making, funding, maintenance, and rehabilitation of any group of coastal structures sharing the same geographical region; poses serious challenges towards the implementation of any sort of macro-level IAM policies with respect to such structures.
- Fourth, little research was aimed at the optimization of both LCC and risk exposure limits as to coastal protection structures, taking into account that such optimization is required to consider the effect of climate change, budgetary constraints, inflation, design versatility, and diversity of deterioration patterns.

The following sections are thus intended to expand on the above problem statement.

1-2.1. Climate Change and Eustatic SLR

Various natural and anthropogenic elements have collectively contributed to the endangerment of Egypt's northern coastline in general, and the city of Alexandria in particular. The global eustatic sea-level rise induced by the climate change phenomenon was identified as the major risk factor (El-Raey et al., 1995; Frihy, 2003; El-Nahry & Doluschitz, 2010; El-Sharnouby et al., 2010; Hassaan & Abdrabo, 2012). The projected sea-level rise in Alexandria based on tidal gage measurement compiled by Frihy (2003) is shown in Figure 1-1.

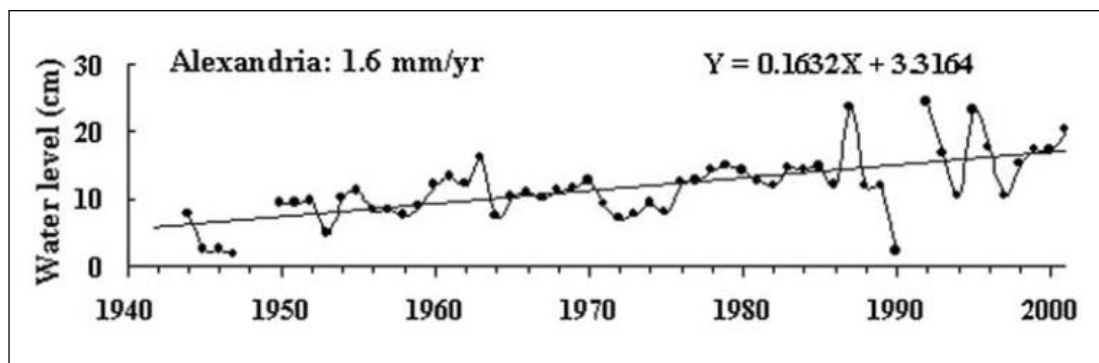


Figure 1-1: Sea-level rise data in Alexandria (Frihy, 2003).

Figure 1-2 depicts the northern Egyptian coastal areas most susceptible to sea inundation as a result of RSLR for various scenarios suggested by Hassaan & Abdrabo, based upon previous studies by Rahmstorf (2007) and Pfeffer et al. (2008); where Alexandria is shown among the highest vulnerable areas, located to the north of the International Coastal Highway, which represents an unintended protection to the areas at its lee. This further ascertains the significance of coastal protection works in reducing the risk to life and property.

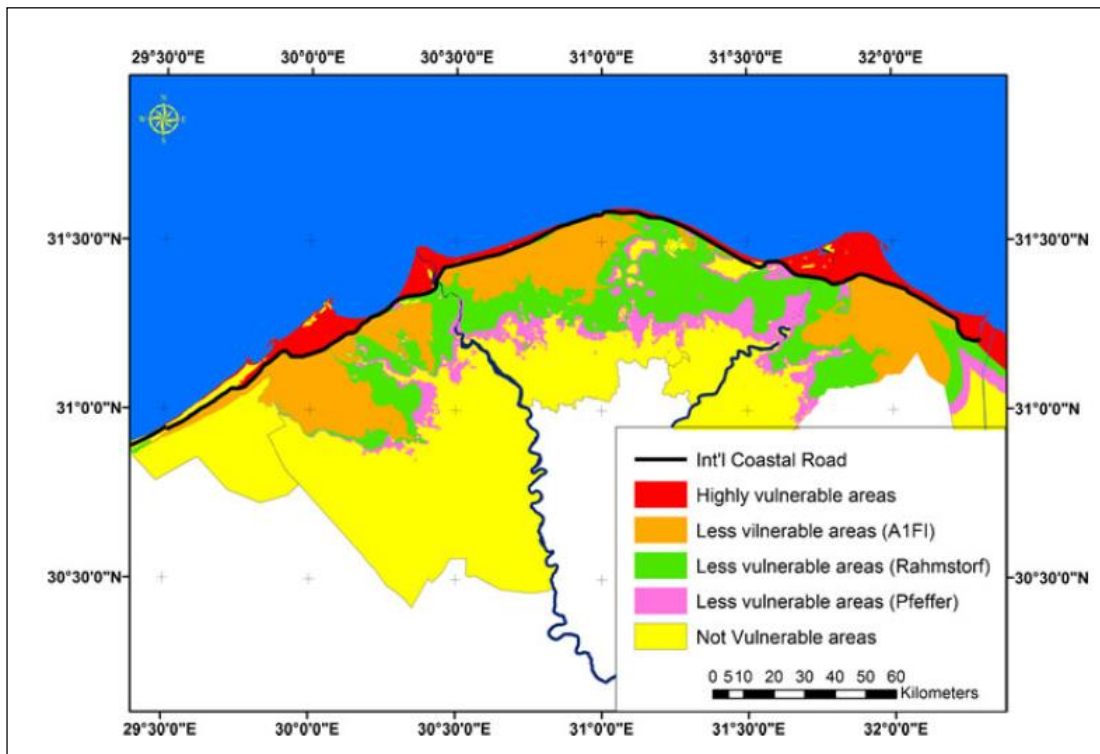


Figure 1-2: Vulnerable areas to RSLR in the Nile Delta (Hassaan & Abdrabo, 2012).

Climate was also blamed for the recent increase in storm surges and change in wave characteristics along Egypt's Mediterranean coasts, posing further risks on Alexandria's beaches, especially during winter storms (Iskander, 2013). In 2003, a heavy winter storm caused the flooding of the Pharos Promenade tourist area in addition to the busy Al-Manshiya district in the Eastern Harbor. Moreover, a severe winter storm in December 2010 inflicted critical damages to the Cornice Road, and caused severe erosion of recreational beaches in several places. Figures 1-3 and 1-4 show examples of the damage of assets, infrastructure, and flooding caused by excessive wave run-up induced by the storm surge in two winter storms in December 2003 and December 2010, respectively. Figure 1-4 shows the impact of the winter storm in the following areas: (a) Engineers Club, Saba Pacha; (b) Armed Forces Club, Mustapha Kamel Pacha; (c) Western Harbor; and (D) Tharwat area (Photos are courtesy of AF Co. and Dr. Mahmoud Fayez Zaki Consulting Office).



Figure 1-3: Storm surge in Al-Mandara area in 2003 (Courtesy of Arab Contractors).



Figure 1-4: Impact of the December 2010 storm in Alexandria.

1-2.2. Seismic and Geological Subsidence and its effect on RSLR

Seismic studies revealed that Alexandria is subjected to an annual subsidence; whereby seismic activity along the existing active fault lines induces the low-lying coastal zones to tilt downwards relative to the Mean Sea-Level (MSL) (Frihy, 2001; Hassaan & Abdrabo, 2012). Parts of the site of Alexandria were submerged down to 6-8 m below MSL following a major earthquake that took place in the 6th century AD (Iskander, 2000). A further risk is imposed by the existence of a 30 m to 40 m-thick layer of Holocene mud resting below the northern waterfront of the Nile Delta, whose expected compaction under the advance of underground seawater is foreseen to

induce further land subsidence of the northern Nile Delta region, in addition to its neighboring Alexandria, as shown in Figure 1-5. Seaward land subsidence rates ranges between -1.6 and -4 mm per year in Alexandria and its surroundings (Frihy, 2003).

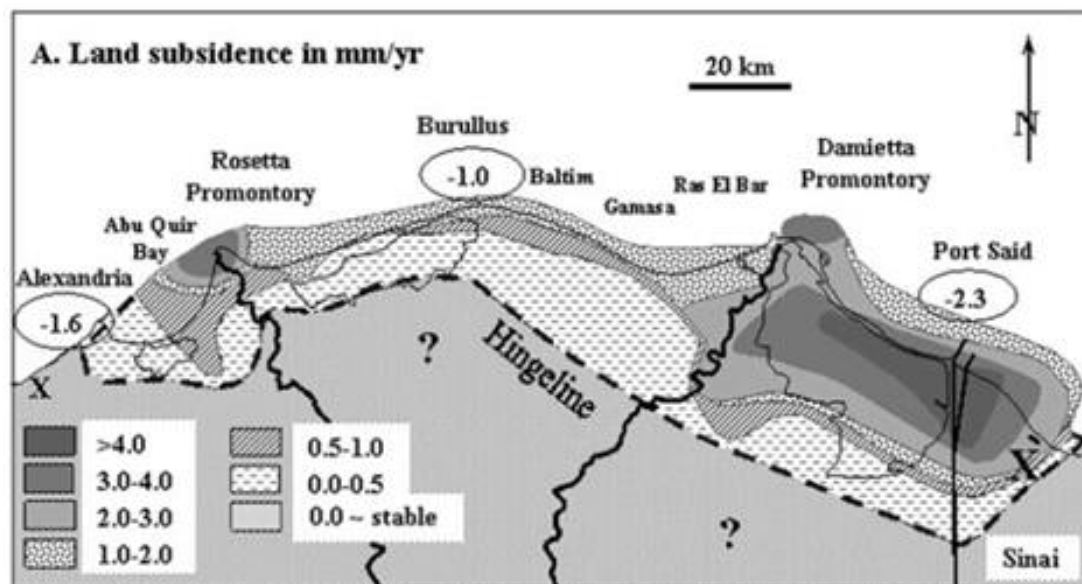


Figure 1-5: Land subsidence along Nile Delta coast (Frihy, 2003).

1-2.3. Flooding Risk Areas

Although relatively distant from Alexandria, several studies indicate that the consequences of failure of the Muhammad Ali Seawall could be extremely costly to the city of Alexandria, as it may cause the immediate inundation of the former Mareotis Lake and Abu Qir Lagoon area, which could physically transform Alexandria into an isolated island (Frihy, 2003; El-Nahry & Doluschitz, 2010; El-Sharnouby et al., 2010; Frihy et al., 2010; Hassaan & Abdrabo, 2012). The locations of Muhammad Ali's Sewall at Al-Tarh area, the former Abu Qir Lagoon and Mareotis Lake are shown in Figure 1-6.

Limited research has been performed with regards to the economic impact of sea inundation of Alexandria in particular, as most of the research dealt collectively with the entire Nile Delta. However, the most thorough analyses of economic and demographic consequences with regard to Alexandria was carried out by El-Raey et al. (1995:1999). From the cultural perspective, the UNESCO had launched a program which aims at studying the effect of Relative Sea-Level Rise (RSLR) and coastal structures on Alexandria's coastal heritage, as outlined in its report published in 2003

(UNESCO, 2003). As a result of RSLR, Alexandria has recently been subjected to severe winter storms in 2003 and 2010 especially. El-Sharnouby and Soliman (2011) discussed seasonal changes brought up in Alexandria's vulnerable coastal areas during severe storm surges, and presented a case study of the severe storm that took place in the winter of 2010, and caused a settlement failure of the Corniche Road in Al-Mandara area. Their research included the responsive coastal defense measures that followed this hazard. Frihy et al. (2010) identified Al-Mandara as the most vulnerable location with respect to storm surge inundation along Alexandria's coastline; this is shown in Figure 1-6. The figure on left shows the location of the former Abu Qir Lagoon and Mareotis Lake, and the position of the Mohamed Ali Sewall (Risk area # 2), as well as Risk Area # 1 at Al-Mandara. Further the figure indicates on the right the altitude measured above MSL of the Corniche Road along Alexandria's waterfront from Al-Silsila to Al-Montaza area

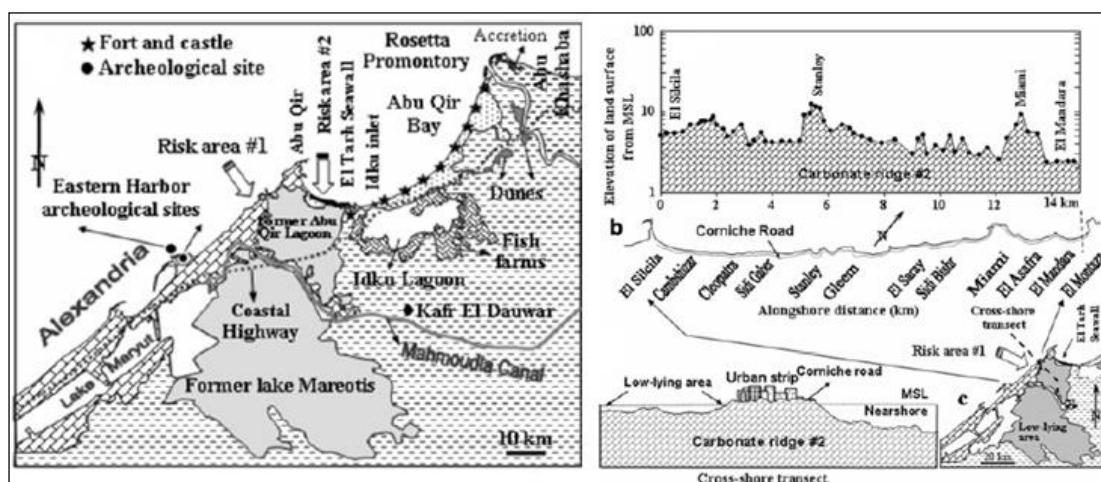


Figure 1-6: Flooding risk areas in Alexandria, Egypt (Frihy et al., 2010).

1-2.4. Need for Effective and Collective Coastal IAM

A problem that is peculiar to all types of coastal infrastructure worldwide is the involvement of numerous governmental and non-governmental agencies and bodies, which makes it difficult in terms of coordinating a sound and effective overall national or regional IAM plan (Quinn, 1971). This is evident in the case of Alexandria, where some of the structure owners can be listed as in Table 1-1:

Table 1-1: Coastal structures in Alexandria and their owning entities.

Zone or Structure	Owner
Qaytbey Fort Marine Protection	SCA
Eastern Harbor Breakwaters	SPA
Marine Scouts Club	Marine Scouts Authority
Al-Manshiya Revetment	Alexandria Governorate
Al-Silsila Cape	Ministry of Defense
Al-Chatby to Sidi Gaber Revetment	Alexandria Governorate
Mustapaha Kamel Armed Forces Club	Ministry of Defense
Teachers Club	Egyptian Teachers Syndicate
Police Club	Ministry of Interior
Professional Clubs Area	Professional Syndicates (Engineers, Medical Professions, Lawyers, Judges, Administrative Auditing)
Glim Bay Groins	Alexandria Governorate
San Stefano Breakwaters	Talaat Mostafa Holding Group and Four Seasons Hotels
26 th of July Club	Ministry of Defense
Laurent Revetment	Alexandria Governorate
Automobile Club	Egyptian Automobile Club
Bir Masoud, Miami, and Al-Mandara Submerged Breakwaters	Alexandria Governorate

The presence of numerous stakeholders may result in conflict of interest between various bodies, which culminates eventually in the form of lack of coordination in the execution of some marine protection works, as will be discussed in further detail considering Alexandria in Chapter IV.

In view of such issues rises the need to implement an efficient collective IAM plan encompassing all coastal structures within a single region, with the aim to achieve the optimum utilization of resources towards meeting the minimum reliability requirements; which is the protection of life and property. Such plan is required to encompass the communication and coordination difficulties imposed by the presence of various owning and managing bodies.

1-2.5. Need for Optimization

From a purely mathematical perspective, the amount of variables as to the design and environmental attributes is enormous. The criticality of areas and assets protected by such structures is an additional variable. Nevertheless, the effect of intermediate and design storms on such structures is not equal, and depends primarily on the armor layer weight and shape, as well as the seaside slope of the structure, the structure crest level, and the significant wave height, in addition to other design and environmental variables.

From an end-user perspective, any sort of model that comprises a group of public and privately-owned infrastructure assets, would be required to possess the ability of segregating the optimization according to the end user. This means possessing the ability to run the optimization for single structures, zones, as well as for the entire area with the same efficiency. For the purpose of illustration, the coastal structures and assets in Alexandria, the case study of this research, are owned and managed by various government and private bodies, which include the SCA, SPA, Governorate of Alexandria, Egyptian Armed Forces, professional syndicates, hotels, and clubs. As such, this research offers an optimization tool for these establishments with regards to their coastal infrastructure within the study area. From another perspective, the presence of various types of coastal structures gives rise to the need of another mode of optimization based upon structure type. This is necessary to visualize the long-term and the single-event deterioration on each category of structures separately. Last but not least, the budgetary constraints faced by both governmental and private institutions further ascertain the need for an optimum LCC optimization module for coastal structures.

1-3. Research Scope and Objectives

This research aims to establish a decision-support system for coastal infrastructure asset managers and designated governmental institutions, with regards to coastal infrastructure assets. The system aims to provide its users with tools to balance risks of failure with total LCC's of coastal structures. This integrated model includes an Asset Inventory Database (AID), an established procedure for inspection, condition assessment and condition rating, a deterioration model which takes into account both the long-term deterioration pattern and the single-event deterioration due to seasonal storms, and finally an optimization module with pre-set action

thresholds triggering predefined intervention policies with the aim to achieve the least LCC corresponding to the minimum acceptable condition state levels. The concept behind this integrated optimization module is to be adaptable to be applied to the level of individual structures, zones, as well as the entire study area. The case study as is the city of Alexandria, with a study area stretching along 18.5 km, and comprising 7 distinct zones, 43 structures, and 198 reaches and sub-reaches. The study area includes four distinct types of coastal infrastructure:

1. Rubble-mound breakwaters and groins;
2. Rubble-mound revetments'
3. Non-rubble seawalls and quaywalls; and
4. Composite breakwaters.

Thus, in order to achieve the targeted scope of work, the following objectives are considered:

1. Establishment of an AID for all reaches, structures, and zones within the study area, given the lack of information, followed by establishing of visual inspection and condition rating criteria and guidelines. The end product is conducting of visual inspection and condition rating of all structures within the study area, to be considered as a single-point inspection given the lack of data as to previous inspections and rating.
2. Modeling of structural deterioration of structures in both regular and storm conditions. This starts by obtaining Deterioration Transition Matrices (DTM's) for all structures, zones, and reaches, with the ability to run the model for every type of structures solely, and is then followed by expressing the deterioration trends obtained from the forward Markovian deterioration modeling in terms of mathematical equations using regression tools. The sudden effect of intermediate and design storms on each structure is taken into account.
3. Formulating an LCC Optimization Module, which enables decision-makers to select the optimum action plans for maintenance, repair,

rehabilitation, or replacement of coastal structures, all while satisfying the required Priority Index (PI) threshold.

4. Development of the Risk Optimization Module, which provides the end-users with the ability to minimize the risk to life and property associated with the deterioration of coastal structures under preset budgetary constraints.

1-4. Research Motivation

Most of the previous attempts to address coastal risks tackled the problem from individual angles rather than a collective approach. The study area offers a unique case study where a multitude of risks are combined, hence offering a fertile area of research as to the combined effect of all threats on coastal structures within the study area. There were attempts by Tetra Tech (1985:1986) and the Shore Protection Authority (SPA) to conduct the condition assessment of the Eastern Harbor middle breakwater, but the results were in the form of a general report where the condition was not expressed in numerical terms. Moreover, the Supreme Council for Antiquities (SCA) hired AF Co. in 1994 to inspect and repair the Qaytbey Fort ancient seawall, yet again, the way the report was composed does not provide sufficient data. Absent any numerical representation of inspections and condition assessments, such data could hardly be used as an input for a coherent IAM policy. Even for regular marine works projects in Alexandria, most contractors tend to use post-construction underwater camera as-built surveys, which are not translated into numerical condition ratings and indices. Other published works studied post-storm responses of coastal structures, as well as the impact of some other structures on water quality in recreational beaches. However, such works did not consider the entire service life of such structures from a deterioration and LCC optimization perspective. The threats posed by climate change, seismic subsidence, and deterioration of coastal structures, compounded by the considerable lack of previous structured research as to the inspection and condition rating of Alexandria's coastal structure gave rise to the need of performing such work by the author. This has been accomplished for the first time using a structured approach for the entire study area. In addition, the main motive behind this work was to introduce for the first time ever and integrated LCC Optimization Module for coastal structures not only for this specific study area, but for the entire Arab Republic of Egypt, and based upon a

single-point inspection in case of data shortage. In addition, this research includes the effect of single-time events such as storms onto Markovian deterioration patterns, thus enabling modeling the effect of climate change on the deterioration, risk and LCC of coastal protection structures.

1-5. Research Methodology

In this research a literature review is conducted with regard to inspection methods and technologies, including the rationales behind the division of coastal structures into distinct reaches. This part includes a brief outline of the various types of coastal infrastructure and their design components. The next section in the literature review addresses the established methods of condition assessment and rating criteria, both structurally and functionally. In doing so, a summary of previous work on coastal structure damage progression and build-up is presented. Next, the literature review progresses to highlighting empirical formulae and artificial-intelligence modeling techniques for the prediction of deterioration of coastal structures. The literature review ends by going through the various previous approaches of integrated coastal infrastructure asset management.

The following step is the presentation of the AID with a description of the entered attributes and characteristics pertaining to all reaches and structures. This is followed by the results of the visual inspection carried out by the author over the course of the year 2013. The development of damage between the year of construction or last major maintenance and the year of this single-inspection point is then modeled using backward MC modeling. The obtained Deterioration Transition Matrices (DTM's) for every single structure from the Backward MC Module are then projected onto the future, to obtain the deterioration forecasts up to year 2050. This forward MC forecast features the inclusion of the effect of intermediate and design storms which are unique to every structure. After some initial trials, it was determined that running the optimization module directly on the Forward MC Deterioration Module inclusive of the storm simulator consumed significant runtime and computer memory. This led to the need to translate all forward MC deterioration trends for all structures into mathematical functions using best-fit regression. This also enabled re-entering the effect of intermediate and design storms, and provided a further validation of such effects as opposed with the results previously obtained during the MC trials. For the optimization module, four sets of decision-making

policies are presented along with their corresponding unit costs and triggering condition state thresholds. Those policies are namely: (1) Do Nothing; (2) Routine Maintenance; (3) Rehabilitation; and (4) Replacement. LCC optimization modeling is carried out under various preset deterioration scenarios then simulated, where design and intermediate storms are set at defined years for the entire study area. The results of this scenario are then presented and discussed. The optimization modules are primarily concerned with LCC and risk optimization. For the LCC Optimization Module, the objective is the minimization of the total LCC for all assets while meeting a minimum risk level threshold. As for the Risk Optimization Module, the objective is to minimize the total risk for the entire study area while being constrained by different budget sets. Both modules are run for various storm occurrence scenarios, and finally conclusions and recommendations for future work are addressed.

1-6. Thesis Organization

This thesis comprises six chapters. Chapter I – Introduction, introduces the significance of coastal structures worldwide in general, and in the study area in particular. In addition, it explains the problem statement and methodology according to which this work has been carried out. Chapter II – Literature Review, discusses the various inspection methods and technologies, condition rating procedures and criteria, previous empirical and AI-based research surrounding structural deterioration, and integrated asset management systems for coastal infrastructure. Chapter III – Research Methodology Framework, outlines the development of the scope of works, the encountered challenges during data acquisition, field work, and expert interviews, in addition to presenting the research objectives. It then expands in detail into the general framework of the thesis, and expands with detailed discussions on every stage of the framework, along with a discussion of the LCC model scenario runs. Chapter IV – Case Study and Discussion of Results, considers the detailed description of the study area, its attributes and characteristics, and continues with the discussion and analysis of the various running modes of the optimization and the associated scenarios. The final chapter, Chapter V – Conclusion and Recommendations for Future Work, includes the conclusion and the recommendations for future work building upon the findings and outcomes of this work.

CHAPTER II - LITERATURE REVIEW

2-1. Introduction

The objective of this literature review is to discuss the most notable previous work with regard to coastal infrastructure asset management. As such, this chapter first presents the conventional and modern methods and techniques for the inspection of coastal structures. This includes an introduction to the main types of coastal structures, including their typical design cross-sections and attributes, and the methods used to divide such structures into reaches and components. The next section describes the distress types and mechanisms, together with the condition rating criteria and methods of calculations of component indices, reach indices (RIs), and structural indices (SIs) for both rubble and non-rubble structures, along with their functional indices (FIs) and overall condition indices (CIs). The following section presents the previous work performed on deterioration prediction using both empirical and AI-based techniques. The chapter ends by presenting various integrated coastal infrastructure asset management approaches from past literature, and includes a discussion on common repair and maintenance construction methods and techniques.

2-2. Coastal Structure Inspection Methods and Technologies

2-2.1. Subdivision of Structures into Reaches and Sub-Reaches

For the purpose of facilitating the process of inspection of coastal structures, which are in essence linear in nature, and in order to ease the reporting of distresses and condition rating, several studies suggested the subdivision of individual coastal structure into distinct reaches. Among these studies were Oliver et al. (1997:1998), Hughes (2003), and Pirie et al. (2005). The suggested procedure entails the subdivision of each coastal structure into major reaches. It does not go by default that all reaches within a certain structure should be equidistant; however, each individual major reach shall correspond to a unique cross-section, type of construction, design feature, or rehabilitated section (Hughes, 2003). The type of structure and its cross-section components dictate the way such structure would be divided into major reaches. Figure 2-1 illustrates the method by which an arbitrary rubble-mound shore-connected or semi-detached breakwater is divided into root, trunk, and head sections, and indicates the various cross-section components of the structure, including the

core, under-layer, armor stone, and crest or cap. Part (a) represents typical layouts of a shore-connected or semi-detached breakwater, and detached breakwaters; whereas part (b) shows the typical components of a rubble-mound breakwater. In addition, Figure 2-2 presents a sample of a non-rubbles breakwater along with its superstructure and substructure components.

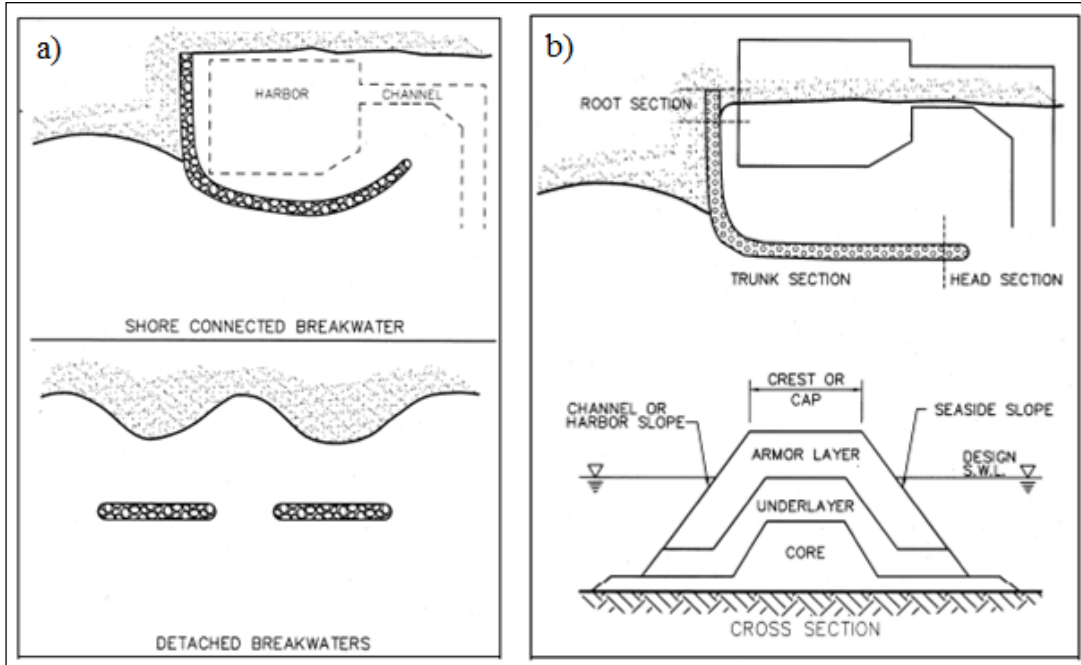


Figure 2-1: Design concept of rubble-mound coastal structures (Oliver et al., 1998).

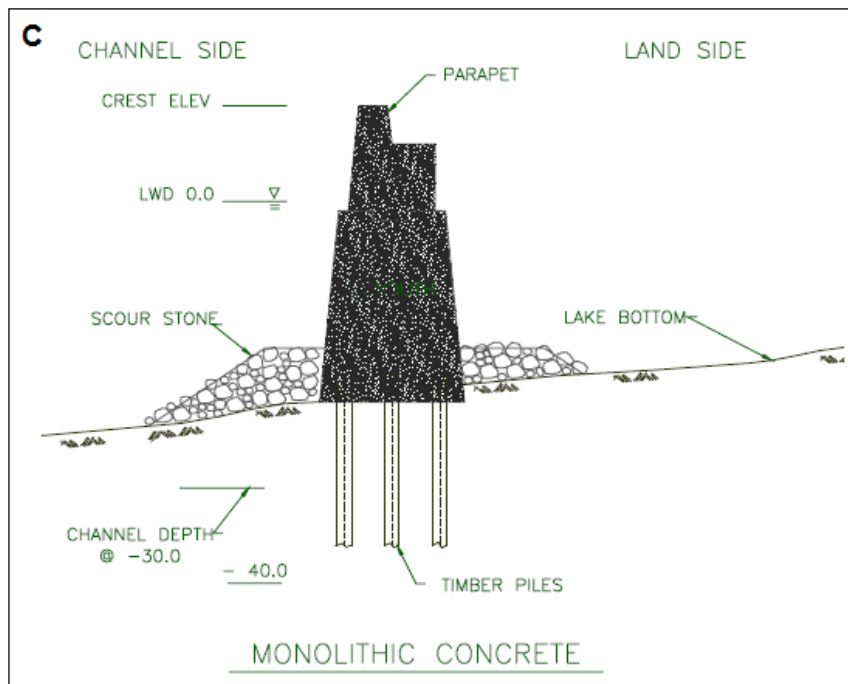


Figure 2-2: Sample non-rubble monolithic concrete structure (Pirie et al., 2005).

In addition, Figure 2-3 provides the subdivision layout of a typical jetty into separate structural reaches and sub-reaches. The figure legend refers to the cases of: (a) a jetty; (b) a shore-connected breakwater; and (c): a detached shore-parallel breakwater. Reaches are based on function, with the head usually being around 30.00m long, at least. Sub-reaches are based upon changes in construction, armor type and size, change in cross-section, and rehabilitated sections. The procedure specified in Oliver et al. (1997), Hughes (2003), and Pirie et al. (2005) limits the length of every sub-reach at 500 ft, which is approximately 150.00 m. From this standpoint, and had the coastal structure to be inspected been divided into a defined set of reaches and sub-reaches that reflect specific geometrical or functional features, or represent a certain stretch not exceeding 150.00 m. Reaches are defined based on function, with the head should always be a separate reach around at least 30.00m long. Sub-reaches are based upon changes in construction, armor type and size, change in cross-section, and rehabilitated sections. The recommended numbering system for surveying stations starts from the shore and proceed seawards. The first number in the sub-reach demarcation relates to the reach number, while the alphabetical letter relates to the division within the major reach. Permanent markers or spray paint should be utilized to identify the positions of surveying stations along the reach for future inspection and monitoring. The next step is to define the suitable inspection methodology for the structure under concern, for both under-water and above-water parts. This is discussed in the following section.

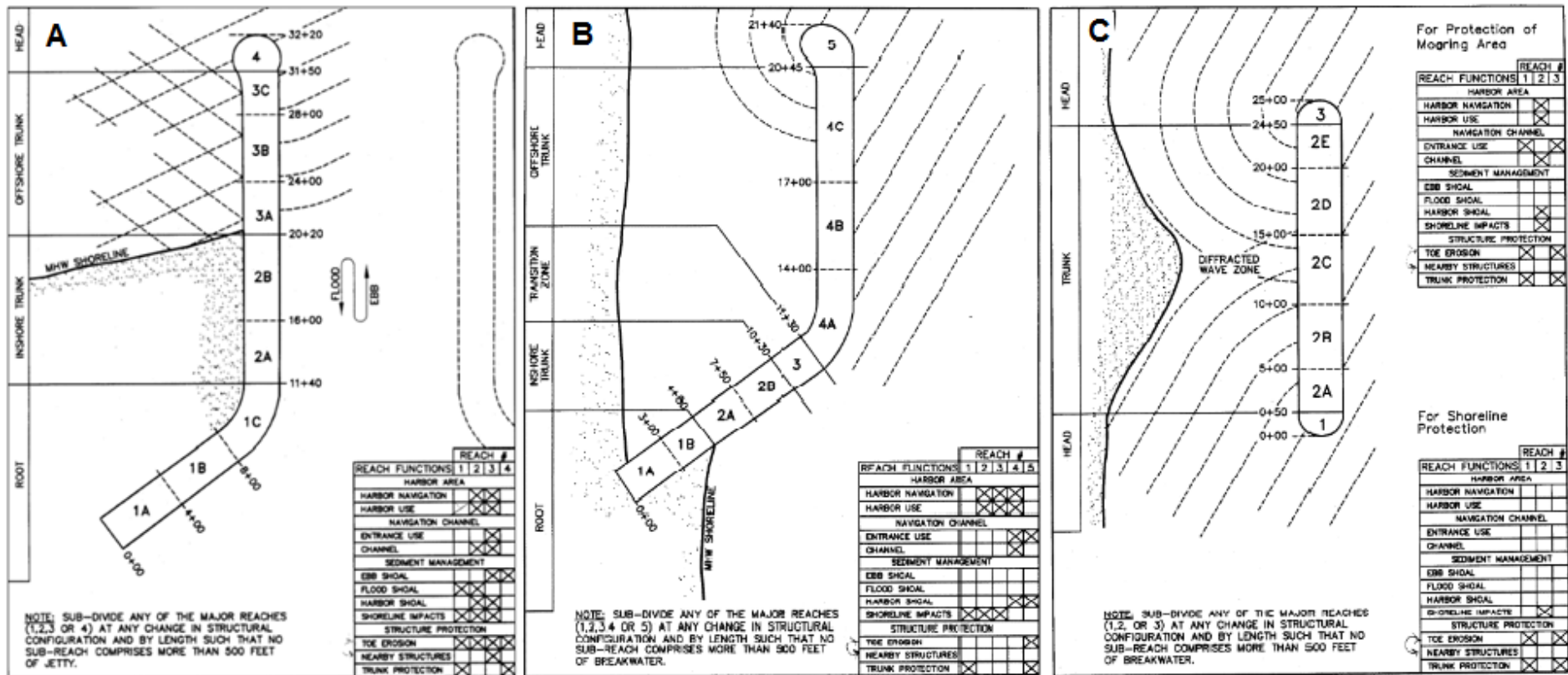


Figure 2-3: Division of coastal structures into reaches and sub-reaches (Hughes, 2003).

2-2.2. Coastal Structures Distress Types and Mechanisms

2-2.2.1. Non-Rubble Structures

Non-Rubble coastal structures may include concrete seawalls, gravity quaywalls, sheet-pile piers, and other various sorts of composite structures. The study area featured in this research includes concrete and composite sheet-pile seawalls and piers. The typical distresses modes that may occur to non-rubble coastal structures, which are mostly concrete, steel sheet-pile or composite structures, are centered on the following observations, after Pirie et al. (2005): (1) Loss of elevation and alignment; (2) Material deterioration; (3) Structural damage or defects; (4) Loss of scour and wave protection; and (5) Loss of foundation support.

For the loss of elevation or alignment, few deviations from as-built alignment may be observed in the form of slight progressive differential settlement of the structure's crest that is only a couple of inches. A further extent of deterioration is when some waviness is depicted in the crest elevation and the horizontal alignment, with no signs of structural movement yet. Without further action, deviations from the as-built alignment become more significant causing the structure's freeboard to be reduced with time by 10% to 25 % of its original height due to structural movements. Had this stage of distress been reached without intervention, the following stage witnesses the appearance of at least one breach along the structure's length, and a reduction of the freeboard by up to 40% of its design value, with an irregular crest. Absent any corrective action, most of the structure becomes prone to structural breaches with 75% of its freeboard height lost; causing most of the structure to be easily overtopped by storm condition waves, until it ultimately fails (Pirie et al., 2005).

Regarding material deterioration, the first distresses that may appear are some ageing or wear of material, with slight imperfections such as superficial steel corrosion, some hair cracks, honeycombing or scaling in non-critical concrete sections, but that do not expose the steel reinforcement. With no response, the cracks in concrete become more visible on the surface, and exposed steel surfaces start having some pitting. Such cracks then develop to allow the steel reinforcement to be further exposed and corroded, with rust staining being clearly visible. With time cracks start to get even deeper in various locations along with spalling. Concrete near the surface starts being ruptured, further exposing steel reinforcement already

corroded. The damage of steel and concrete then reaches the stage of general material failure, with concrete surfaces lost in large portions and steel corrosion dangerously widespread, affecting the stability of the structure (Pirie et al., 2005).

Structural damage and defects start by small imperfections in the main structural members such as piles, sheet piles, walers, and caps. With further exposure and no treatment, such non-critical components exhibit minor signs of distress due to the structure's loading. This may be visible in the form of strain at connections and joints. Such components then when left further develop significant deformation, such as a hole in a sheet pile wall, and minor deformation or impact damage of connections. Beyond this stage, damage can then affect critical components of the structure. This may be evident in cracks in the parapet or cap of the structure, broken connections, gaps between interlocking gravity quaywall blocks, and voids behind sheet piles. The lack of adequate response leads to the progression of damage to a stage where serious collision damage may be present, holes and gaps become large enough to allow the wash-away of backfill material at the leeside of the structure or of the core stone in case of composite structures. The structure ultimately fails when all connections are broken or severely weakened (Pirie et al., 2005).

Loss of scour and wave protection typically starts with a small displacement of the toe of the structure in isolated parts, with a slight displacement of armor stone that is within 25% of the armor stone size. This next develops into minor settlement of the toe, with armor displacement within 75% of armor stone size. The further development of damage is characterized by exposing the toe of the structure caused by excessive armor stone displacement, albeit in small locations. Scour then becomes clearly evident in long sections of the structure's reaches, exposing the structure itself or its core to wave attack. The next stage is when the structure exhibits some settlement and loses its stability, leading gradually to localized structural failure, which then develops into large failures around the initially failed section (Pirie et al., 2005).

The loss of foundation support starts by observing a slight foundation settlement. Such slight settlement then further develops to inflict noticeable loss of the structure's alignment and elevation, putting the structure's stability at risk. Without action, the loss of alignment increases and the structures subsides and leans (Pirie et al., 2005).

2-2.2.2. Rubble-Mound Structures

Rubble-mound structures include breakwaters, groins, jetties, and revetments. The study area featured in this research includes all these structure types less jetties. The typical distresses modes that may occur to rubble-mound coastal structures are as listed below, after Oliver et al. (1998): (1) Armor loss; (2) Breach; (3) Core exposure; (4) Armor quality defects; (5) Loss of armor contact and interlock; and (6) Slope defects.

The earliest signs of armor loss are slight movement observed in the armor layer in few spots, leaving a depression within 25% of the armor unit nominal diameter. Further levels of degradation are reached when there is some waviness along the structure's slope with depression size within 75% of the armor stone nominal diameter. There might be some bridging over such voids within 50% of the armor unit nominal diameter, making the under-layer visible, although not yet suffering from loss. Further stages of deterioration include the increase of inter-armor voids to be almost equal to the size of a single armor stone, in several locations. Units adjacent to the void are prone to rocking and gradual displacement, leaving the under-layer and core stone visible, but still without being lost. Bridging in such case may span over a distance almost equal to the armor stone diameter. Without appropriate response, the situation can further escalate to the point where armor units are lost or have moved out of place in some portions of the structure reach lengths, with voids sizable enough to permit the loss of under-layer and core stone. Any further displacement of armor stone may eventually inflict further losses in the under-layer and core stone, leaving the structure vulnerable to being washed away by regular storm conditions (Oliver et al., 1998).

Breach in the structure's section may first be observed in slight settlement of the crest that is within 25% the nominal diameter of an armor unit. The following degradation stage is marked by a slight waviness along the crest profile, accompanied by settlement within 50% of the armor stone nominal diameter. At that stage, no core or under-layer has been lost. Hence, it is possible to conduct repair work by the addition of few armor units to replace the displaced ones. If no repair is performed, the situation further aggravates with the appearance of short breaches reaching down to the under-layer and core stone. The crest has now settled down by a height equivalent to 200% of the armor stone nominal diameter, or equivalent to the entire

depth of the armor layer. Under-layer and core stone may suffer insignificant losses, meaning that repair by the addition or repositioning of armor units is still possible. Leaving the structure without action leads to the following stage of deterioration causes considerable disturbance and loss of under-layer and core stone. A serious breach in the structure now takes place, putting the structure's integrity at peril under overtopping wave load. Further exposure to wave load at that stage inflicts large losses of armor, under-layer, and core stone, and causes the breach section to widen, settle and ultimately fail (Oliver et al., 1998). Figure 2-4 displays the mechanism and detail of a typical breach occurring along a rubble-mound breakwater.

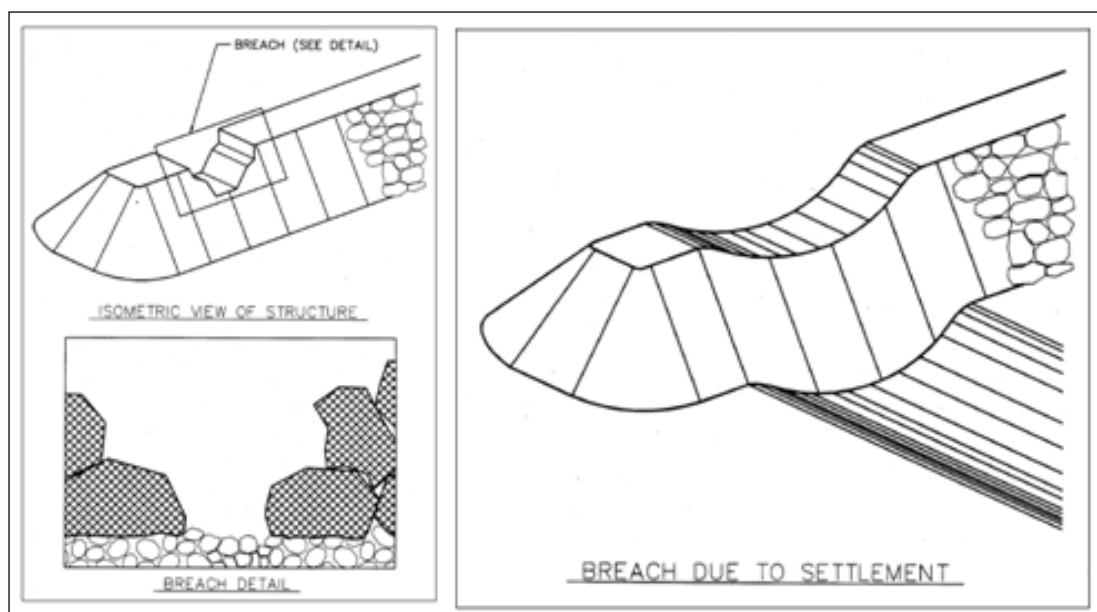


Figure 2-4: Structural breach in a rubble-mound breakwater (Oliver et al., 1998).

Core exposure comes primarily as a result of inter-armor gaps allowing wave energy to reach the core and under-layer and cause their loss. The first signs of alarm are when the under-layer stone can be occasionally visible between openings in the armor layer, yet such openings are smaller than the under-layer stone nominal diameter, and hence do not allow any losses to take place. Negligence of the deterioration grade may lead to further complications, manifesting in the form of enlarged inter-armor gaps allowing the wash-away of under-layer and core stone under wave attack (Oliver et al., 1998).

Loss of under-layer and core stone in several locations results in the dispersion of armor units, and the overall structural stability starts to be jeopardized

and with time becomes seriously affected. Further loss of core stone deprives the armor layer from any support from beneath, and it is easily displaced by stormy wave conditions, leaving the core either lost or exposed over full reaches of the structure (Oliver et al., 1998). Figure 2-5 and 2-6 illustrate core and under-layer loss resulting from armor stone displacement, and from loose nesting of armor after initial slope settlement, respectively.

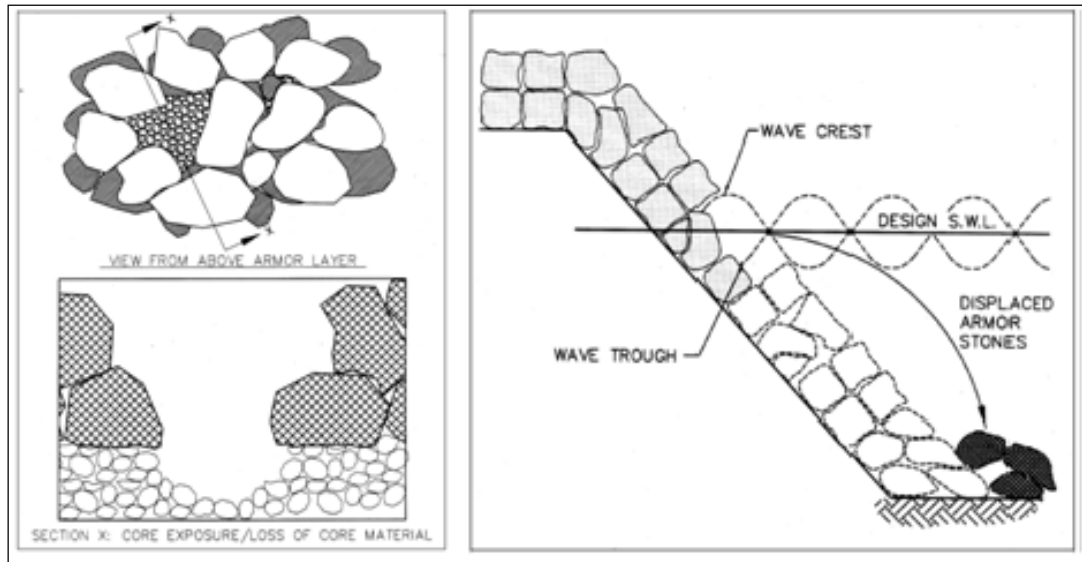


Figure 2-5: Core exposure resulting from armor loss (Oliver et al., 1998).

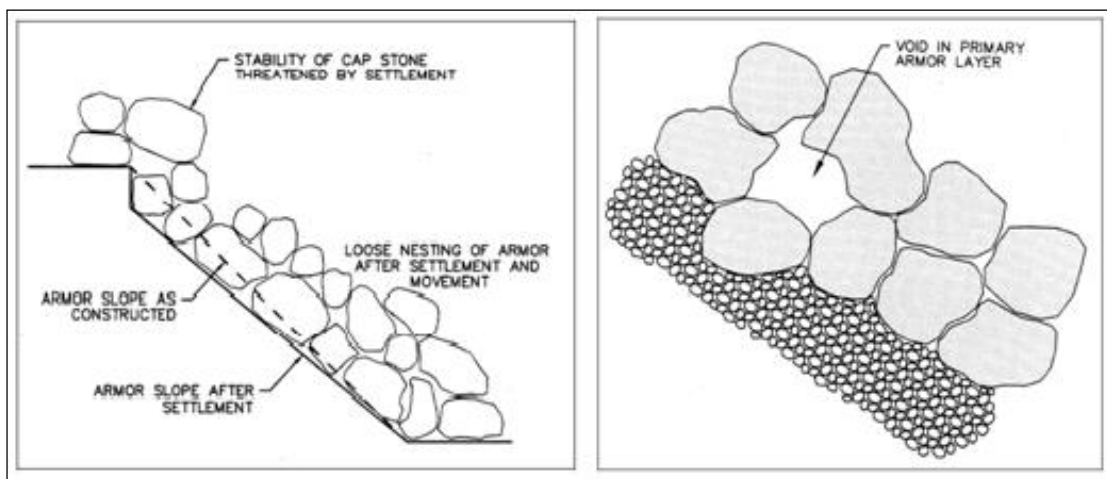


Figure 2-6: Armor loss after initial settlement (Oliver et al., 1998).

Another major deterioration field is armor stone quality defects. This starts by slight rounding of edges, spalls, and small cracks on few armor stones. Without monitoring and appropriate response, these minor defects become common for most armor stones, and deep cracks may be seen in few armor units in a certain reach of

the structure. Corrosion stains may appear around steel lifting hooks, but cracks do not exposed the embedded steel reinforcement (if any). With time, more armor units develop deeper cracks, embedded steel hooks starts to be visible, and few units become entirely fractured. The situation reaches complete deterioration when most armor units are fractured or seriously damaged (Oliver et al., 1998). Figure 23 (LHS) illustrates the consecutive degradation stages of an individual rock armor stone.

The earliest sign of loss of inter-armor contact and interlock is when few adjacent armor units are spaced by 25% the size of their nominal diameter. Further alarm signs appear when this spacing between adjacent units is within 50% of the nominal diameter, with occasional bridging along any particular reach of the structure. When the inter-armor spacing exceed 50% of the armor stone nominal diameter, individual units start acting independently, and become vulnerable to rocking out of place under normal wave attack. The situation become further critical when the inter-armor spacing reaches 100% the diameter of an armor unit, and most armor units might have been already lost along the structure slopes (Oliver et al., 1998). Various mechanisms of loss of armor contact and interlock see Figure 2-7. The left part of the figure shows the deterioration stages in the quality of rock armor stone, while the middle and right parts illustrate the loss of armor contact and interlock due to armor displacement and spalling. The armor stones on the bottom right are Dolosse armor units.

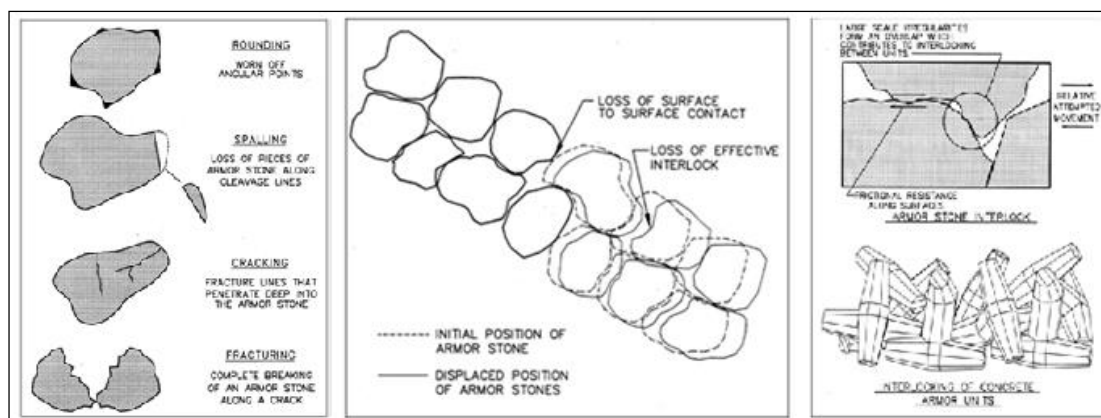


Figure 2-7: Armor quality degradation and loss of armor contact (Oliver et al., 1998).

Slope defects start by observing a minor sliding or steepening of the structure’s slope. The outer surface becomes uneven with visible waviness. In the

event where such waviness and sliding increase, the under-layer and core stone begin to be exposed, and the stability of such sections starts to be affected. The next deterioration stage is when such sliding and waviness is common across the entire structure's slope, leaving the core exposed in various locations to wave attack. Without appropriate action, the slope deterioration becomes a mean observation across the entire reach, until reaching the point when the extent of slope deformation deprives the structure from its stability (Oliver et al., 1998). Figure 2-8 displays the impact of slope defects and toe erosion on the overall structure and on the armor stone effectiveness.

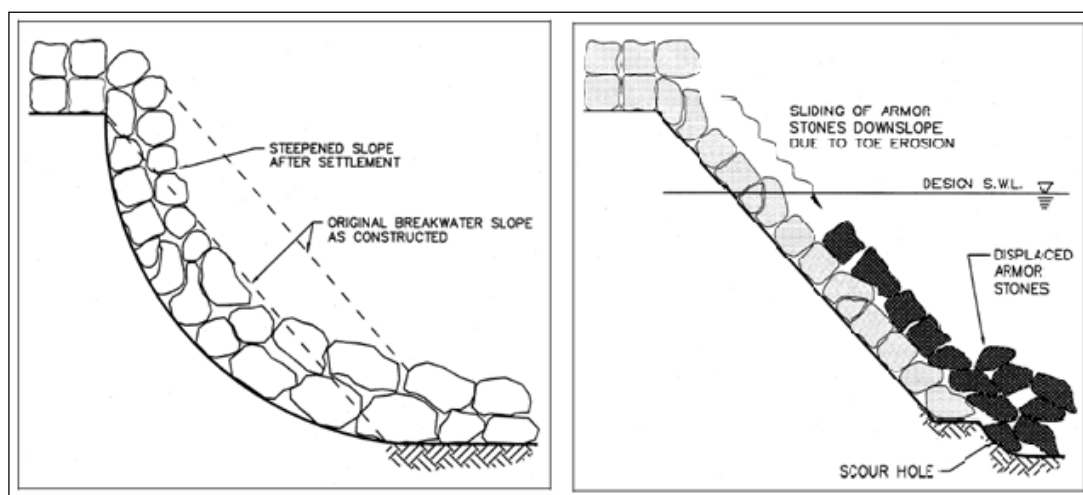


Figure 2-8: Slope defects and toe erosion impact on armor layer (Oliver et al., 1998).

2-2.3. Inspection Methods and Technologies

2-2.3.1. Visual Inspection

Visual inspection is the most widespread and most important inspection technique (Oliver et al., 1998; Hughes, 2003). According to Hughes (2003), the visual inspector has to be to a great extent familiar with the structure being assessed and its past history in terms of inspection, repair, maintenance, and deterioration records. Reach boundaries should also be well identified as discussed earlier in this research, prior to conducting the visual inspection. The assessor should bring a hard copy of the previous inspection report, laminated in a transparent plastic cover to prevent it from being wet by seawater. It is also of great importance to possess recent site maps, photographs, satellite imagery, digital cameras, tape measures, hand-held spirit levels, as well as tidal and meteorological information of the region where the

structure is situated (Hughes, 2003). In a typical above-water inspection, the inspector should at the start walk the entire length of the structure, noting the observed defects and scribing down where the defects are in terms of station locations, and indicating the severity of such defects. The inspector then conducts a return walk, in which he re-examines the depicted distresses and defects, and using a standard condition assessment form, starts putting his/her ratings and other comments on the form (Hughes, 2003). The condition rating process is covered in section 2-3 of this chapter.

For below-water visual inspection, a trained diver is the most common option, according to interviews conducted throughout 2013 and 2014, with engineers belonging to several Egyptian companies that work in both construction and supervision of coastal structures: Abdessalam El-Fiky Co., Arab Contractors Co., FZ Consulting Office, and Suez Canal Co. for Port Works and Mega Projects. Most inspections requiring trained divers and underwater cameras in previous projects in Alexandria dealt primarily with either post-construction underwater inspection or after a structural failure had occurred. Underwater videotaping of structures is common in Alexandria immediately after construction or immediately after record seasonal storms as in the case of the 26th of July Club breakwaters.

2-2.3.2. Modern Inspection Technologies

Limited studies have discussed other inspection methods and technologies for coastal and marine structures. Along with the traditional visual inspection custom, which works well with above-water portions of coastal structures, various modern inspection methods and technologies for underwater portions of jetties, breakwaters and groins are discussed in Prickett (1998) and Hughes (2003). These include aerial photogrammetry and multibeam sonar, which can accurately predict underwater inconsistencies in structure toes, armor layers, and under-layer stone. Aerial photogrammetry, depends on frequent photographs taken from the air, of coastal structures, and is mainly concerned with depicting above-water defects. This is illustrated in Figure 2-9.

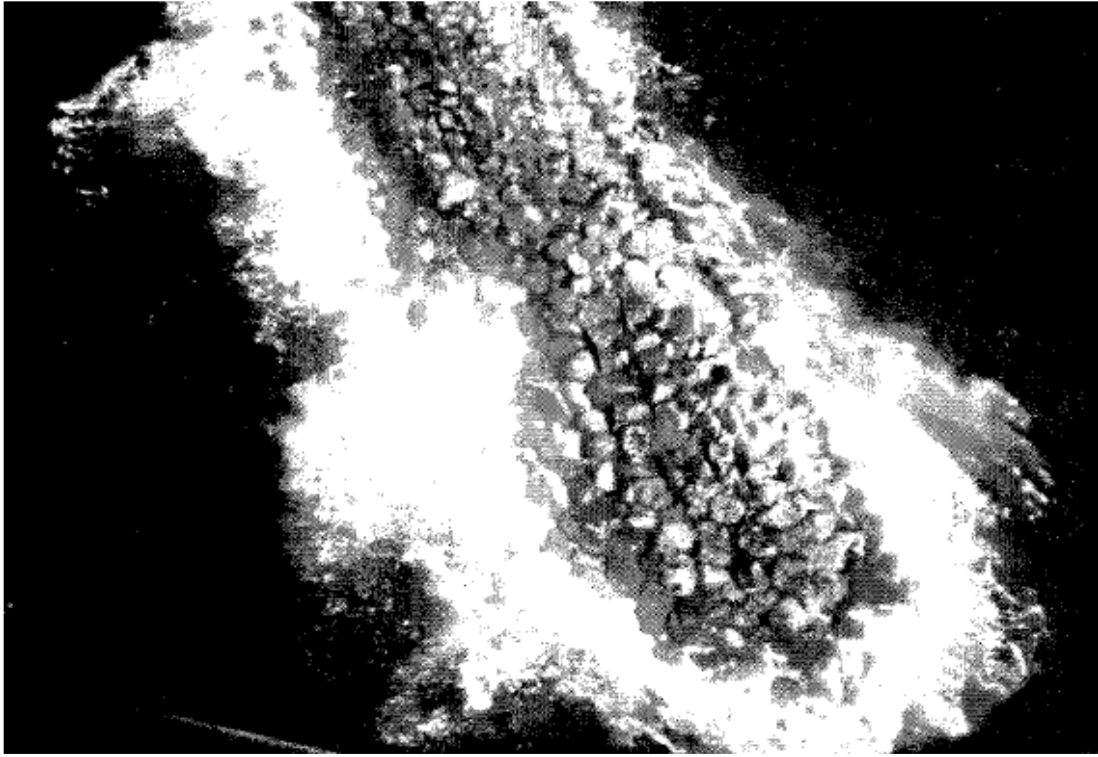


Figure 2-9: Aerial photo of a breakwater's head under wave attack (Prickett, 1998).

Another relatively modern technology described in Prickett (1998), is the Coastal Structure Acoustic Raster Scanner (CSARS) system. Developed by the US Army Corps of Engineers in the late 1980's, the CSARS system is an assembly consisting of an acoustic transducer operating at a 300 kHz frequency, mounted on a pan-and-tilt diving motor, and resting on a seabed-deployed tripod. The assembly can be lowered down to seafloor opposite to the coastal structure under concern from a vessel or even from a helicopter. The tripod contains an inclinometer and a pressure sensing device, enabling it to be accurately adjusted and to detect water depth. The transducer emits a conical beam of acoustic waves towards the inspected structure, "mapping the underwater target as a two-dimensional array or raster of ranges which, once processed, results in a data set of x-y-z coordinates", providing a 3D representation of steep coastal structures such as rubble mound breakwaters (Prickett, 1998). The tripod is connected to a ship-based computer system providing on-the-spot graphical display and quick data processing. Figure 2-10 illustrates the CSARS assembly and its operational concept as displayed by its computer software screen. Part (a) shows the CSARS system set-up comprising of the tripod and the diffuser head; and part (b) illustrates the pattern followed by the CSARS device in covering

underwater sections of coastal structures by emitted acoustic waves, as displayed by this screenshot from the CSARS computer software.

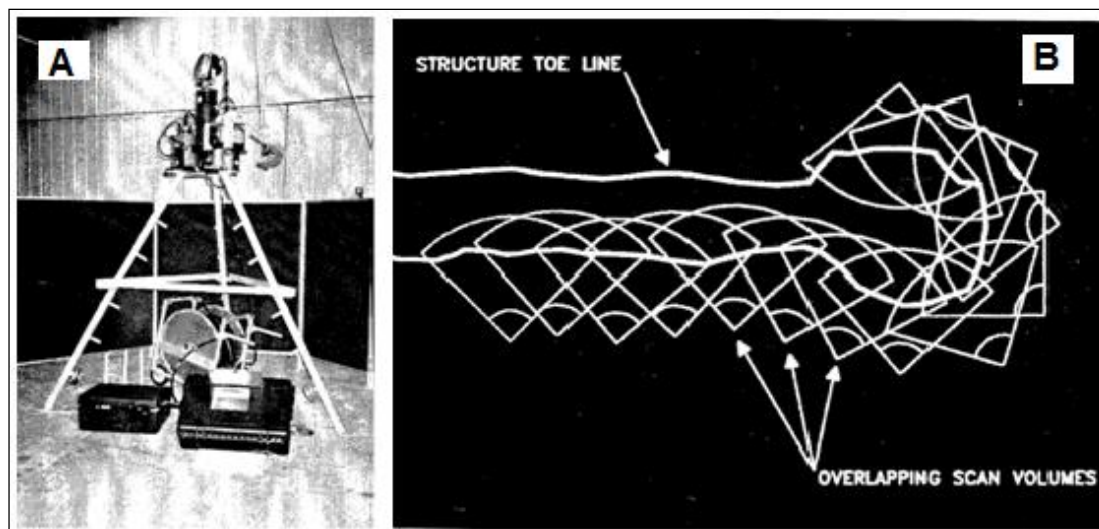


Figure 2-10: CSARS system set-up and mode of operation (Prickett, 1998).

Prickett (1998) also presents another modern tool for underwater inspection; the vessel-mounted Seabat™ device, equipped with a multibeam sonar system. The SeaBat™ was developed by RESON, Inc. of Goleta, California. The device was originally developed for high resolution, Remotely-Operated Vehicle (ROV) mounted surveys. However, it can be adapted to small vessel deployment. The SeaBat™ is a portable, downward and forward-looking single-transducer multi-beam sonar system. The main component of the system is an acoustic sonar head operating at 455 kHz that transmits 60 sonar beams spaced at 1.5° in a fan pattern to provide a maximum sounding coverage of 90° as shown in Figure 2-11. This configuration enables coverage of 2 to 4 times the water depth (Prickett, 1998). The sonar head is cabled to an external computer or data logger that controls the display, data processing, and output in real time. A pointer device such as joystick is used for operational control of the sonar head. The sonar head is tilt-able for mapping steeply-sloped or vertical structures.

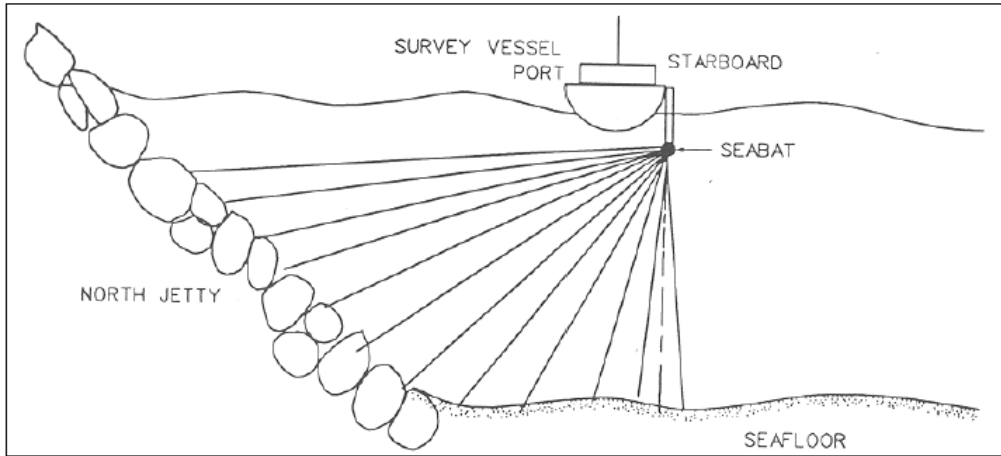


Figure 2-11: SeaBat™ sonar device fan pattern (Prickett, 1998).

The SeaBat™ provides accurate, high-resolution hydrographic data on the underwater condition of coastal structures. Cost is another constraint where it is costly but it guarantees a much more rapid dataset collection and presentation, and also provides a 100% bathymetric coverage to the water's edge (Prickett, 1998). Since the device was developed in the 1990's, Reson Inc. has been systematically upgrading its capabilities and software applications and data processing efficiency (Reson Inc., 2009). Figure 2-12 provides an example of the user interface for the device's software in recent eco-sound survey in Helsinki, Finland, using Seabat™ 7125, in 2010. Above-ground features appear in the 3D representation, with water depths represented with a color scale

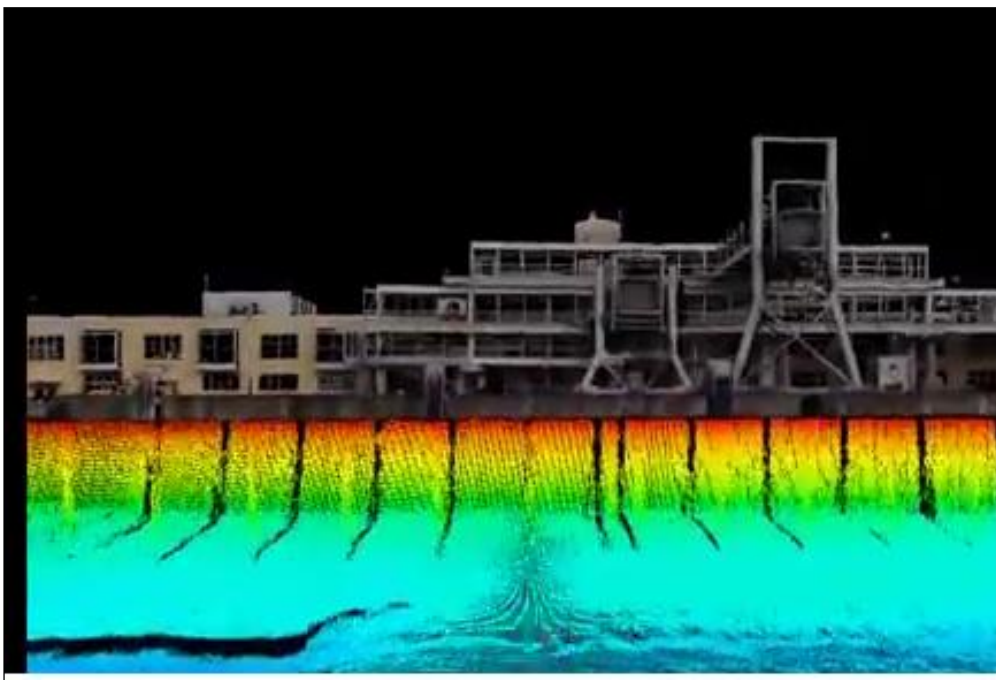


Figure 2-12: Underwater survey for a marine wharf (Teledyne Reson, 2010).

2-3. Condition Assessment and Rating

2-3.1. General Condition Index

The Condition Index (CI) system is a rational and consistent method for long-term evaluation of coastal structure condition based on periodic inspection (Hughes, 2003). Condition rating procedures for rubble-mound coastal structures are discussed in Plotkin et al. (1991), Oliver et al. (1997:1998), and Hughes (2003). Moreover, Pirie et al. (2005) describe the condition rating process for non-rubble coastal structures. All previously stated studies featured two separate condition rating processes for the structural condition and functional performance of structures. In accordance with general process, the structural condition and functional performance is reflected by a Structural Index (SI) and a Functional Index (FI), such that the general CI of the structure is a factor of both the SI and the FI. Plotkin et al. (1991), for instance, summarized three various rationales adopted to obtain the CI depending upon various relationships between SI's and FI's. The three rationales depend upon calculating SI's and FI's for each individual reach, then the relationship and order of priority between SI's and FI's is the point of difference between all three concepts. Concept "C" was later on expanded by Oliver et al. (1998), where the process of rating particular structural aspects for the reach components is first carried out to obtain the reach's SI, then the reach's FI is determined against the rating of specific functional criteria, prior to finally determining the CI for the reach. Oliver et al. (1997) applied the same concept adopted by Plotkin et al. (1991) for obtaining the SI for entire structures, but this time to obtain the FI value for the entire structure. The components and rating categories this time for functional rating were as shown in Table 2-1, columns (1) and (2).

For an individual structure, hence, the main target is to obtain a General CI, which is expressed in numerical terms (Plotkin et al., 1991; Oliver et al, 1997:1998; Aguirre & Plotkin, 1998; Hughes, 2003; Pirie et al., 2005). The main reasons which all cited studies agreed upon to justify the adoption of a unified numerical scale for CI's, are to reduce evaluation subjectivity by devising this uniform and consistent evaluation CI-based numerical method. Oliver et al. (1997) suggested the deterioration scale shown in Table 2-2 for the General CI for rubble-mound structures, while Pirie et al. (2005) suggested the same deterioration scale but this time for non-rubble structures, shown in Table 2-3.

Table 2-1: Condition rating guidelines for rubble-mound structures (Oliver et al., 1997).

Functional Area (1)	Functional Rating Categories (2)	Structural Rating Categories (3)
Harbor area	<ul style="list-style-type: none"> • Harbor navigation • Harbor use 	<ul style="list-style-type: none"> • Breach • Core exposure / loss • Armor loss • Loss of armor contact / interlock • Armor quality defects • Slope defects
Navigation channel	<ul style="list-style-type: none"> • Entrance use • Channel 	
Sediment management	<ul style="list-style-type: none"> • Ebb shoal • Flood shoal • Harbor shoal • Shoreline impact 	
Structure protection	<ul style="list-style-type: none"> • Nearby structures • Toe erosion • Trunk protection 	

Table 2-2: General CI scale for rubble-mound structures after Oliver et al. (1997).

Damage Level	Zone	CI Range	Condition Level	Description
Minor	1	85 to 100	EXCELLENT	No noticeable defects. Some ageing or wear may be visible.
		70 to 84	GOOD	Only minor deterioration or defects.
Moderate	2	55 to 69	FAIR	Some deterioration or defects are evident, but function is not significantly affected.
		40 to 54	MARGINAL	Moderate deterioration. Function is still adequate.
Major	3	25 to 39	POOR	Serious deterioration in at least some portions of the structure. Function is inadequate.
		10 to 24	VERY POOR	Extensive deterioration. Barely functional.
		0 to 9	FAILED	No longer functions. General failure or complete failure of a major structural component.

Table 2-3: General CI scale for non-rubble coastal structures after Pirie et al. (2005).

Damage Level	Zone	CI Range	Condition Level	Description
Minor	1	85 to 100	EXCELLENT	Only slight imperfections may exist.
		70 to 84	GOOD	Only minor deterioration or defects.
Moderate	2	55 to 69	FAIR	Deterioration is clearly evident, but the structure still appears sound.
		40 to 54	MARGINAL	Moderate deterioration.
Major	3	25 to 39	POOR	Serious deterioration in some portions of the structure.
		10 to 24	VERY POOR	Extensive deterioration.
		0 to 9	FAILED	General failure.

2-3.2. Structural Condition Index

Having explained the general concept of obtaining SI, FI and CI values for individual structural reaches, the following step would be to determine SI, FI, and CI values for the entire structure. For the SI value for the entire structure, Plotkin et al. (1991) visualized it as originating from reach components, then entire reaches, then the entire structure. The SI rating scale used by both Oliver et al. (1998) and Pirie et al. (2005) is illustrated in Table 2-4. Based upon a collective review of inspection steps as outlined in Aguirre & Plotkin (1998), Oliver et al. (1997:1998), Hughes (2003), and Pirie et al. (2005); the typical condition rating steps are summarized as follows:

1. Determine the function of the structure;
2. Divide the structure into major reaches according to the function;
3. Subdivide major reaches into sub-reaches according to structural and dimensional characteristics;
4. Set out the functional performance criteria;
5. Set out the structural requirements;
6. Inspect the structure and formulate a structural rating for component indices, sub-reaches, reaches, then obtain total SI;
7. Formulate a functional rating and calculate the general CI; and
8. Review structural requirements.

Table 2-4: SI rating scale based upon Oliver et al. (1998) and Pirie et al. (2005).

Observed Damage Level	Distress Zone	SI Range	Condition Level
		85 to 100	Excellent
Minor	1	70 to 84	Good
		55 to 69	Fair
Moderate	2	40 to 54	Marginal
		25 to 39	Poor
Major	3	10 to 24	Very Poor
		0 to 9	Failed

Determining the SI of a particular reach is further described in Plotkin et al. (1991), as being a three-phase procedure; starting by separate seaside and leeside components ratings, followed by rating of the entire structure, and ending by separate ratings for various categories of the seaside, the leeside, and the crest of the structure. This concept is illustrated in Table 2-5. Please refer to Oliver et al. (1998) and Pirie et al. (2005).

Table 2-5: Structural rating sequence for rubble-mound structures (Plotkin et al., 1991).

Phase 1	Phase 2	Phase 3
1. Breaching of section	1. Breach / Loss of cross-section	1. Breach
2. Change in side slopes	2. Side slope / Head (Seaside, leeside)	2. Slope defects
3. Armor condition	3. Armor damage	3. Armor quality defects
4. Condition of cap	4. Damage to cap / crest	4. Armor loss
5. Below water indicators	5. Below water indicators	5. Lack of armor contact / interlock
6. Exposure of under-layer / core material		6. Core exposure / loss
7. Armor displacement		

The calculation of structural component indices whether for rubble-mound or non-rubble structures can be described using Equation 2-1:

$$CI_C = DR_L + 0.3 (DR_H + DR_L) [\sum_{i=1}^n DR_i - (DR_H + DR_L) / 300]$$

Equation 2-1: Cross-section component index (Oliver et al., 1998).

Where:

- “ CI_C ” is the Cross-Section Component Index;
- “ DR_L ” is the lowest distress type rating;
- “ DR_H ” is the highest of the distress type rating; and
- “ DR_i ” is the rest of the distress type ratings, where “ i ” is the number of rated distress and “ n ” is the total number of rated distress types.

Every reach or sub-reach consists of all cross-sectional components; therefore, Equation 2-2 describes the relation that combines all cross-sectional components within the same reach or sub-reach, to obtain the reach or sub-reach index:

$$RI = CI_{CL} + 0.3 (CI_{CH} - CI_{CL}) [(\sum_{i=1}^n CI_{Ci} - (CI_{CH} - CI_{CL})) / 100]$$

Equation 2-2: Reach / sub-reach structural index (Oliver et al., 1998).

Where:

- “ RI ” is the Reach/Sub-reach Structural Index;
- “ CI_{CL} ” is the lowest Cross-section Component Index;
- “ CI_{CH} ” is the highest Cross-section Component Index; and
- “ CI_{Ci} ” is the rest of Cross-section Component Indices, where “ i ” is the number of cross-section component indices and “ n ” is their total number for the same reach or sub-reach.

Combining RI values corresponding to all reached within a certain structure, Oliver et al. (1998) expressed the structural index for the entire structure using Equation 2-3:

$$SI = RI_L + 0.3 (RI_H - RI_L) * [\sum_{i=1}^n (RI_i * i \%) / 100]$$

Equation 2-3: Structural index for the entire structure (Oliver et al., 1998).

Where:

- “*SI*” is the overall Structural Index for structure;
- “*RI_L*” is the lowest Reach/Sub-reach Structural Index;
- “*RI_H*” is the highest Reach/Sub-reach Structural Index;
- “*RI_i*” is the rest of Reach/Sub-reach Structural Indices; and
- “*i%*” is the percentage of structure’s length belonging to reach/sub-reach “*i*”.

Furthermore, the typical frequencies of walking inspections for structural rating for both rubble-mound and non-rubble structures is outlined in Hughes (2003), as per Table 2-6. Several examples of structural inspection forms are presented in Plotkin et al. (1991) for each of the three inspection phases. Furthermore, other examples built upon the Phase 3 inspection form presented initially in Plotkin et al. (1991) were presented in Oliver et al. (1998), as shown in Figure 2-13, providing the rationale by which the sheet is being filled by the inspector. For non-rubble structures, Pirie et al. (2005) developed similar inspection forms.

Table 2-6: Typical frequencies of visual inspection (Hughes, 2003).

Inspection Frequency (Years)	Description
1	By default
1	Recently completed structures and repairs; less frequent inspections for older structures
2	By default
3	If structure has not changed for 4 consecutive years
Response inspection	After major storm events
Opportunistic inspection	When personnel are in the region of other purposes
Emergency inspection	Local users report a problem

STRUCTURAL RATING FOR RUBBLE BREAKWATERS AND JETTIES Page _____ of _____

PROJECT NAME: Example Harbor Reach 3A

STRUCTURE NAME: South Jetty Sta: From 22+22 To 24+00

INSPECTOR: J.T.O. Inspection Date: 8/30/95 Time: Begin 8:00 End 12:00

WAVE HEIGHT (ft) 3-4 WAVE ACTION ON: B TIDE LEVEL: C WEATHER DAY OF A

TYPE OF INSPECTION: A WALKING B. BOATING C. OTHER

RATING CATEGORIES: Rate all items (Circle applicable lettered items)	CREST / CAP		SEASIDE (or HEAD)		CHANNEL / HARBOR SIDE	
	Rating 0-100	Comment Numbers	Rating 0-100	Comment Numbers	Rating 0-100	Comment Numbers
Breach: <u>A</u> Displaced Cap/Armor B) Settling Cap/Armor	10	1				
Core (or Underlayer) Exposure / Loss	10	1	10	1	10	1
Armor Loss: <u>A</u> Displaced C) Bridging B) Settling	10		10		10	
Loss of Armor Contact / Armor Interlock	10		10		10	
Armor Quality Defects: A) Rounding B) Cracking C) Spalling D) Fracturing	95		95		95	
Slope Defects: A) Steepening B) Sliding			55		20	2

FOUNDATION FAULT SUSPECTED IN: A) Armor Displacement B) Slope Steepening C) Slope Sliding
 Caused By: (a) Scour (b) Settlement (c) Shear (d) Liquefaction
 Item (A) (B) (C) (D) (a) (b) (c) (d) Sta 22+40 to 23+40

WARNING SIGNS/GATES _____
 AUXILIARY STRUCTURES (walkways, stairs, navigation lights, etc.) _____
 AMOUNT OF DEBRIS IN ARMOR (rubble, trash, logs, etc.) _____

SUGGESTED ACTIONS: A) Immediate Action B) Action Soon C) Watch D) Defer E) Investigate Further

Comment Number	Suggested Action	Station Location(s)	COMMENTS AND SKETCHES
1	A		300 feet of reach has been breached to about MLLW.
2	A		Scour hole noted on last 2 annual surveys on channel side. Resurvey immediately.

SUGGESTED ACTIONS: A) Immediate Action B) Action Soon C) Watch D) Defer E) Investigate Further

Comment Number	Suggested Action	Station Location(s)	COMMENTS AND SKETCHES
2	A		(Continued) Waves presently steepening at previous scour location. That wing shift apparent.
3	A		Warning signs needed to alert public until reach is repaired.

Figure 2-13: Structural rating form for a rubble-mound jetty (Oliver et al., 1998).

2-3.3. Functional Condition Index

The functional design purpose of the structure is a crucial field of assessment when it comes to condition rating. Plotkin et al. (1991) based the functional rating of any structure based upon its intended primary and secondary purposes. In that study, a typical set of primary and secondary objectives were listed as shown in Table 2-7.

Table 2-7: Primary and secondary coastal project purposes (Plotkin et al., 1991).

Primary Purpose (Project Authorization)	Secondary Purpose (Supplementary benefits)
Small boat - recreational	Protection of land and facilities
Small boat – commercial	Public safety
Small boat – refuge	Navigation aid
Deep draft – commercial shipping	Public access: recreation
National defense - military	Fishing
	Commercial benefits

Plotkin et al. (1991) defined three distinct groups of functional evaluation categories that can be accommodated to suit various types of coastal structures. The first group includes the following categories:

1. Reduced wave protection within the harbor area;
2. Reduced wave protection at the entrance / channel;
3. Increased sediment management needs; and
4. Reduced navigational safety.

The second group of functional criteria comprises the following items:

1. Changed current velocities;
2. Damage to vessels or facilities; and
3. Risk to public safety / access.

Finally, the third group included the following assessment fields:

1. Environmental damage;
2. Adverse impacts on water level in the harbor / mooring area; and
3. Erosion or flooding of harbor shores.

Meanwhile, Oliver et al. (1998), using the same lines of Plotkin et al. (1991), developed functional rating criteria for breakwaters and jetties. Such criteria apply equally to rubble and non-rubble coastal structures, and include the following items:

1. Harbor area, including whether the structure is serving its purpose for harbor navigation and harbor use by vessels, and how well the harbor structures are protected.
2. Navigational channel, in case of jetties, including the impact of the jetty on the quality of navigation and on the channel itself.
3. Sediment management, including assessment of the structure's impact on the effect of ebb shoal, flood shoal (in case of jetty located at a river promontory) and harbor shoal.
4. Structure protection, which indicates the extent to which the head of the breakwater or jetty is protecting the rest of the structure such as the trunk, and the entire structure against toe erosion.
5. Other functions, including public access, recreational use, environmental effects, and aids to navigation.

Please refer to Oliver et al. (1998) and Pirie et al. (2005) for the condition rating numerical ranges for functional rating categories of rubble-mound and non-rubble structure, respectively. Oliver et al. (1998), for instance, developed the FI rating scale similar to the previously-discussed SI rating scale. As for the overall functional rating of the structure, while Plotkin et al. (1991) had developed the FI numerical rating scale shown in Table 2-8; they also listed the appropriate management decisions for each of the FI value ranges.

Table 2-8: Suggested intervention actions against FI ranges (Plotkin et al., 1991).

Impact Level	FI Range	Description
None	100	Action is not required, structure fully functional.
Minor	70--99	Immediate action not required. May have some minor impact on secondary function.
Moderate	40-69	Economic analysis of repair alternatives versus benefits is recommended to determine appropriate action. Only limited loss of primary function. Project still serviceable.
Major	0-39	Detailed engineering and economic analysis recommended determining the need for repair or rehabilitation. Primary function has been seriously impaired or completely lost. Public safety or economic justification at risk.

By the same token of Equations 2-1, 2-2, and 2-3 for the structural condition rating of coastal structures, Oliver et al. (1998) set Equations 2-4 and 2-5 for the functional rating of reaches and structures:

$$FI_R = R_L + 0.3 (R_H - R_L) [(R_2 / 100 + R_3 / 100 + R_4 / 100 + \dots) / N]$$

Equation 2-4: Reach functional index (Oliver et al., 1998).

Where:

- " FI_R " is the functional index for the reach;
- " R_L " is the lowest of the reach's functional ratings;
- " R_H " is the highest of the reach's functional ratings;
- " $R_2, R_3, R_4 \dots$ " are the values of the second, third, fourth functional ratings, and so on; with a maximum of 7; and
- " N " is the number of rated functions for the reach; with a maximum of 9.

$$FI = FI_{RL} + 0.3 (FI_{RH} - FI_{RL}) [(FI_{R2} / 100 + FI_{R3} / 100 + FI_{R4} / 100 + \dots) / N]$$

Equation 2-5: Functional index for the entire structure (Oliver et al., 1998).

Where:

- "FI" is the functional index for the structure;
- "FI_{RL}" is the lowest reach functional index;
- "FI_{RH}" is the highest reach functional index;
- "FI_{R2}, FI_{R3}, FI_{R4}..." are the values of the second, third, fourth reach functional indices, and so on; and
- "N" is the number of reaches in the structure.

Figure 2-14 provides an example of a filled functional inspection form for a rubble-mound jetty. As per the procedure set out in Oliver et al. (1998) and Pirie et al. (2005); a functional evaluation matrix is first developed, listing the various design features and purposes of the structures before proceeding to the actual inspection.

FUNCTIONAL RATING FOR BREAKWATERS AND JETTIES					
FUNCTION		RATING 0-100	COMMENT NUMBER	PROJECT	
HARBOR AREA	Harbor Navigation	20	8	Example Harbor	
	Harbor Use a. Moored Vessels b. Harbor Structures c. Other Facilities	30 35 35 35	30 9		South Jetty
	NAVIGATION CHANNEL	Entrance Use	100		REACH
		Channel	30	3, 10	3
SEDIMENT MANAGEMENT	Ebb shoal	85		RATER J. O.	
	Flood Shoal	—			
	Harbor Shoal	30			
STRUCTURE PROTECTION	Shoreline Impacts	75	6	DATE OF RATING 9/8/95	
	Nearby Structures	70	7		
	Toe Erosion	90			
OTHER FUNCTIONS	Trunk Protection	—		Has a structural inspection been recently completed? <input checked="" type="radio"/> YES <input type="radio"/> NO	
	Public Access		1		
	Recreational Use		2		
	Environmental Effects		None		
Are there functional deficiencies which are not related to structural defects?		<input checked="" type="radio"/> YES	<input type="radio"/> NO	4	
Is there risk of further loss of function within the next budget cycle?		<input checked="" type="radio"/> YES	<input type="radio"/> NO	5	
SUGGESTED ACTIONS: A) Immediate B) Soon C) Watch D) Defer E) Investigate Further					
COMMENT NO.	ACTION	COMMENTS AND SKETCHES			
1	A	Access to outer end of jetty (across this reach) is hazardous at all tide levels.			
2	A	Pedestrian access needs to be blocked and danger signs posted.			

FUNCTIONAL RATING FOR BREAKWATERS AND JETTIES (CONTINUED)		
SUGGESTED ACTIONS: A) Immediate B) Soon C) Watch D) Defer E) Investigate Further		
COMMENT NO.	ACTION	COMMENTS AND SKETCHES
3	A	Aids to navigation need to be shifted to identify channel location.
4	E	See project background information.
5	A	Deterioration in function expected to increase.
6	A	Assessment of design and impact of intermediate storm levels needed as structure may be lost if major breach recession occurs.
7	A	Rating based on low intensity storm experience. Further evaluation may indicate a lower rating.
8	A	Harbor navigation unsafe for small boats during low intensity storms.
9	A	Low intensity storms stop commercial activities and cause vessel and facility damage.
10	A	Thalweg migration causes channel shift.

Figure 2-14: Functional rating form for a jetty (Pirie et al., 2005).

The inspector needs to possess full awareness of all such aspects prior to conducting the visual inspection. An extensive functional evaluation matrix for

rubble-mound jetties and breakwaters is presented in Oliver et al. (1998), while a similar one for non-rubble structures is presented in Pirie et al. (2005).

2-4. Prediction of Deterioration and Damage Progression

2-4.1. Empirical Relationships based on Laboratory Testing

Extensive research has been carried out to study the damage occurrence probability and progression on breakwaters. The end objective was the attainment of a comprehensive risk analysis for breakwater maintenance and rehabilitation purposes. Various studies focused around estimating the probability of failure resulting from armor layer instability, based upon estimating the deterioration progression on armor stone, whether rock or concrete. Typical failure modes of rubble-mound breakwaters are presented in Bucharth (1991) and for earth dikes in Vrijling (2001), as shown in Figure 2-15.

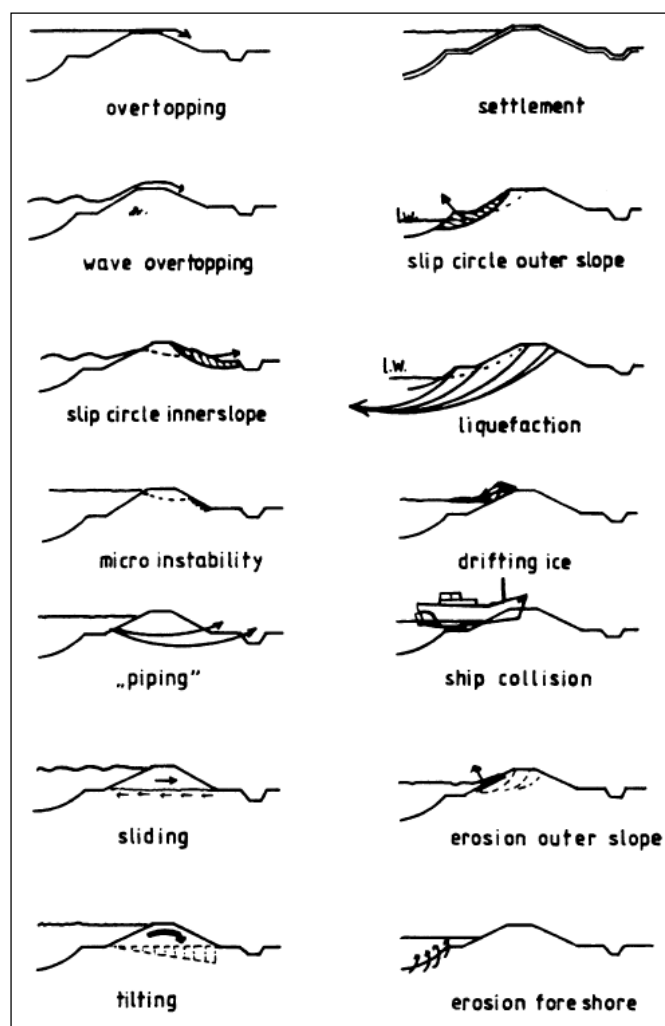


Figure 2-15: Failure modes for a rubble-mound earth dike (Vrijling, 2001).

Most of the studies tackling the damage progression from this particular angle assume that the seaside section of the breakwater exposed to constant wave loading

end up reaching an equilibrium profile, while other studies rather describe this assumed equilibrium as a mere reduction in the damage rate (Castillo et al. ,2012). Such studies were made by Bucharth (1984; 1994; 1997; 2000), Bucharth and Sorensen (1998), Castillo et al. (2004; 2006), and Minguez et al. (2006). The main approaches dealing with damage accumulation in breakwaters tackled either damage progression, armor stability, or both. Several studies featured the empirical modeling of armor stability under regular wave loading, while taking into account the effect of armor weight and shape, as well as the structure's slope angle, on the overall armor stability. This general concept was discussed by Iribarren (1938), Hudson (1958:1959), Ahrens and McCartney (1975), Thompson & Shuttler (1975), Losada & Gimenez-Curto (1982), Pilarczyk & Den Boer (1983), and also by Van der Meer (1988).

Nevertheless, Medina (1996) suggested a method for exponential modeling of damage progression on breakwaters under regular wave conditions. This work was further refined in Medina et al. (2003) to accommodate the effect of every individual incident wave. Other studies discussed the effect of irregular wave loading on breakwaters, and then to analyze the structure's stability. They featured experiments on test flumes under a given distribution of wave heights at certain sea states and storm durations. This particular approach was adopted by Medina & McDougal (1990), Vidal et al. (1991:1995:2003:2004:2006), and Jensen et al. (1996), as cited in Castillo et al. (2012).

Some other studies tackled damage progression modeling on various types of breakwaters through the exposure to irregular breaking and non-breaking waves and their associated wave periods, such as, for instance, Ahrens (1975), Ahrens & McCartney (1975), SPM (1984), and Carver & Wright (1991). While the SPM (1984) analyzed the damage progression for various types of armor layer rock gradations, Medina & McDougal (1990) studied the effect of the number of incident waves on damage progressions on breakwater test flumes. However, Pfeiffer (1991) compared all of the above models and concluded that none of them can be entrusted to predict extended long-term damage (Castillo, et al., 2012).

One of the few early published studies by Thompson & Shuttler (1975) envisaged the issue from that dimension, by exposing riprap armor prototypes placed

on impermeable core to short-term storm damage as well as to long-term degradation. The main outcomes of the study were of paramount importance, where the damage extent was found proportional to the significant wave height. The study also observed that erosion rates tend to decrease with respect to time until attaining an equilibrium state (Castillo, et al., 2012). Nevertheless, it was observed that the chronological progression of damage is highly influenced by the method of placing the armor stones. While all of the above-mentioned studies provide useful tools for predicting short-term damage under stormy conditions, they are hardly applicable in accurately estimating the damage progression process over the lifetime of the structure, due to the involvement of a complexity of uncertainties (Castillo, et al., 2012).

Several other studies focused on exploring the initiation of damage in rubble-mound breakwaters. Font (1968) observed the direct effect of the armor laying method on the timing of damage initiation; however, the model did not offer any applicability in predicting the future damage of an already-damaged structure. Furthermore, Torum et al. (1979) and Davies et al. (1994) observed the relation between the remaining depth along the armor layer profile, and the long-term capacity of the armor layer to endure further wave attack. In doing, so the eroded depth perpendicular to the structure's slope provides an indication of the extent to which the structure is progressing towards failure, defined as the exposure of the under-layer stone (Castillo, et al., 2012). Experiments on breakwater stability under irregular wave attack were conducted on test flumes by Carver & Wright (1991) in an attempt to explore the initial damage initiation in case of different armor stone placement methods and various wave periods.

A further approach for estimating damage progression for rubble-mound coastal structures is presented in Van der Meer (1988), which envisions the damage analysis in light of damage profile statistics (Castillo, et al., 2012). Experiments were carried out on prototypes in order to determine the mean damage and its timely progression. The damage parameter S developed by Broderick (1983), which is a dimensionless factor that is function of the eroded area and the size of the armor stone. In his experiments, Van der Meer (1988) analyzed the mean and standard deviations for the damage parameter S , along with the armor layer cover depth and the eroded depth. The results were then compared to normal distributions, and the main outcome was that higher damage degrees could be predicted with less error.

Based upon these results, Van der Meer (1988) developed empirical formulas predicting damage progression in breakwaters under depth-limited wave condition. Variables were the stability number N_s for armor stone, mean wave period T_m , and duration of the test t . Other factors contributed to the damage progression patterns, including the side slope angle α , the armor stone characteristics such as porosity, method of placement, shape and gradation, (Castillo, et al., 2012). Furthermore, a statistical approach for modeling damage progression on rubble-mound breakwaters is presented in Melby & Kobayashi (1998) and Melby (1999), and was further extended by Castillo et al. (2012). Kamali & Hashim (2009) present a summarized schematic comparison between the three major philosophies of damage evaluation adopted in all of the previous research, as shown in Figure 2-16. In the figure, part (a) shows the intact structure profile; part (b) shows the damaged profile using the armor stone counting method; and part (c) shows the damaged profile using the eroded area (A_e) and eroded depth method.

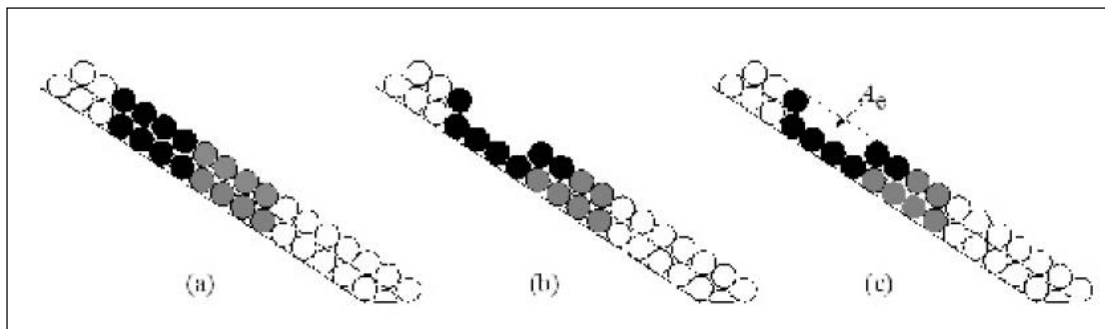


Figure 2-16: Various methods of damage evaluation (Kamali & Hashim, 2009).

As many as 20 different empirical relationships were developed between 1933 and 1988 for predicting the stability of armor layer in rubble-mound breakwaters (Kamali & Hashim, 2009). However, Kamali & Hashim (2009) note that while the empirical formulae for armor stability prediction may provide an indication of the damage extent of structures, they are based in their essence on experiments conducted in laboratory small-scale test flumes, and are hence prone to inaccuracies due to the scale effect. While this makes such formulae of particular usefulness during the design stage, their uncertainty should well be considered in the form of model testing prior to construction (Kamali & Hashim, 2009).

2-4.2. New Trends in Deterioration Modeling for Coastal Structures

2-4.2.1. Artificial Intelligence Deterioration Modeling

Few studies tackled the issue of damage modeling with regard to coastal protection structures, from an Artificial Intelligence (AI) approach. Mase et al. (1995) conducted one of these earliest attempts, and analyzed the stability of rock armor in rubble-mound breakwaters using artificial neural networks (ANN's) and compared their findings with experimental results, revealing close trends. However, this attempt did not address the damage progression patterns against time for these types of structures. Moreover, Medina et al. (2003) presented two methods to estimate the rubble-mound breakwater armor damage evolution in non-Rayleigh sea states. The first method is based on the exponential model on individual waves proposed by Medina (1996), while the second method is based on ANN's combined with evolutionary algorithms. While both methods gave reasonably good agreement with laboratory observations, more work was still suggested for Rayleigh sea states and for other types of coastal protection structures.

A study by Yagci et al. (2005) featured the estimation of breakwater slope damage ratios using three different ANN models and a fuzzy logic model. The main finding in their study is that the more data is trained regarding slope attributes and environmental data, the more ANN's are accurate in matching experimental results. Nevertheless, the fuzzy logic model produced close results to the ANN's, due to its execution that closely mimics environmental conditions, suggesting the potential usefulness of AI to successfully model the breakwater damage ratio especially when conducting an adequate number of experiment is not an available option (Yagci et al., 2005).

An alternative method for modeling the deterioration of coastal structures was performed using ANN's by El Hakea et al. (2014). Information relating to the design and environmental data structural reaches were extracted from an inventory database and utilized for training and testing. The structure of the ANN model consisted of an input, a hidden, and an output layer. The number of training entries for the model comprised 162 cases divided onto structural reaches. Entry fields included: (1) type of structure and its design concept; (2) age of structure; (3) water depth at toe; (4) significant wave height (5) type and weight of seaside armor stone; (6) type and weight of core or under-layer stone; (7) type of crest or cap; (8) position of the reach

whether head, trunk, or root; (9) reach length; (10) seaside slope; (11) leeside armor stone type and weight; (12) seabed type; (13) toe material; and (14) measured SI's as of the date of last inspection. 80% of entries were for training of the model while 20% were for testing. This ANN featured a single-point inspection, and was designed to model the past deterioration between the date of construction of the structure, and the date of the single-point condition rating, where the SI value is known. The error margin was 12% for training and 6% for testing. The hidden layer in that ANN module contained 13 hidden neurons, and the objective function was to match the SI values, as per the results of the single-inspection point. The ANN then determined the SI at any given year during the forecast period. One of the limitations of the model was its large dependence on condition rating procedures, which, although performed according to a structured methodology, are still largely dependent on the experience of the condition rater and the accuracy of records and observations, which could be significantly more accurate with the inclusion of modern inspection technologies along with visual inspection and historical satellite imaging. Furthermore, while the developed model did not deal with major storm events as single events, it distributes their effect equally on the structural deterioration forecast time interval; which represents an indicative long-term decision-support tool for coastal structure IAM.

2-4.2.2. Markov-Chain (MC)-based Deterioration Modeling

Yokota & Komure (2003) applied the Markov-Chain (MC) deterioration modeling concept on various deterioration build-up methods corresponding to several individual components of coastal structures in Japan. The concept presented in their studies assumes four distinct grades of structural deterioration. El Hakea et al. (2014) however, as show in Figure 2-17, suggested seven deterioration grades, all while using the same analogy provided in Yokota & Komure (2003).

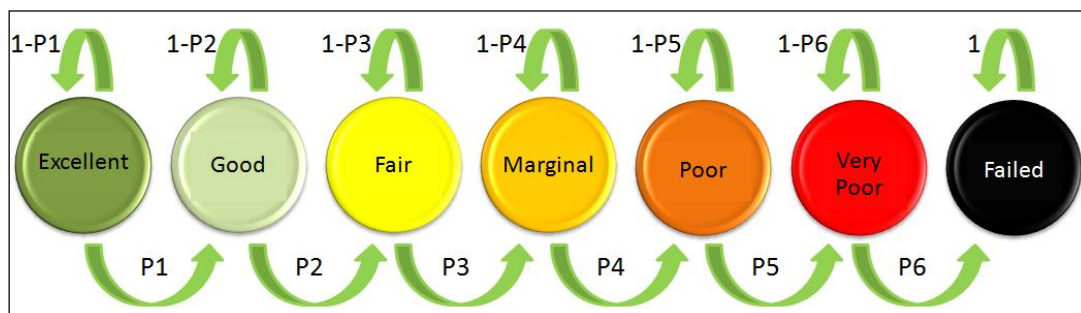


Figure 2-17: MC-based transition probabilities for structural deterioration.

Furthermore, while the transition probabilities between all consecutive deterioration grades is assumed constant in Yokota & Komure (2003), El Hakea et al. (2014) used the same equation but featured six different transition probabilities to represent the transition between each deterioration stage and its successor, as shown in Equation 2-6, assuming a No-Action policy, which was developed to obtain the transition probabilities between structural conditions, which was modified by El Hakea et al. (2014) based upon Yokota & Komure (2003).

$$\begin{pmatrix} \% \textit{Excellent} \\ \% \textit{Good} \\ \% \textit{Fair} \\ \% \textit{Marginal} \\ \% \textit{Poor} \\ \% \textit{Very Poor} \\ \% \textit{Failed} \end{pmatrix} = \begin{pmatrix} 1-P1 & 0 & 0 & 0 & 0 & 0 & 0 \\ P1 & 1-P2 & 0 & 0 & 0 & 0 & 0 \\ 0 & P2 & 1-P3 & 0 & 0 & 0 & 0 \\ 0 & 0 & P3 & 1-P4 & 0 & 0 & 0 \\ 0 & 0 & 0 & P4 & 1-P5 & 0 & 0 \\ 0 & 0 & 0 & 0 & P5 & 1-P6 & 0 \\ 0 & 0 & 0 & 0 & 0 & P6 & 1 \end{pmatrix}^t \begin{pmatrix} 1 \\ 0 \\ 0 \\ 0 \\ 0 \\ 0 \\ 0 \end{pmatrix}$$

Equation 2-6: Backward MC formulation (El Hakea et al., 2014).

Where:

- “% *Excellent*” through “% *Failed*” are the percentage of the structure’s length corresponding to the excellent condition and so on;
- “*P1*” through “*P6*” are the transition probabilities between each two consecutive deterioration grades, respectively; and
- “*t*” is the deterioration forecast period in years.

Thus, substituting (*t*) with the number of years between the construction or the latest maintenance date of the structure, and its current condition rating date, then solving for the transition probabilities between successive deterioration ranges; *P1* to *P6*, yields the characteristic 1-year Deterioration Transition Matrix (DTM) for the structure. Using this equation, El Hakea et al. (2014) used a backward-MC analysis of the past deterioration which led to the current condition state of the structure, represented in the form of a seven-cell matrix, then used the calculated probabilities to project the future condition state at any given year. Using Microsoft Excel

Evolver™ application, exact values of transition probabilities were calculated with a 2% total error (El Hakea et al., 2014).

2-4.2.3. Deterministic AI-based Modeling versus Stochastic MC-based Modeling

Furthermore, El Hakea et al. (2014) compared the stochastic MC deterioration model with the deterministic ANN model. The ANN was the same module described in Section 2-4.2.1 of this Chapter. The results showed close deterioration patterns produced by both ANN's and MC's, with an error margin in estimating the actual SI at the year of the single-point inspection ranging between 5% and 12% for a group of 17 coastal structures in Alexandria, Egypt. An example of one of such structures is shown in Figure 2-18, for the Eastern Harbor Middle Breakwater in Alexandria, Egypt, where MC and ANN deterioration modeling was performed between 1986 (Age = 0) and 2050. It was observed that the MC-based deterioration modeling was more accurate in simulating the deterioration of structures between their year of construction and year 2013 with a 2% error as opposed to 12% for the ANN (El Hakea et al., 2014).

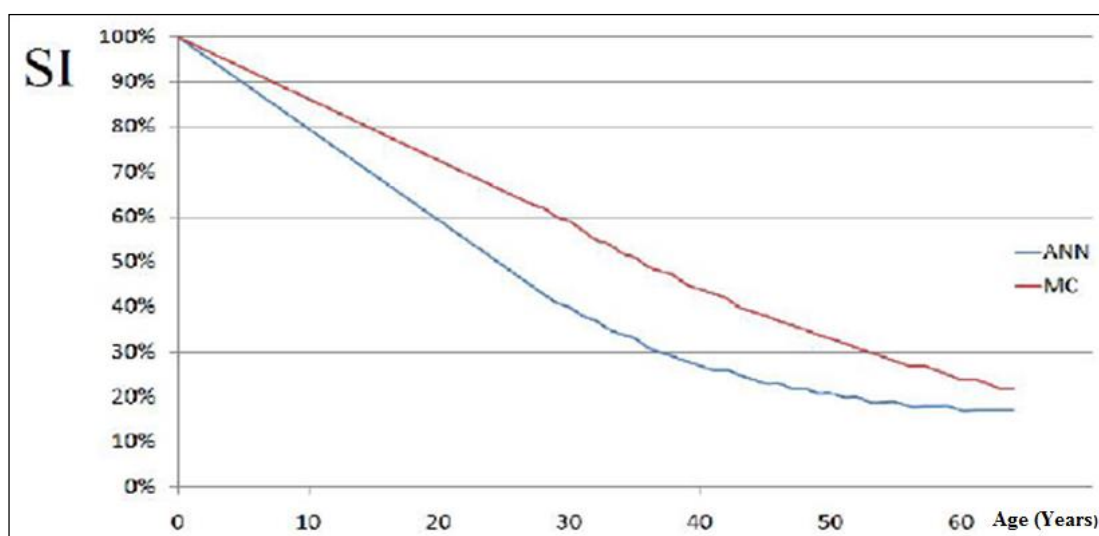


Figure 2-18: Eastern Harbor Middle Breakwater deterioration (El Hakea et al., 2014).

2-5. Maintenance and Repair Methods and Equipment for Coastal Structures

2-5.1. General Overview

Discussing repair methods and equipment for coastal protection structures can best be started by an overview of the general construction practices in this field.

However, this discussion needs to be related to the general aspects governing coastal construction in the city of Alexandria, and in the study area in particular. In general, several interviews were conducted by the author with construction and technical managers of three different coastal engineering firms in Alexandria. Additional interviews were also conducted by the author with experts in the subject matter. From the interviews, attention is to be made to the various site considerations in terms of space requirements, temporary facilities, as well as electricity and water sources. The nature and accessibility of the structure being repaired pretty much dictate the construction method and equipment used for the repair job. When the structure is parallel to the shore such as in the case of revetments and seawalls, land-based construction is preferred over water-borne construction, given the limited water depth at the toe of these structures which hinders the use of floating derricks and marine barges. Waterborne operations are generally more costly than land-based construction considering structures that are detached or close to the shore. In some structure such as semi-detached shore-perpendicular breakwaters and groins, combining both land-based and waterborne construction techniques and equipment might be necessary to achieve the optimum time schedule and cost. Waterborne operations are also best suited in harbor basins where there is enough room to accommodate the draft of loaded barges and tugboats.

For rubble-mound structures, there is a general consensus among experts that maintenance works include the addition of supplementary armor units or rock in lieu of the displaced or lost units, periodically. Repair is often associated with the extension of the seaside toe of the structure and the creation of a new armor layer on top of the degraded initial armor layer, which shall be deemed to act as a core or under-layer after the addition of the new repair section. As for non-rubble structures, namely concrete seawalls and quaywalls, if we were to consider the study area, they could be either locally repaired or completely modified to incorporate new rubble-mound slopes. The main aspects governing coastal construction and maintenance operations could be summarized as follows:

1. Site considerations (wave climate, geotechnical aspects, wind, bathymetry, space requirements, temporary facilities, storage areas).
2. Number of days per year where works can take place (In Alexandria the calm sea state is around 75 days per year in winter season, such that while

seasonal storms occur in winter, it is preferable to conduct coastal construction works in winter to avoid any interference with the summer tourism season, and given that the calm sea state in winter is more convenient for construction than the calm sea state in summer).

3. Optimization of the use of land-based and waterborne construction equipment depending upon the project needs.
4. Optimal choice of on-site or off-site cast yard for precast concrete armor units, and associated delivery and lifting equipment.
5. Choice of core and under-layer stone type (dolomite or basalt in the case of Alexandria).
6. Choice of armor stone aggregate type (dolomite or gravel).
7. Choice of cement type and content in the mix design of concrete armor units.
8. Choice of characteristics weights for core, under-layer and armor stone.

Due coordination is the responsibility of the contractor for all matters pertaining to site organization, access and egress arrangements, logistics, working hours, material deliveries, and required permits. Legal and governmental stakeholders in the study area include for instance the SPA, CoRI, Alexandria Governorate, the Egyptian Naval Forces (Coast Guards), and the SCA with regards to the eastern harbor archeological sites and sunken monuments.

2-5.2. Common Construction and Repair Methods

2-5.2.1. Land-Based Construction

Land-based construction is most commonly used for shore-connected rubble-mound breakwaters and groins. The construction starts by tipping and spreading the core stone from the root section moving towards the trunk then the head, all while paying respect to the design seaside and leeside slopes. Figure 2-19 illustrates the various typical stages of land-based construction of a rubble-mound breakwater.

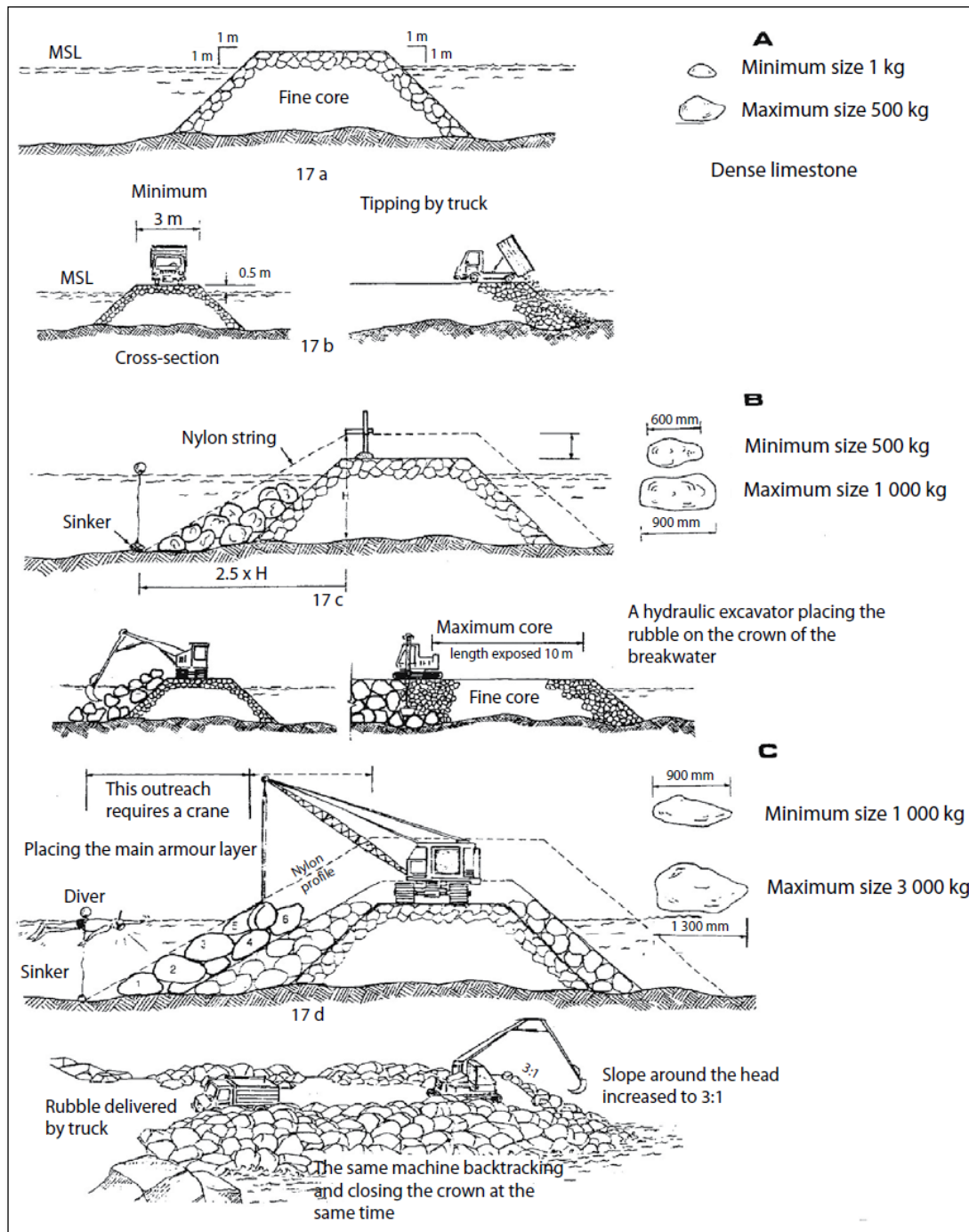


Figure 2-19: Land-based construction schematic (Breakwaters, 2000).

Adjustment of slopes above-water is conducted using timber stakes and nylon stings, while in the below-water section the slopes are adjusted using the extension of the nylon string such that its below-water end is attached to the seafloor using a sinker, whose location is marked by a buoy. A diver typically watches the slope alignment of stones as they are being dropped in place. The design needs to account for the space requirements needed to allow for a smooth equipment access and egress, by providing the optimum crest width, as shown in Figure 2-20, where the

crest should allow for smooth traffic of adjacent combinations of excavators, trucks, and cranes.

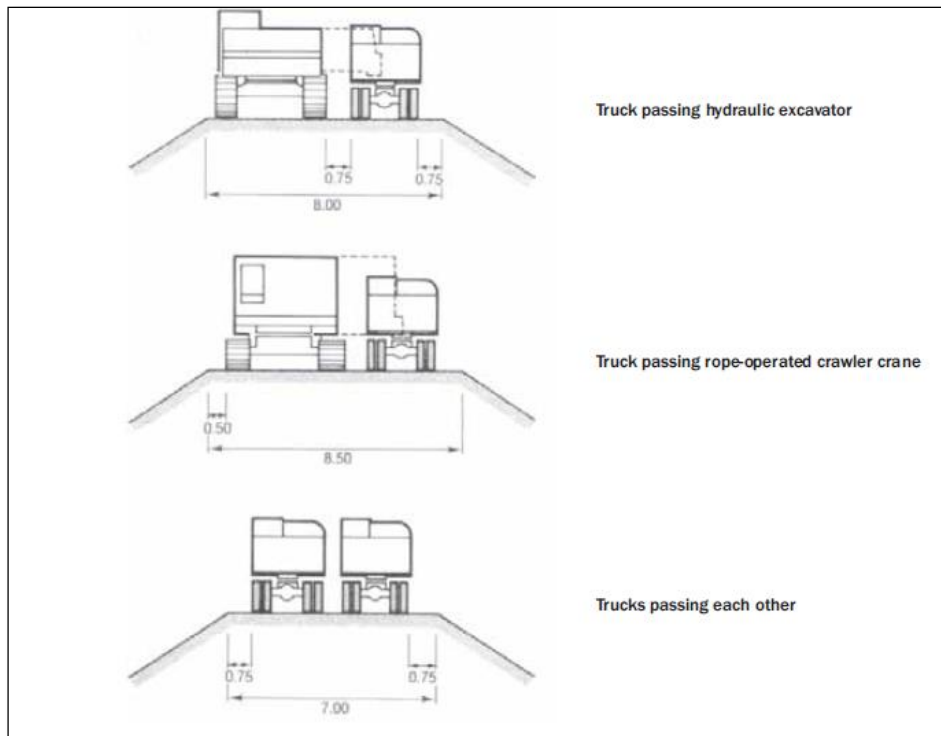


Figure 2-20: Space requirements for construction equipment (CIRIA, 2007).

For low-crest and submerged breakwater construction works, land-based construction could be applied in the same way as in elevated structures. However, upon the completion of the core and under-layer stone slopes, the excavator starts lowering the structure below water level systematically starting from the head section and moving in the direction of the trunk and the root. As soon as any particular section has been completed, the crawler crane or the floating derrick mounted on the pontoon or barge starts lowering the armor layer in place. Nevertheless, CIRIA (2007) explains the typical sequence of construction for a rubble-mound shore-parallel revetment, starting by dredging of the seafloor, stockpiling of sand material or core stone, spreading of sand and core stone then trimming of slope, placement of geotextile from a waterborne vessel-mounted drum, followed by under-layer and armor stone installation.

Selecting the appropriate excavator size and reach is also the task of the construction manager, based upon the project constraints and requirements. In addition, CRIAI (2007) provides the guidelines for the sizes of excavators required to

place average mass ranges of armor stone, and the maximum excavator reaches for given loads and sizes. Wire-rope crawler cranes are typically used for coastal engineering jobs. Choosing of cranes depends primarily on the access availability, and the maximum required safe working loads, taking into account that the construction manager may benefit from buoyancy to increase the reach of the crane beyond the normal safe working load reach; this is explained in detail in CIRIA (2007).

2-5.2.2. Waterborne Construction

According to the expert interviews, waterborne construction is typically best-suited for detached coastal protection structures. Construction managers usually resort to waterborne equipment whenever the cost of the works governed by such equipment types is more effective than in the case of constructing a temporary rubble road connecting the shore to the structure's location. In other cases where portions of a certain structure, had it even been a shore-connected or semi-detached structure, lie in an area where water depth and wave conditions are considerably severe to allow for land-based operations, construction managers may also resort to waterborne construction methods and equipment. Table 2-9 displays various types of waterborne construction vessels and equipments, categorized by size and significant wave height (H_s) limitations on their use.

Choosing the most suitable vessel for waterborne construction is not an easy task, and is not only governed by the wave climate and corresponding vessel attributes limitations; but also the availability of the required vessel types and cost constraints. The site considerations must also allow for a temporary loading quay and quarry run coffer dam to provide a safe loading, unloading and mooring harbor for the floating equipment and their tugboats. It is to be noted that for floating equipment, especially barges, the size of the vessel dictates what type and size of auxiliary equipment that is to be used. The size of such auxiliary equipment and machinery depends primarily on space availability of the barge deck and on the vessel's strength. Table 2-10 provides examples of typically used combinations of barges and common construction equipment, according to CIRIA (2007).

Table 2-9: Limiting wave conditions for waterborne equipment (CIRIA, 2007).

Type of vessel	Size	Auxiliary Equipment Type and Size	H_s limit for dumping	H_s limit for placing
Large crane barge	60 x 20 m	150 crane	0.80 m	0.60 m
Small crane barge	40 x 15 m	75 t crane	0.65 m	0.50 m
Large excavator on barge	35 x 12 m	70 t excavator	0.65 m	0.50 m
Side stone dumper	650 t		1.25 m	1.00 m
Side stone dumper	1400 t		1.50 m	1.25 m
Split hopper	800 t		1.50 m	N/A
Split hopper	2000 t		2.00 m	N/A
Flat-top barge and wheel loader	2000 t		0.80 m	N/A
Fall-pipe barge	50 x 17.5 m		N/A	0.65 m
Fall-pipe vessel	10 000 t		N/A	3.50 m

Table 2-10: Combinations of waterborne equipment sizes (CIRIA, 2007).

Vessel type and size	Auxiliary equipment type and size
1800 t flat-top barge	30 t wheel loader and 25 t articulated dump trucks
3000 t flat-top barge	30 t wheel loader and 30 t off-highway dump trucks
4500 t flat-top barge	30 t or 50 t wheel loader and 35 t off-highway dump trucks
9000 t flat-top barge	40 t or 50 t wheel loader and 50 t off-highway dump trucks
18000 t flat-top barge	40 t or 60 t wheel loader and 80 t off-highway dump trucks

The seafloor at the temporary harbor should be continuously dredged using wire-rope crane and clamshell. The cost of tugboats differs between downtime and work time depending on the sea state. Inside the temporary harbor small-size vessels are used to pull the barges, while in open sea, large-size tugboats must be used. A key aspect governing loading and unloading of vessels such as barges and pontoons is tidal considerations, however, this is not really applicable to the study area. Loading and unloading of core, under-layer, and armor stone on vessels may be performed using various conveying and lifting equipment and accessories.

2-5.2.3. Combined Land-Based and Waterborne Construction

Figure 2-21 provides a real-life example on the use of land-based and waterborne construction. The photo was taken during the construction of the San Stefano and the 26th of July Club breakwaters in Alexandria, Egypt, 2011. In most situations, optimizing the utilization of both land-based and waterborne methods and their corresponding equipment is key towards achieving the near optimum cost and time schedule in not only marine construction, but also in maintenance and repair jobs. CIRIA (2007) includes a general comparison between land-based and waterborne construction. The comparison criteria include the concept behind determining the structure's cross-sectional dimensions and length, logistics, relation with seabed morphology, limiting factors, environmental constraints, damage to the structure whilst execution takes place.



Figure 2-21: Combining land-based and waterborne equipment (Courtesy of AF Co.).

2-5.3. Integrated Inventory, Condition Rating, Maintenance and Repair Models

2-5.3.1. Repair, Evaluation, Maintenance, and Rehabilitation (REMR) Management and Breakwater™ Software

Since the beginnings of the 1990's, the US Army Corps of Engineers has launched the REMR program with the aim to establish an integrated life-cycle management of all coastal protection and navigation infrastructure across the country. The efforts produced in this specific field of study by Plotkin et al. (1991), Oliver et al. (1997:1998), Aguirre & Plotkin (1998), Hughes (2003), and Pirie et al. (2005) were in fact part of the REMR scheme. The REMR management framework according to Oliver et al. (1998) starts by condition inspection and rating, then logging of the inspection data onto the asset inventory database computerized system, analysis of maintenance and repair alternatives and associated LCC, and finally the production of condition reports, budget reports, and maintenance and repair records. While the works published by Plotkin et al. (1991), Oliver et al. (1997:1998), Hughes (2003); and Pirie et al. (2005) are all dealing with inventory management and condition rating procedures and forms; Aguirre & Plotkin (1998) stand out in the way they introduced the first computer program intended to facilitate the process of life-cycle management of coastal and navigational infrastructure. Envisaging the same process flowchart of the REMR scheme, Aguirre & Plotkin (1998) discussed the concept of the Breakwater™ software, a simple DOS-based program whose main objectives are listed as follows:

1. Establishing an asset inventory database for breakwaters and jetties;
2. Collection of structural and functional inspection data and condition assessment and rating, performed in accordance with the REMR procedures;
3. Calculation of SI, FI, and CI values in accordance with the REMR scheme, as outlined in Equations 2-1, 2-2, 2-3, 2-4, and 2-5; and
4. Produce a group of reports comprising inventory, inspection, and condition indices data.

An "Inventory Summary" is produced by the program, comprising a comprehensive list of all structures and their SI, FI, and CI values, in addition to their chronological inspection data. The software further produces a condition index computation sheet for every inspected reach, a district inventory summary report, and

a historical record of all inspections carried out for all structures within the same zone. Examples such reports are provided in Figure 2-22.

HISTORICAL PROGRESSION OF PROJECT STRUCTURES			
Date: 20 December 1996	Database: NPI	District 1	Page: 1
PROJECT: BAWL HARBOR			
Location: Bawl Harbor			
Structure Historical Index Rating Summary			
Structure	Inspection Start Date	Structural Index	Functional Index
E.BREAKWATER	05/21/1990	49	83
	05/16/1990	49	67
NORTH JETTY	05/18/1990	48	49
S.BREAKWATER	05/16/1990	78	80
SOUTH JETTY	05/17/1990	65	69

Figure 2-22: Breakwater™ software SI and FI report (Aguirre & Plotkin, 1998).

The maintenance policies to be followed during the typical lifetime of any particular structure should be envisioned in light of the level of damage attained by the structure. Against every established warning and action threshold, the maintenance policy should have in place all corresponding measures to be taken. For instance, CIRIA (1991), Oliver et al. (1998), Vrijling (2001), and Ngyuen et al. (2010) all discussed the various inspection, maintenance, and LCC optimization methods for coastal structures. The main methodology in all of these studies is to establish a curve that tracks the change in the structure's CI with respect to time, in its both actual and estimated patterns, as a first step. Figure 2-23 provides an example of these types of CI versus time plots, showing the actual and estimated CI values, and the improvement of the CI resulting from the implementation of two different maintenance policies. CI is shown in its both actual and estimated values, and the enhancement of the CI resulting from the implementation of two various maintenance policies is also shown in the figure.

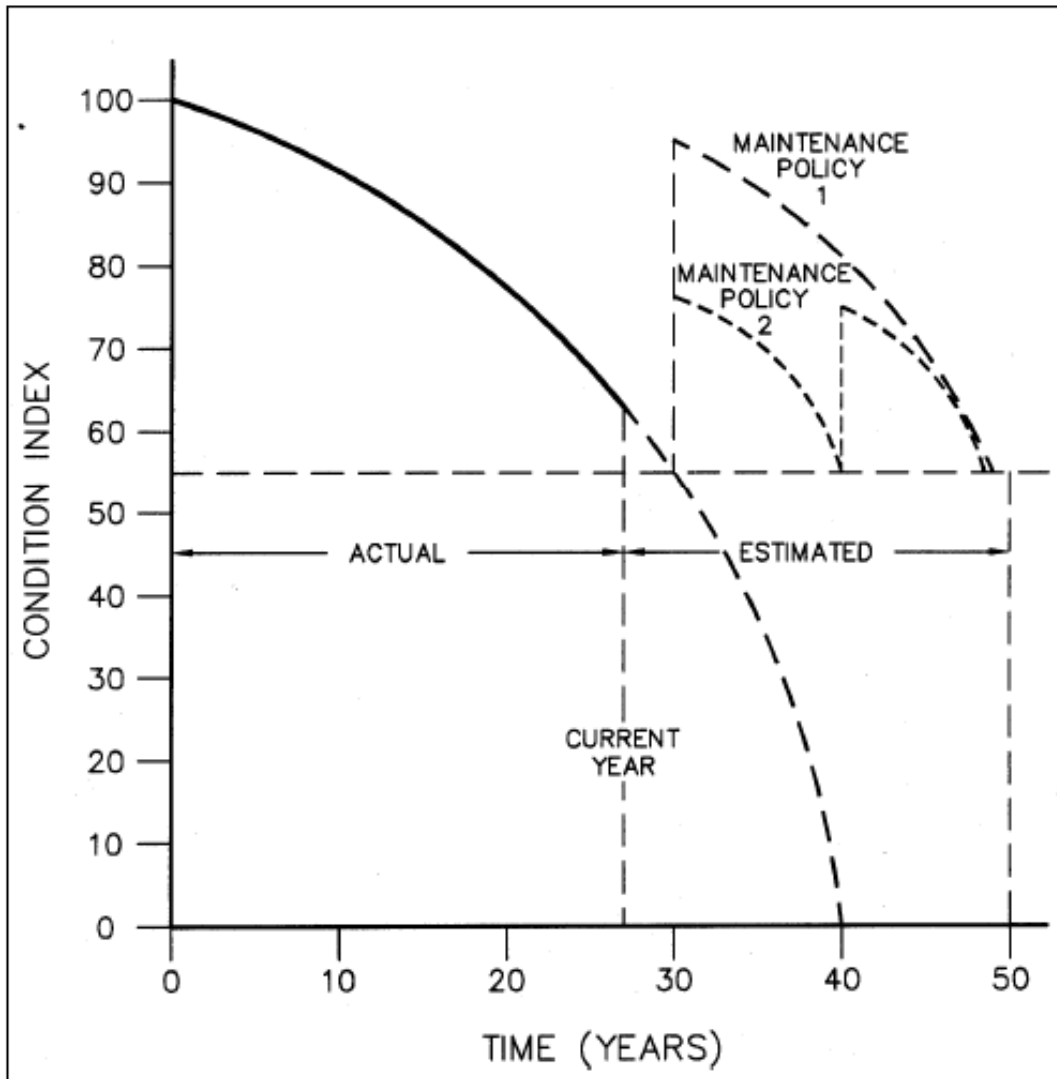


Figure 2-23: CI of a rubble-mound breakwater against time (Oliver, et al., 1998).

2-5.3.2. Coastal Structure Condition Assessment and Standardized Reporting Application (CoSCA™)

As part of the efforts made to improve the REMR management systems, the US Army Corps of Engineers launched the *eCoastal* program, which is a professional training and education scheme for port and navigation operation divisions, branches, and areas personnel, and also for engineering and structural divisions' personnel. The targeted levels of personnel include technical, engineering, and managerial levels. Under the *eCoastal* program, the new CoSCA™ software has been developed, building upon the Breakwater™ software. CoSCA™ is designed to comprise integrated data from various sources regarding inventory, inspection, and condition rating of coastal structures, also using standard inspection and condition assessment forms and procedures. The addition it brings is the use of high-tech surveying equipment to

record, store, monitor, and update the structural coordinates of coastal structures. This enables the use of 3D wire-frame data modeling to compute changes in volume that any structure may exhibit during its lifetime. This reduces by far the subjectivity of condition assessment and rating. The program also feature GIS-based asset inventory (US Army Corps of Engineers, 2008). Figure 2-24 shows the user interface of the CosCA™ software during the inspection data logging; for the selecting the structure and its reach, then describing the defect, respectively. The figure shows selecting and logging of observations for structural rating and associated defects. Figure 2-25 display the 3D representation of the surveying stations, which constitute the data points used to monitor the timely change in the structure's alignment and volume. The figure shows the head on the left and the trunk on the right, and the toe underneath. The schematic displays the various survey lines and stations used for monitoring of the structure during its lifetime.

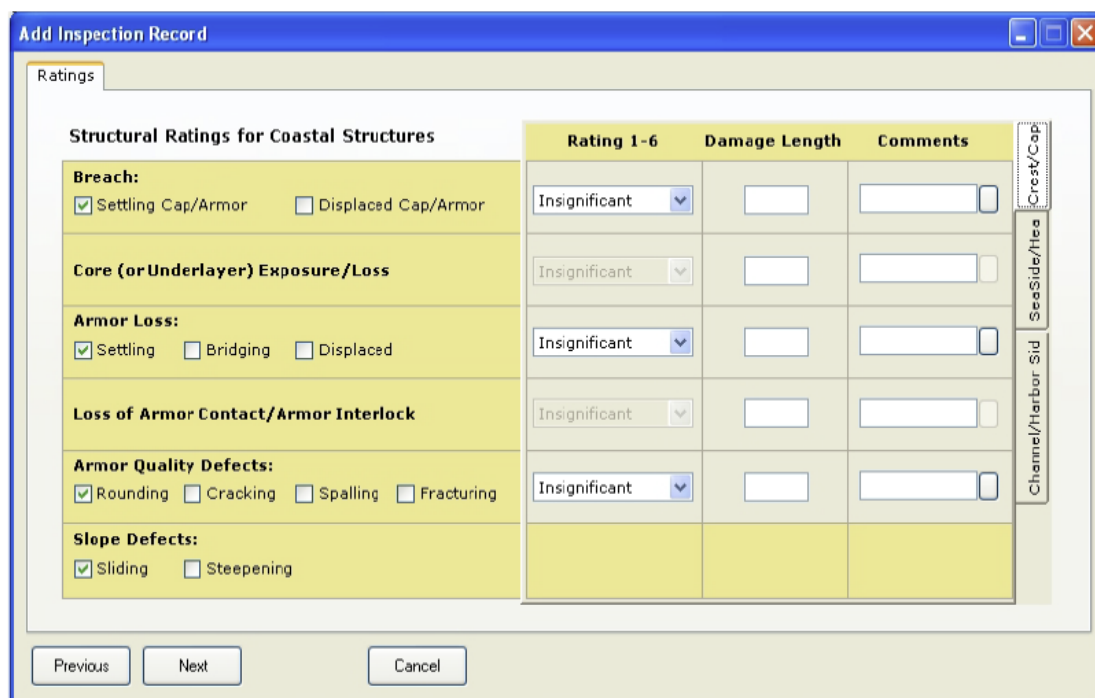


Figure 2-24: CoSCA™ software screenshot (US Army Corps of Engineers, 2008).

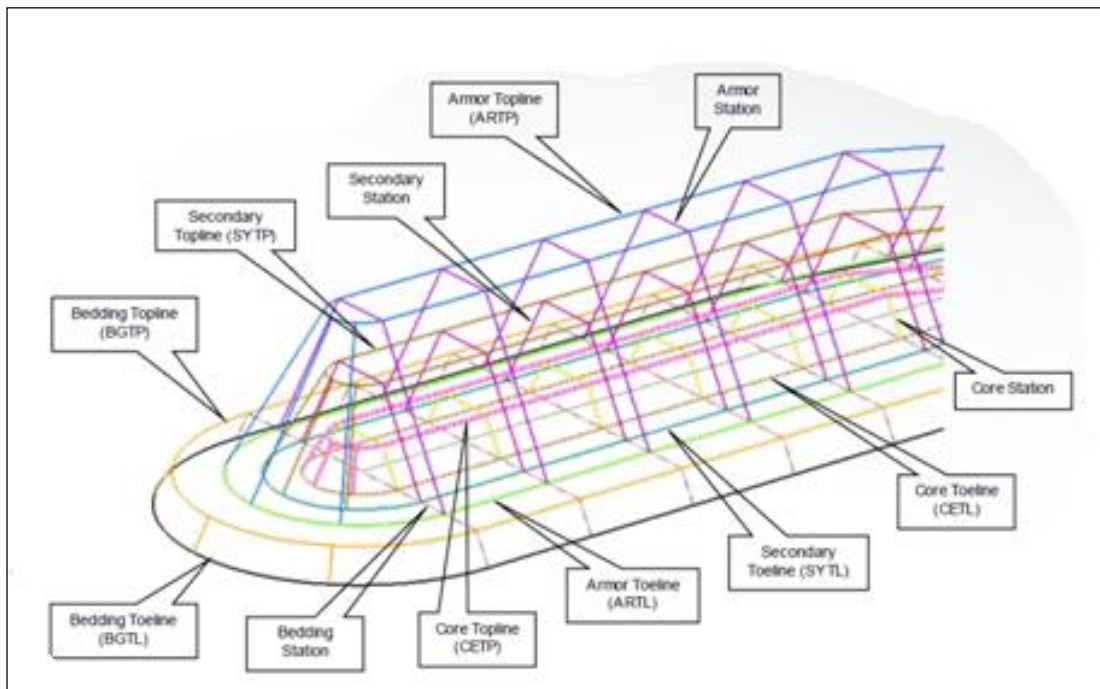


Figure 2-25: CoSCA™ 3D representation (US Army Corps of Engineers, 2008).

Based upon the structural deformation and the associated repair and maintenance policies, the CosCA™ software enables the computation of the cost of repair works based on the overall condition, both for each defected element of the structure and for the structure in its entirety. Given the flexibility of adaptation and response to environmental conditions enjoyed by rubble-mound structures, the CosCA™ scheme depends on a series of surveying prisms mounted on equidistant arrays along the profile of the structure. Such survey points are periodically monitored for X, Y, and Z coordinates using theodolite devices for the above-water parts, and using special submarine surveying equipment for the below-water parts. Upon the compilation of the results of a new survey, the software computes the change that occurred in the dimension of the cross-section. In the event where the amount of displacement and settlement exceed the design limit state, the software computes the cost of reinstating the structural profile to be minimally safe once again. This process benefits from a cost database including predefined bills of quantities for dredging, laying of geotextile filter layer, placing of toe stone, placing of core stone, placing of filter layer, trimming of slopes, and placing and readjustment of armor stones. This database provides for both land-based and water-borne construction operations.

2-5.3.3. Reliability-Based LCC Management of Coastal Infrastructure

Reliability-based maintenance and LCC optimization for coastal structures has been discussed in various sources. Most recent of such efforts were published by Vrijling (2001), Sorensen & Burcharth (2004) and by Nguyen et al. (2010). While Vrijling (2001) introduced the combination of the expected deterioration patterns of rubble-mound structures and the preset thresholds of monitoring, warning, and action, in order to come up with the optimum LCC, Sorensen & Burcharth (2004) introduced the concept of limit states. They suggested three levels of limit states; the Serviceability Limit State (SLS), the Reliability Limit State (RLS), and the Ultimate Limit State (ULS). The SLS is set at 50 years, which constitute the service lifetime of the structure, while the RLS is attained when the structure ceases to perform its intended design function. Moreover, the ULS is reached when the structure fails from a structural perspective. The model includes the design storm return period (T) as a factor that causes single-point deterioration increase to the structure at the year of their occurrence (Sorensen & Burcharth, 2004). Several cases of coastal structures within a Danish harbor were stochastically modelled using this concept with the aim of reaching both the near optimum reliability level and the near optimum total LCC. The main limitation of the model developed by Sorensen & Burcharth (2004) is that it does not consider damage accumulation over time. This is illustrated in further detail in Figure 2-26. The figure shows near-optimal total LCC in a 50-year lifetime for structures with various armor stone weights with no damage accumulation being considered, in case of no harbor downtime cost (left), and with the inclusion of harbor downtime cost (right). The three curves correspond to different interest rates, and present the set of near-optimum solutions.

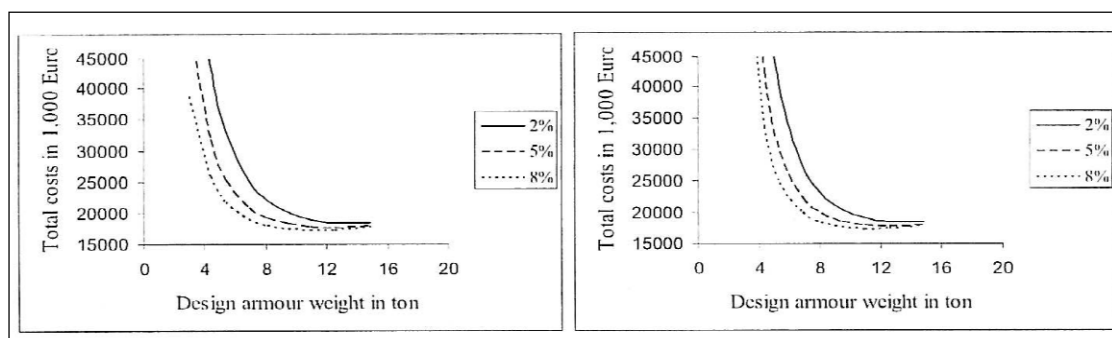


Figure 2-26: Optimizing of armor LCC and weight (Sorensen & Burcharth, 2004).

Later studies by Nguyen et al. (2010) expanded on the limit state reliability-based concept in LCC optimization. Reference is made here to the ULS and SLS, based upon the earlier study made by Sorensen & Burcharth (2004). This concept is further demonstrated using Figure 2-27, which shows the time on the X axis and the structure's both strength and loading of the Y axis. As the cumulative loading increases due to single events such as major storms, and generally due to conventional wave action, the strength of the structure decreases in a certain pattern with time. The figure illustrates the chronological progression of damage and shows the warning and action thresholds triggering the suitable types of intervention. Δt is the time interval between inspections and/or interventions.

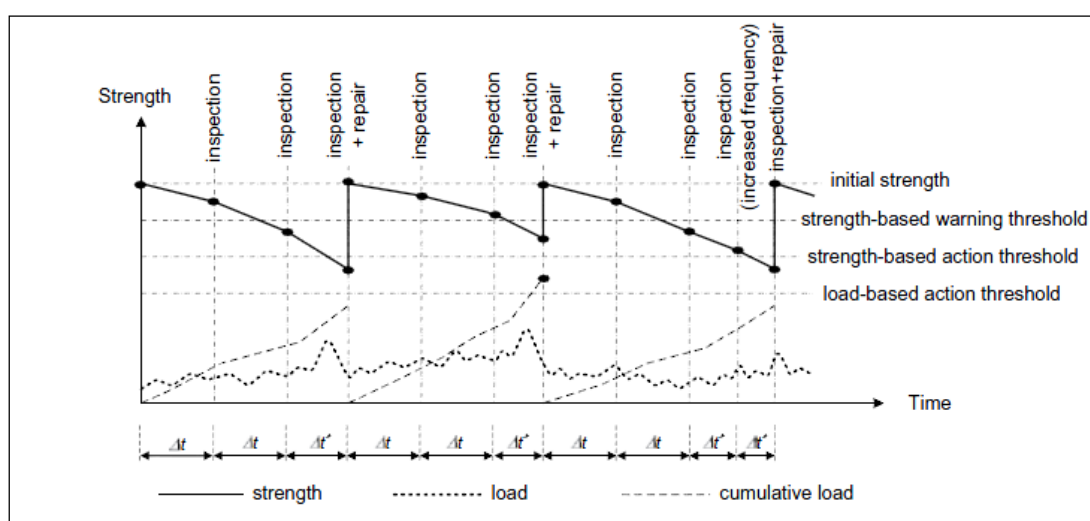


Figure 2-27: Maintenance strategy for a rubble-mound structure (Nguyen et al., 2010).

Established warning thresholds indicate the strength at which warning is to be initiated and the strength at which action is to be taken in the form of inspection, maintenance, or repair. This deals with the fault-based maintenance. The cumulative loading also triggers another load-based action threshold, which initiates the load-based maintenance. In other situation, when the structure's use changes according to the design needs, a use-dependent maintenance may be required. In addition, time-dependent maintenance takes place at fixed time intervals during the structure's lifetime regardless of any other circumstances.

CHAPTER III – RESEARCH METHODOLOGY FRAMEWORK

3-1. Introduction

This chapter highlights the research methodology adopted for this thesis. It commences by addressing the scope and objectives of this research, and then continues with a detailed description of the adopted methodology, prior to discussing the need to establish a CI system for condition rating, which is subsequently used to formulate a MC Deterioration Module, which is then translated into mathematical best-fit regression formulae, on which GA-based optimization for LCC and risk exposure is then applied. This Chapter then discusses in detail each of the steps constituting the LCC and risk optimization framework for coastal structures.

3-2. Methodology Development

Figure 3-1 outlines the stages of the methodology development of this thesis.



Figure 3-1: Research general outline.

This thesis work started by data collection with regard to design and environmental attributes of coastal structures in the study zone. This data was verified through field visits carried out by the author, and through interviews with contracting companies, governmental institutions, private owners, and design offices that are or were involved in marine projects. After the stage of data acquisition, comes the stage of formulating the AID, prior to conducting a visual inspection and condition assessment of all structures using established condition assessment and rating criteria and guidelines. The results of such field work were then verified through expert consultation, and an analysis was performed from a zone perspective as well as in view of the structure categories. Furthermore, the results of this single inspection point were traced back to the initial condition of each structure at the year of construction or the last major rehabilitation, using the backward MC Module. The DTM obtained from the Backward MC Module were then utilized to project future deterioration up to year 2050, while including the single-event impact of intermediate and design storms. The latter forward MC deterioration trends were then expressed in terms of mathematical functions peculiar to each individual structure, using best-fit regression. The following step was establishing a series of CI thresholds triggering their corresponding intervention policies, and taking into account the unit cost of each of such observe and monitor, maintenance, repair, and replacement policies; the end product is there: the LCC Optimization Module. The construction of such module necessitated another wave of data collection, but this time concerning the cost of maintenance and repair policies associated with each structure within the study area. As for the Risk Optimization Module, data collection was primarily guided towards obtaining numerical factors representing the consequence of failure of each structure within the study area through expert opinion and literature review of high-risk areas. Figure 3-1 describes the general work methodology development outline.

3-3. Methodology Framework Outline

The research framework consists of the following module components: (1) Asset Inventory Database (AID); (2) Inspection and Condition Rating Module; (3) Backward MC Deterioration Module; (3) Forward MC Deterioration Module including expressing deterioration patterns using best-fit regression; (4) LCC Optimization Module; and (5) Risk Optimization Module.

In this chapter, each of these six module components shall be separately discussed in detail, through a presentation of the gathered information used to build each of these models and databases, followed by a discussion of the database and model structures, prior to proceeding to a general discussion and analysis of the main outcomes and findings of running the LCC Optimization model for the coastal assets within the study area. Figure 3-2 displays the framework of this research and its various stages.

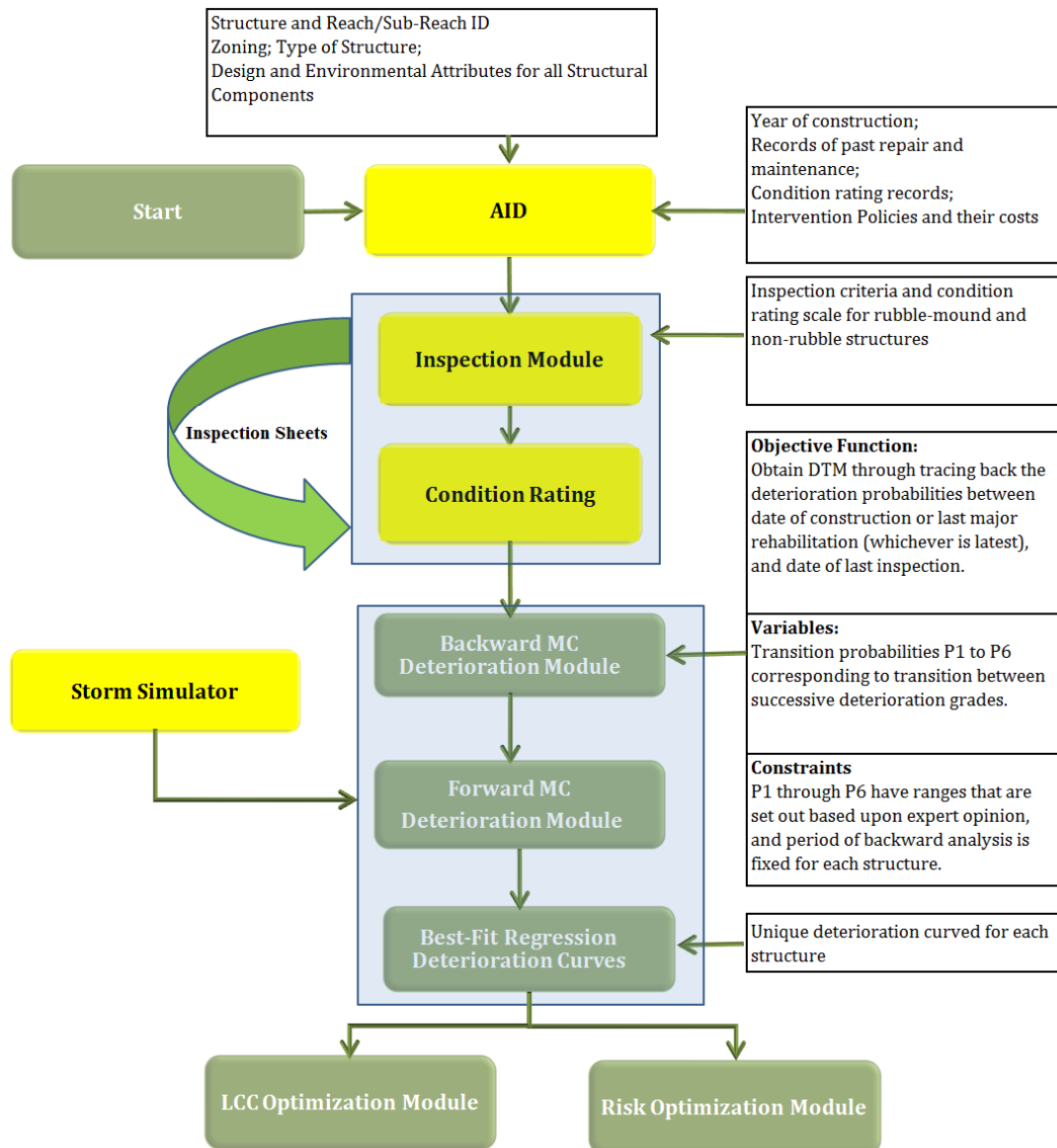


Figure 3-2: Outline of the research methodology framework.

3-4. Asset Inventory Database (AID)

3-4.1. Purpose

The first step in constructing the LCC optimization model consists of establishing an AID encompassing all of the existing coastal assets in the region or area under concern. In addition to design and environmental attributes of all reaches belonging to all structures, the AID also includes information regarding the date of construction, costs of the works, duration of the work, main parties involved, and records of previous maintenance, repair, and rehabilitation.

3-4.2. Zoning and Nomenclature of Assets

The asset ID's for this research are designed on a reach/sub-reach level. The ID refers to all of the following:

1. Asset zone;
2. Asset sub-zone;
3. Asset structure type;
4. Structure's serial number within the sub-zone;
5. Reach number; and
6. Sub-reach number.

A summary of the AID categorized by zones and sub-zones is presented in Appendix 2, entitled, "AID Summary". An example of asset ID naming rationale is also given in Figure 3-3.

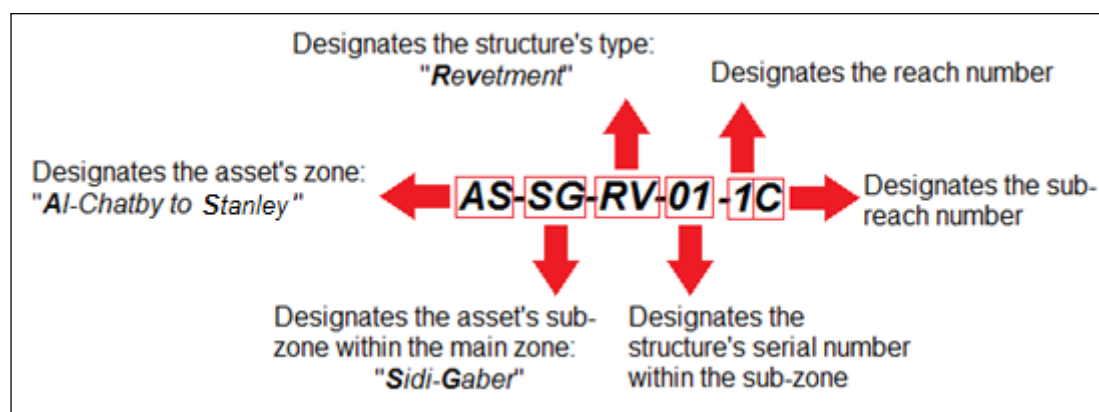


Figure 3-3: ID number configuration for a typical sub-reach.

3-4.3. Logging of Design, Historical, and Environmental Attributes

In this section, extracts of the AID master spreadsheet are presented. Table 3-1 provides an extract of the AID for area typical rubble-mound breakwater. It shows the division of the breakwater into reaches, and the basis on which such reaches are set out. Under the general information on the structure, the year of construction as well as that of the last major repair or maintenance is included. The type of structure is referred to using a two-letter abbreviation code that is explained as follows:

- *RV* stands for "*Revetment*";
- *GR* stands for "*Groin*";
- *BW* stands for "*Breakwater*";
- *SW* stands for "*Seawall*";
- *QW* stands for "*Quaywall*"; and
- *PR* stands for "*Pier*".

Stations and reaches for a typical breakwater were determined using field survey, design drawings, and Google Earth measurement option. This is shown in Figure 3-4 for the Pharos promenade breakwater. The division of structures into reaches following this arrangement, as explained also in Chapter II, is a standard practice in this research. The design concept also features the same coding scheme, and is explained as follows:

- *RM* stands for "*Rubble-Mound*";
- *RR* stands for "*Rip-rap*";
- *PC* stands for "*Plain Concrete*";
- *RC* stands for "*Reinforced Concrete*";
- *SP* stands for "*Sheet Pile*"; and
- *CO* stands for "*Composite*".

The relationship of the structure with the SWL is denoted as follows:

- *EL* stands for "*Elevated*";
- *SM* stands for "*Submerged*"; and
- *LC* stands for "*Low-Crest*".

Table 3-1: Structure general data as logged in the AID.

Reach / Sub-Reach	Stations		Basis of Reach Division	General Information						Structure Dimensions			
	From	To		Year of Construction	Last Major Repair / Maintenance / Rehab	Type of structure (RV/GR/BW/SW/QW/PR)	Design Concept (RM/RR/PC/RC/SP/CO)	Relation to SWL (EL/SB/LC)	Protection Type (P/S)	Length (m)	Max Width (m)	Min Width (m)	Max Height above SWL (m)
Reach 1	+00.00	+75.00	Root and Inshore Trunk	2011	-	BW	RM	EL	P	75.00	48.00	48.00	5.00
Reach 2	+75.00	+115.00	Offshore Trunk	2011	-	BW	RM	EL	P	40.00	48.00	48.00	5.00
Reach 3	+115.00	+190.00	Head	2011	-	BW	RM	EL	P	75.00	66.00	66.00	5.00

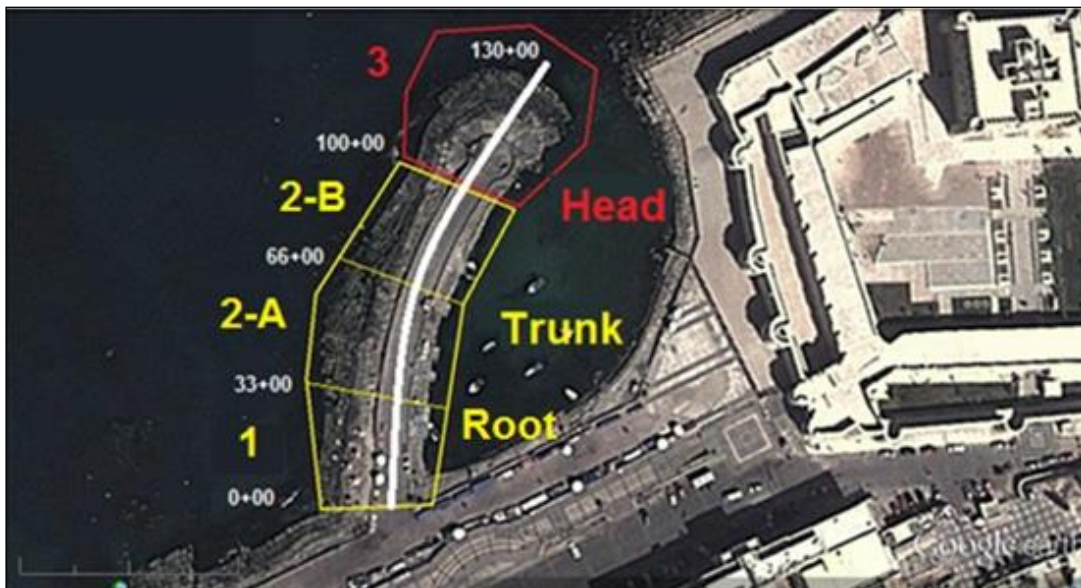


Figure 3-4: Subdivision of the Pharos Promenade breakwater (El Hakea et al., 2014).

The protection provided by the structure is either Primary "P" or Secondary "C". Primary protection is where the structure encounters open sea, whereas secondary protection is where the structure is located at the leeside of another coastal protection structure; such as in the case of all structures inside the Eastern Harbor basin, located at the lee of the Eastern Harbor breakwaters. Nevertheless, the cross-sectional dimensions of every reach and its height above SWL are also included.

Moreover, the AID includes the design data pertaining to the core stone and under-layer as shown in Table 3-2. The abbreviation coding in the table is deciphered as follows:

- *BA* stands for "*Basalt*";
- *DO* stands for "*Dolomite*";
- *CO* stands for "*Concrete*"; and
- *GR* stands for "*Gravel*".

Tables 3-3 and 3-4 provide the data included under the seaside and leeside armor stone, and the slope attributes, respectively; for the 26th of July Club Breakwater. Armor stone types are denoted by the following coding:

- *AN* stands for "*Antifer*";
- *AP* stands for "*Accropode*";
- *BA* stands for "*Basalt*";
- *CU* stands for "*Cubes*";
- *DO* stands for "*Dolomite*";
- *MC* stands for "*Modified Cubes*"; and
- *TP* stands for "*Tetrapod*".

Table 3-2: Core stone and filter layer attributes for a typical breakwater.

Reach / Sub-Reach	Stations		Basis of Reach Division	Core Stone			Seaside Filter / Under-layer			Leeside Filter/ Under-layer		
	From	To		Type (BA/DO/CO)	Min Weight (ton)	Max Weight (ton)	Type (DO/GR)	Min Weight (ton)	Max Weight (ton)	Type (DO/GR)	Min Weight (ton)	Max Weight (ton)
Reach 1	+00.00	+75.00	Root and Inshore Trunk	DO	0.01	0.30	DO	0.50	1.50	DO	0.50	1.50
Reach 2	+75.00	+115.00	Offshore Trunk	DO	0.01	0.30	DO	0.50	1.50	DO	0.50	1.50
Reach 3	+115.00	+190.00	Head	DO	0.01	0.30	DO	0.50	1.50	-	-	-

Table 3-3: Armor stone attributes for a typical breakwater.

Reach / Sub-Reach	Stations		Basis of Reach Division	Seaside Armor Stone					Leeside Armor Stone						
	From	To		Predominant Type (AN/AP/BA/CU/DO/MC/TP)	Weight (ton)	Concrete Aggregate (GR/DO)	% New	% Reused	Nominal Diameter (m)	Predominant Type (AN/AP/BA/CU/DO/MC/TP)	Weight (ton)	Concrete Aggregate (GR/DO)	% Leeside Armor (New)	% Leeside Armor (Reused)	Nominal Diameter (m)
Reach 1	+00.00	+75.00	Root and Inshore Trunk	CU	10.00	DO	100%	0%	1.73	DO	0.5-1.5	DO	100%	0%	2.00
Reach 2	+75.00	+115.00	Offshore Trunk	CU	10.00	DO	100%	0%	1.73	DO	0.5-1.5	DO	100%	0%	2.00
Reach 3	+115.00	+190.00	Head	CU	10.00	DO	100%	0%	1.73	-	-	-	-	-	-

Table 3-4: Armor stone attributes for a typical breakwater.

Reach / Sub-Reach	Stations		Basis of Reach Division	Slope and Toe Attributes								
	From	To		Seaside Slope (H:V)	Leeside Slope (H:V)	Geotextile Fabric	Seaside Toe Material	Min Weight (Ton)	Max Weight (ton)	Leeside Toe Material	Min Weight (Ton)	Max Weight (ton)
Reach 1	+00.00	+75.00	Root and Inshore Trunk	1:1.5	1:1.5	Y	DO	0.01	0.30	DO	0.01	0.30
Reach 2	+75.00	+115.00	Offshore Trunk	1:1.5	1:1.5	Y	DO	0.01	0.30	DO	0.01	0.30
Reach 3	+115.00	+190.00	Head	1:2	-	-	DO	0.01	0.30	-	-	-

The various attributes included in the AID for the crest, as well as the hydraulic, bathymetric, and armor stability attributes for the reaches of the 26th of July Club Breakwater; are listed in Table 3-5. The seabed type is either rock “*RK*” or sand “*SN*”. In shallow water, H_s is taken as 78% of SWL at the toe of each reach, as per the provisions of the US Army Corps of Engineers Shore Protection Manual (1984). This process has been followed through the entire the AID for all rubble-mound structures, in a spreadsheet format. The armor stone shape coefficient “ K_D ” values for each type of armor units is taken as recommended by SPM (1984), in this case, it is recommended to be 6 for armor cubes at breakwater trunks, and 5 for armor cubes at head reaches.

Table 3-5: Design and environmental attributes for a typical breakwater in year 2013.

Reach / Sub-Reach	Stations		Basis of Reach Division	Crest Attributes					Hydraulic Attributes, Bathymetry, and Stability				
	From	To		Crest Type	Crest Length (m)	Max Crest Width (m)	Min Crest Width (m)	Parapet Type	Seaside Max Water Depth (m)	Seaside Cotan Alpha	Seaside Armor K_b	Hs Max (Seaside)	Seabed Type (RK/SN)
Reach 1	+00.00	+75.00	Root and Inshore Trunk	PC Slab	48.00	6.00	6.00	PC	2.45	1.5	6	1.91	RK
Reach 2	+75.00	+115.00	Offshore Trunk	PC Slab	48.00	25.00	25.00	PC	2.90	1.5	6	2.26	RK
Reach 3	+115.00	+190.00	Head	PC Slab	66.00	11.00	11.00	PC	3.65	2	5	2.85	RK

3-5. Visual Inspection and Condition Assessment

3-5.1. Structural Condition Assessment

3-5.1.1. Rubble-Mound Structures

Condition rating is first conducted for structural features of each reach. The rating is estimated by the inspector based on a preset 0 to 100 deterioration severity scale corresponding to various sets of observations indicating the extent of structural distresses, all in line with the REMR procedures. Various distress types for cross-section components of the reach are rated, such that separate indices are obtained for the Crest/Cap (*CR*), the Seaside/Head (*SE*), and the Channel/Harbor Side (*CH*). Typical categories of rating include breach, core and under-layer exposure, armor loss, loss of armor contact and interlock, armor quality, and slope defects, as previously discussed in this research.

Calculation of structural indices for component indices, reaches or sub-reaches, and entire structures are based upon the equations provided in Plotkin et al. (1991), Oliver et al. (1998), Hughes (2003) and Pirie et al. (2005). The structural Cross-Section Component Indices, whether (*CR*, *SE*, or *CH*) for rubble-mound structures or their equivalent indices for composite and non-rubble structures are developed using Equation 2-1, by Plotkin et al. (1991), Oliver et al. (1998), Hughes (2003) and Pirie et al. (2005). The combination of all Cross-Section Component Indices for a single reach or sub-reach is then performed to calculate the Reach/Sub-reach Structural Index. Equation 2-2 denotes the structural index for a single reach or

sub-reach, and is used in the Inspection and Condition Rating Module. The overall SI for a single coastal structure is calculated then using Equation 2-3.

The same concept of Equations 2-1, 2-2, and 2-3 applies for both rubble-mound and non-rubble structures alike (Pirie et al., 2005). Table 3-6 shows the various rating fields under each of the three structural components: (1) Crest / Cap; (2) Seaside / Head; and (3) Channel / Harbor / Leaside. The structural component indices for each reach are listed under CR, SE, and CH for the three previous component indices in the same order. Having inspected each individual reach while using the forms in Appendix 3, all the data stemming from such inspection sheets are logged in the way showed in Table 3-6.

Table 3-6: CI_C values for reaches of the Glim Bay East Groin in year 2013.

Reach / Sub-Reach	Stations		Basis of Reach Division	Crest / Cap			Seaside / Head					Channel / Harbor / Leaside						
	From	To		Breach	Core Exposure	CR	Core Exposure	Armor Loss	Loss of Armor Contact and Interlock	Armor Quality Defects	Slope Defects	SE	Core Exposure	Armor Loss	Loss of Armor Contact and Interlock	Armor Quality Defects	Slope Defects	CH
1	+00.00	+60.00	Inshore Root	95	95	95	95	60	60	54	60	61	95	60	60	54	60	61
2-A	+60.00	+120.00	Offshore Trunk	95	95	95	95	58	58	54	58	61	95	90	90	90	90	91
2-B	+120.00	+210.00	Offshore Trunk	95	95	95	95	60	60	54	60	61	95	60	60	54	60	61
2-C	+210.00	+290.00	Offshore Trunk	95	95	95	95	77	77	60	69	68	95	90	65	55	65	64
3	+290.00	+320.00	Head	80	90	80	84	74	70	65	72	69	NA	NA	NA	NA	NA	NA

The spreadsheet calculates the component indices, the sub-reach/reach indices, before ending with the overall SI for the entire structure, as shown in Table 3-7, which is an extract of the Inspection and Condition Rating Module, showing sample SI's for each individual sub-reach, then for each reach, prior to ending with the SI for the structure, expressed in both numerical and alphabetical terms. Data correspond to the Glim Bay East Groin located in Alexandria, Egypt, in year 2013. In the table, the SI values were calculated using Equation 2-3, following the REMR scheme condition rating process.

Table 3-7: Extract of the Inspection and Condition Rating Module.

Sub-Reach	Stations		Basis of Reach Division	SI				
	From	To		Sub-Reach	Description	Reach	Structure	Description
1	+00.00	+60.00	Inshore Root	71	GOOD	71	72	GOOD
2-A	+60.00	+120.00	Offshore Trunk	71	GOOD	71		
2-B	+120.00	+210.00	Offshore Trunk	71	GOOD			
2-C	+210.00	+290.00	Offshore Trunk	73	GOOD			
3	+290.00	+320.00	Head	72	GOOD	72		

3-5.1.2. Non-Rubble and Composite Structures

A clear example on non-rubble and composite structures can be found in the old Eastern Harbor Seawall, located between Al-Raml Station and Al-Silsila Cape, and extending over a length of 1.65 km. The structure was built in 1934 along with the construction of the Alexandria Cornice Road, with the last major rehabilitation taking place in 1986, as documented in Tetra Tech (1986), with the addition of concrete cube armor units at the toe of the structure, with weights ranging between 10 and 30 tons. Concrete seawalls are considered as non-rubble structures; however, the addition of armor units, an inherent feature of rubble-mound structures, puts the structure into the composite category. For the non-rubble part, Table 3-8 shows the various component indices corresponding to the reaches of the seawalls along with their SI values.

Table 3-9 displays the inclusion of the rubble-mound aspect, namely the seaside armor, into the condition rating of the same old Eastern Harbor Seawall. Thus, the component indices are determined for each sub-reach, followed by the overall SI's for the entire reach of the seawall, which in this particular case corresponds to the structure's SI.

Table 3-8: Cl_c values for the Eastern Harbor Seawall in year 2013.

Sub-Reach	Stations		Basis of Reach Division	Superstructure				Substructure				Foundation				Structural Features						
	From	To		Elevation / Alignment	Structural Damage	Material Deterioration	SPI	Elevation / Alignment	Structural Damage	Material Deterioration	Fill	SBI	Structural Damage	Material Deterioration	Scour / Wave Protection	Foundation Support	FDI	Parapet	Cap / Crest	Concrete Walls	Others	SFI
1-A	+00.00	+150.00	Length	95	95	54	58	90	69	54	NA	56	NA	NA	80	NA	80	65	80	65	NA	66
1-B	+ 150.00	+300.00	Length	95	95	54	58	70	45	50	NA	46	NA	NA	80	NA	80	64	80	64	NA	65
1-C	+ 300.00	+450.00	Length	95	95	54	58	69	40	45	NA	41	NA	NA	80	NA	80	65	80	65	NA	66
1-D	+450.00	+600.00	Length	95	95	54	58	54	40	40	NA	41	NA	NA	75	NA	75	60	74	60	NA	61
1-E	+600.00	+750.00	Length	95	95	60	63	45	40	35	NA	35	NA	NA	65	NA	65	54	69	54	NA	55
1-F	+750.00	+900.00	Length	95	95	45	50	90	69	35	NA	39	NA	NA	65	NA	65	60	20	60	NA	22
1-G	+900.00	+1,050.00	Length	95	95	45	50	95	74	40	NA	44	NA	NA	70	NA	70	63	60	63	NA	60
1-H	+1,050.00	+1,200.00	Length	95	95	45	50	95	74	54	NA	57	NA	NA	80	NA	80	65	64	65	NA	64
1-I	+1,200.00	+1,350.00	Length	95	95	54	58	74	60	54	NA	55	NA	NA	85	NA	85	64	69	64	NA	64
1-J	+1,350.00	+1,500.00	Length	95	95	60	63	90	69	54	NA	56	NA	NA	85	NA	85	69	74	69	NA	69
1-K	+1,500.00	+1,650.00	Length	95	95	60	63	95	74	54	NA	57	NA	NA	90	NA	90	70	90	70	NA	71

Table 3-9: Seaside armor structural ratings for the Eastern Harbor Seawall in year 2013.

Sub-Reach	Stations		Basis of Reach Division	Seaside Armor							SI			
	From	To		Core Exposure	Armor Loss	Loss of Armor Contact and Interlock	Armor Quality Defects	Slope Defects	SE	Sub-Reach	Description	Reach	Structure	Description
1-A	+00.00	+150.00	Length	NA	50	50	54	NA	50	59	FAIR	39	39	POOR
1-B	+ 150.00	+300.00	Length	NA	50	55	54	NA	50	56	FAIR			
1-C	+ 300.00	+450.00	Length	NA	48	50	54	NA	48	53	MARGINAL			
1-D	+450.00	+600.00	Length	NA	45	54	50	NA	45	51	MARGINAL			
1-E	+600.00	+750.00	Length	NA	40	45	45	NA	40	44	MARGINAL			
1-F	+750.00	+900.00	Length	NA	30	20	45	NA	21	34	POOR			
1-G	+900.00	+1,050.00	Length	NA	45	40	45	NA	40	49	MARGINAL			
1-H	+1,050.00	+1,200.00	Length	NA	60	54	50	NA	51	59	FAIR			
1-I	+1,200.00	+1,350.00	Length	NA	69	54	54	NA	55	64	FAIR			
1-J	+1,350.00	+1,500.00	Length	NA	65	54	54	NA	55	64	FAIR			
1-K	+1,500.00	+1,650.00	Length	NA	65	60	54	NA	55	66	FAIR			

Equally to the inspection procedures for rubble-mound structures, the REMR procedures explained in Oliver et al. (1998) are used for condition inspection and rating for non-rubble and composite structures. The rubble-mound features of composite structures are dealt with under the procedures outlined in Chapter II. The structural rating guidelines for non-rubble structures are provided in Pirie et al. (2005).

3-5.2. Functional Condition Assessment

3-5.2.1. General Procedures and Guidelines

The guidelines for functional condition assessment for coastal structures are provided in Oliver et al. (1998) and Pirie et al. (2005) for rubble-mound and non-rubble structures, respectively. Table 3-10 provides an example of functional condition rating for the Glim Bay East Groin. However, for the purpose of the LCC model, and as it was impractical to conduct structural condition rating for submerged structures within the study area, the FI values for these types of structures is considered as equivalent to the SI values.

Table 3-10: FI values for Glim Bay East Groin in year 2013.

Sub-Reach	Stations		Basis of Reach Division	Harbor / Beach Area		Navigation Channel		Sediment Management		Structure Protection			FI			
	From	To		Harbor Navigation	Harbor / Beach Use	Entrance Use	Channel	Harbor / Beach Shoal	Shoreline Impact	Nearby Structures	Toe Erosion	Trunk Protection	Sub-Reach	Description	Reach	Structure
1	+00.00	+60.00	Inshore Root	80	80	NA	NA	85	60	85	75	NA	64	FAIR	64	64
2-A	+60.00	+120.00	Offshore Trunk	80	80	NA	NA	85	60	85	85	NA	64	FAIR	64	
2-B	+120.00	210.00	Offshore Trunk	80	80	NA	NA	85	60	85	85	NA	64	FAIR		
2-C	+210.00	+290.00	Offshore Trunk	80	80	NA	NA	85	60	85	75	NA	64	FAIR		
3	+290.00	+320.00	Head	80	80	NA	NA	85	60	85	80	80	64	FAIR	64	

Selected photographs documenting observations recorded during the functional inspection of various types of structures are shown in Figure 3-5. The figure is the courtesy of the author, and the legend is explained as follows: (a) Waste accumulated on top of the Glim Bay West Groin crest; (b) waves breaking on the Glim Bay East

Groin; (c) Seawater flooding a pedestrian tunnel at the lee of Al-Chatby Revetment; and (d) Waves breaking on the submerged Miami Breakwater creating safe haven for beach users and protecting the beach from erosion.



Figure 3-5: Functional inspection by the author in Alexandria, Egypt, 2013.

3-6. Deterioration Module

3-6.1. General Overview

In this section the method of expressing numerical values of CI's for reaches and sub-reaches into single-line SCM's is presented. Next, such SCM's are used in the Backward MC Module to determine the DTM for each reach/sub-reach. Having done so, comes then the discussion of the Forward MC Deterioration Module, which integrates the single-time effect of intermediate and design storms on coastal structures within the study area. Before that, expert opinion was sought to estimate the approximate magnitude ranges of the single-time impacts on all reaches and sub-reaches.

3-6.2. Development of SCM's for Reaches and Sub-Reaches

The first step towards establishing a MC-based Deterioration Module is to express the numerical values of CI's in terms of a SCM. As discussed in Chapter II,

Yokota & Komure (2003) represented the structural condition at the year of construction, and considering four successive levels of deterioration, using a single-liner matrix. Using the same concept but this time spanning seven levels of deterioration as per the REMR guidelines, the following matrix denoted by Equation 3-1 shall represent the condition of the structure at the year of construction or last major repair or maintenance:

$$SCM = [1 \quad 0 \quad 0 \quad 0 \quad 0 \quad 0 \quad 0]$$

Equation 3-1: SCM at the year of construction or last major repair.

Where:

- The digit "1" placed on the left cell means that 100% of the structure lies within the "Excellent" condition state, and none of the structural components fall into the following condition states. The conversion of any numerical value of the CI into a single-liner matrix is performed as denoted by Equation 3-2.

$$RI = [7 * (\%Excellent) + 6 * (\%Good) + 5 * (\%Fair) + 4 * (\%Marginal) + 3 * (\%Poor) + 2 * (\%Very\ Poor) + 1 * (\%Failed)] / 7$$

Equation 3-2: Expression of RI by a single-liner matrix.

Where:

- “*RI*” is the Condition Index of the reach/sub-reach and the percentages correspond to the portion of the reach belonging to each of the seven condition state ranges.
- The constants 7, 6, 5, 4, 3, 2, and 1 are arbitrarily chosen as consecutive numbers, and reflect the weights of their corresponding percentages, as suggested through expert consultation. The main issue is to choose constants with the same increments.

3-6.3. Backward MC Deterioration Module

Using the SCM for any particular reach or sub-reach, the problem is illustrated by Equation 2-6.

Where:

- The LHS of the equation represents the current SCM of the reach or sub-reach based upon the field inspection in 2013; such that each row corresponds to the % reach or sub-reach length falling in the indicated condition rating category.
- "*P1*" through "*P6*" are the transition probabilities between each two successive deterioration grades in the DTM.
- "*t*" is the period of time in years separating the date of construction or that of last major repair or rehabilitation, and the date of the last condition rating (i.e. 2013 in this case).
- The RHS single-column matrix represents the condition state at the year of construction, or at the time of the last major repair or rehabilitation.

Thus, the only unknowns in Equation 2-6 are the values of *P1* through *P6* (*P7* is equal to 1.00). The constraints represented the values provided by experts for the acceptable ranges of *P1* through *P7*, which reflects a deterioration rate that increases with age and is common for infrastructure deterioration patterns as follows:

$$\begin{array}{rclcl}
 0.90 & > & P1 & \geq & 0.80 \\
 0.80 & > & P2 & \geq & 0.70 \\
 0.70 & > & P3 & \geq & 0.60 \\
 0.60 & > & P4 & \geq & 0.50 \\
 0.50 & > & P5 & \geq & 0.40 \\
 0.40 & > & P6 & \geq & 0.30 \\
 & & P7 & = & 1.00
 \end{array}$$

The list of experts consulted and surveyed throughout this work is included in Section 4-7 of Chapter IV.

3-6.4. Forward MC Deterioration Module

In the forward MC Deterioration Module, the DTM's of all reaches obtained using the Backward MC Module are used to predict future deterioration. This is carried out through raising the DTM to the power " t " as in Equation 3-6, where " t " corresponds to the time interval in years between 2013 and the year of the CI forecast. The time limit for the forward MC deterioration forecast is up to year 2050. The forward MC deterioration prediction model is designed in such a way as to offer asset managers with running modes that can be categorized according to the following:

1. Type of structure (Rubble-mound breakwaters and groins, rubble-mound revetments, non-rubble seawalls and quaywalls, and composite structures);
2. Reach / sub-reach level;
3. Structure level;
4. Zone level; and
5. Entire study area level.

The results obtained through the forward MC module were then represented using mathematical formulae pertinent to each individual structure using best-fit regression.

3-6.5. Intermediate and Design Storm Simulator

The typical return periods considered for design storms in this research is 50 years, while the intermediate storm return period are 25 years. From past meteorological records, the last design storm occurred in 2010, while the last intermediate storm occurred in 2003. Using these return periods and indicated storm dates as the simulator's baseline, a random number has been assigned over the study period spanning between years 2013 and 2050. This random number is between 0 and 25 for the intermediate storm case, and between 0 and 50 for the design storms. Once the simulator is run, the obtained intermediate and design storm years of occurrence are then fixed as a first step prior to obtaining the effect of such storms on the respective coastal structures.

Accordingly, the single-time effect on the CI of every reach and sub-reach in the study area was obtained through expert survey. The survey did not present exact

names or ID's of structures or reaches, but it rather included certain sets of design attributes and environmental characteristics that cover all types of structures within the study area. The surveyed experts were handed survey template containing various combinations of design and environmental attributes, against which they were required to estimate the percent reduction in the CI value upon the occurrence of intermediate and design storms. The list of experts consulted and surveyed throughout this work is included in Section 4-7 of Chapter IV. Design data included comprised the following:

1. Toe stone attributes;
2. Filter layer attributes;
3. Seaside armor layer attributes;
4. Seaside slope attributes; and
5. Latest calculated CI values.

On the other hand, environmental data included:

1. Still-water depth at toe;
2. Seabed attributes; and
3. Maximum H_s and T_m .

Thus, the percent reduction in the CI of each reach was then logged in the simulator to represent the single-time effect of each type of storm. The calculation of the overall reduction in the CI value for the entire structure was then performed using Equations 2-1, 2-2, and 2-3, as shown in Table 3-11.

Table 3-11: Average CI drop for Alexandria's coastal structures due to storms.

SN	Structure	Int. Storm CI Average Reduction	Design Storm CI Average Reduction
1	26 th of July Club East Breakwater	15.00%	21.67%
2	26 th of July Club Submerged Breakwater	12.50%	17.50%
3	Al-Chatby to Sidi Gaber Revetment	10.00%	20.00%
4	Al-Mandara Breakwater	15.63%	20.63%
5	Al-Manshiya Revetment	10.00%	15.00%
6	Al-Montaza Breakwater	15.00%	20.00%
7	Al-Silsila to Al-Chatby Casino East Revetment	15.00%	30.00%
8	Al-Silsila to Al-Chatby Casino West Revetment	20.00%	35.00%
9	Armed Forces Club Revetment	20.00%	35.00%
10	Automobile Club Revetment	20.00%	30.00%
11	Bahari Revetment	20.00%	25.00%
12	Bir Masoud Breakwater	10.83%	21.67%
13	Bir Masoud Revetment	15.00%	24.83%
14	Engineers Club Revetment	15.00%	25.00%
15	Engineers Club West Breakwater	13.75%	22.50%
16	Glim East Groin	14.00%	23.00%
17	Glim East Revetment	20.00%	30.00%
18	Glim Middle Revetment	20.00%	30.00%
19	Glim West Groin	15.00%	23.75%
20	Glim West Revetment	20.00%	30.00%
21	Laurent Revetment	15.00%	25.00%
22	Marine Scouts Quaywall	10.00%	15.00%
23	Marine Scouts Revetment	15.00%	20.00%
24	Miami Breakwater	15.00%	20.00%
25	Middle Breakwater (Eastern Harbor)	15.00%	30.00%
26	Pharos Promenade Breakwater	16.25%	31.25%
27	Pharos Promenade East Revetment	15.00%	30.00%
28	Pharos Promenade West Revetment	15.00%	30.00%
29	Police Club East Breakwater	14.00%	23.00%
30	Police Club Middle Breakwater	17.50%	27.50%
31	Police Club Quaywall	5.00%	10.00%
32	Police Club West Breakwater	16.67%	26.67%
33	Professional Clubs Breakwater	15.00%	25.00%
34	Qaytbey East Seawall	15.00%	30.00%
35	Qaytbey North Revetment	15.00%	30.00%
36	Raml Station to Al-Silsila Seawall	10.00%	15.00%
37	San Stefano East Breakwater / Headland	13.75%	22.50%
38	San Stefano North Breakwater	17.50%	27.50%
39	San Stefano Quay	17.50%	27.50%
40	San Stefano South Pier	16.67%	26.67%
41	Stanley Beach Seawall	5.00%	10.00%
42	Teachers Club Breakwater	15.00%	24.29%
43	West Breakwater (Eastern Harbor)	15.00%	30.00%

3-7. Optimization Modules

3-7.1. General Overview

The Optimization Module features the following steps arranged according to the sequence of their analogy as follows:

1. Initial Condition Index Calculation;
2. Calculation of Storm Effect on Initial Condition Index;
3. Calculation of Intervention Policy Effect on Condition Index after Storm Occurrence;
4. Priority Index Calculation;
5. LCC Optimization Module; and
6. Risk Optimization Module.

3-7.2. Initial Condition Index Calculation

The deterioration data peculiar to every single structure was obtained from the results of the Forward MC Deterioration Module as explained early in this chapter. These results were then expressed in terms of mathematical relations using best-fit regression. From this standpoint, characteristic deterioration equations were obtained for each structure, and the initial Condition Indices at each year were obtained. For the purpose of illustration, Equation 3-3 displays the characteristic regression curve for the Eastern Harbor West Breakwater, obtained as a direct result of mathematically representing the Forward MC deterioration pattern using best-fit regression in this research:

$$CI_{Oij} = -2 \times 10^{-6} (Y_j - Y_{oi})^3 + 0.003 \times (Y_j - Y_{oi})^2 - 0.0101 (Y_j - Y_{oi}) + 0.5452$$

Equation 3-3: Obtained regression equation for the Eastern Harbor West Breakwater.

Where:

- " CI_{Oij} " is the initial CI for structure " i " at year " j " in case no storms take place and also in case no intervention action is implemented. This value for each year is represented by the characteristic regression deterioration curve

for each structure, obtained in its turn from the Forward MC Deterioration Module;

- “ Y_j ” is the current year of CI calculation; and
- “ Y_{oi} ” is the structure “ i ” year of construction or its year of last major repair, whichever is more recent.

3-7.3. Calculation of Storm Effect on Initial Condition Index

As previously discussed, the storm effect on each structure is reflected by the sudden single-time percent reduction it inflicts on the initial CI value. This percent reduction has been obtained through expert survey, for each structure within the study area, for both cases of design and intermediate storms. In this research, the formulation of the storm effect on the CI value is denoted by Equation 3-4, which is suggested by the author to represent the CI adjustment after storm occurrence:

$$CI_{Sij} = (1 - S_{ij}) CI_{Oij}$$

Equation 3-4: Developed equation of the adjusted CI value after storm occurrence.

Where:

- “ CI_{Sij} ” is the CI of structure “ i ” at year “ j ” after the occurrence of either an intermediate or design storm at year “ j ” or at any previous year.
- “ S_{ij} ” is the percent reduction in the CI value caused by the storm for structure “ i ” at year “ j ”.

3-7.4. Calculation of Intervention Policy Effect on Condition Index

After calculating the value of CI_{Sij} , the following step in the LCC Optimization Engine analogy is the adjustment of that latter value in accordance with the type of intervention policy. Four sets of intervention policies are considered as shown in Table 3-12. The Intervention Policy ID is denoted by “ M ” in the model formulation, and “ ΔCI_M ” is the increase in the CI as a result of the policy.

Table 3-12: Intervention policies and their effect on CI values.

<i>M</i>	ΔCI_M	Intervention Policy	Description	Cost
0	None	Do Nothing	<ul style="list-style-type: none"> Visual inspection and condition rating after storm occurrences and each 2-3 years. 	None
1	Increased by 25%	Routine Maintenance	<ul style="list-style-type: none"> Compensate displaced and lost armor for rubble-mound structures; and Replace damaged mooring accessories, fenders, ladders; and fill small voids for non-rubble structures. 	2% of initial construction cost of the structure.
2	Increased by 50%	Rehabilitation	<ul style="list-style-type: none"> Extend toe and place new armor layer for rubble-mound structures; and Same as routine maintenance with the repair of crest / cap for non-rubble structures. 	6% of initial construction cost.
3	Increased to 100%	Replacement	<ul style="list-style-type: none"> Remove all armor, compensate under-layer and core loss, extend toe, and install new armor for rubble-mound structures; and Install sheet pile or any vertical structure on the seaside and apply mass concrete between new and old structure, reinstate crest and accessories, for non-rubble structures. 	100% of initial construction cost.

As suggested in CIRIA (2007) and further to the findings of expert interviews, routine maintenance, which is the second intervention policy, corresponds generally to the compensation of lost armor units for rubble-mound structures, and to minor repairs for non-rubble structures. The third intervention policy, which is the rehabilitation, includes the extension of the toe stone for rubble-mound structures, and the placement of a complete new layer of armor stones. For non-rubble structures, this method corresponds to structural repairs, and may include upgrading the structure with the addition of armor stones. Replacement, which is the fourth intervention policy, is not the most efficient way, but considering the relatively lengthy modeling horizon, it represents a last resort. Replacement of rubble-mound

structures may consist of removing all armor stones, compensation of degraded core and under-layer, reinstatement of seaside slope and toe, and installation of new seaside armor. However, in many cases it consists of removing the entire armor stones and either re-arranging them to prevent excessive wave run-up, or replacing them after reinstating the core and under-layer materials. The associated costs of intervention policies are logged per unit length for each structure for modeling purposes. Such unit costs per linear meter were estimated depending upon expert consultation for all four intervention policies. The list of experts consulted and surveyed throughout this work is included in Section 4-7 of Chapter IV. Appendix 6, entitled, "*Summary of Intervention Policy Unit Cost Database for the Study Area in 2013*", provides a list of unit costs per meter runs for intervention policies 1, 2, 3, considering all 43 structures within the study area. Moreover, there was a general consensus among expert that between 2% and 6% of the initial construction cost is spent annually for the routine maintenance and rehabilitation of coastal protection structures, as per the standards norms of the marine construction industry.

In view of the above, the suggested adjustment of CI_{Sij} values to account for the intervention policies is formulated in this research according to the developed Equation 3-5:

$$CI_{Fij} = \begin{cases} CI_{Sij} [1 + \Delta CI_{Mij}]; & M_{ij} = 0, 1, 2; \quad j = 1 \\ [CI_{Fi(j-1)} - \Delta CI_{Fij}] \times [1 + \Delta CI_{Mij}]; & M_{ij} = 0, 1, 2; \quad j > 0 \\ 100\%; & M_{ij} = 3; \quad j > 0 \end{cases}$$

Equation 3-5: Adjusted CI value to account for intervention policy effect.

Where:

- " CI_{Fij} " is the final CI of structure " i " at year " j " considering previous storm effect and also considering the effect of the implementation of any of the intervention policies at year " j " or before.
- " M_{ij} " is the intervention policy applied to structure " i " at year " j ".

- “ ΔCI_{Mij} ” is the increase in CI value resulting from applying the intervention policy “ M ” to structure “ i ” at year “ j ”.
- “ $CI_{Fi(j-1)}$ ” is the adjusted CI accounting for both storm effect and previous intervention policies for structure “ i ” the year immediately before year “ j ”
- “ ΔCI_{Fij} ” is the decrease in the value of “ $CI_{Fi(j-1)}$ ”, for structure “ i ”, between age “ $j-1$ ” and year “ j ” according to the initial regression deterioration pattern for the structure.

3-7.5. Calculation of Priority Index

The Priority Indices (PI's) for all structures in the study area were obtained using both data obtained from literature and expert opinion. The priority indices were taken as the result of multiplying the probability of failure of the structure by the impact level of the structure's failure. The probability of failure is taken as $(1-CI)$, and a scale from 1 to 4 is also used to quantify the levels of impact; with 1 being the lowest impact and 4 being the highest. This is further explained by Equation 3-6, and uses the same concept of reliability-based maintenance as outlined in Nugyen et al. (2010).

$$PI_{ij} = (1 - CI_{Fij}) * (RF)$$

Equation 3-6: Priority Index calculation for structures, after Nugyen et al. (2010).

Where:

- “ PI_{ij} ” is the risks Priority Index for structure of the structure “ i ” at year “ j ”.
- “ RF ” is the Risk Impact Factor, which represents the magnitude of the structure's failure impact on a scale from 1 to 4 considering ascending impact levels.

In this study, PI ranges were classified in accordance with Table 3-13, based upon expert consultation. The list of experts consulted and surveyed throughout this work is included in Section 4-7 of Chapter IV. The Red range represents the High Risk PI Values, the green range represents the low-risk PI values, and the amber range represents the medium risk values.

Table 3-13: PI risk ranges as per expert consultation in year 2014.

		Impact Level			
		1	2	3	4
Probability of Failure	0.90	0.90	1.80	2.70	3.60
	0.80	0.80	1.60	2.40	3.20
	0.70	0.70	1.40	2.10	2.80
	0.60	0.60	1.20	1.80	2.40
	0.50	0.50	1.00	1.50	2.00
	0.40	0.40	0.80	1.20	1.60
	0.30	0.30	0.60	0.90	1.20
	0.20	0.20	0.40	0.60	0.80
	0.10	0.10	0.20	0.30	0.40

3-7.6. LCC Optimization Module

In early attempts to run the model, the optimization was performed directly on the Forward MC Deterioration Module, without transforming the deterioration patterns for sub-reaches and reaches into mathematical relations using regression techniques. This arrangement features 4 sets of policies listed against structural sub-reaches and reaches. This caused a significant runtime for the model and made it extremely impractical to run the model and obtain results in an efficient manner considering a long analysis time interval. From this standpoint, the translation of MC deterioration patterns into mathematical functions using regression tools was introduced, which greatly helped reduce the size of the model and eliminated the runtime issues when running the GA-based optimization module. The runtime issues and redundancy of variables were further mitigated by switching the level of optimization to the structure level rather than reach and sub-reach level.

The objective function of the LCC Optimization Module is the LCC minimization. Obtaining the yearly set of decisions pertaining to maintenance, rehabilitation and repair of coastal structures, while being constrained by the minimum acceptable reliability level expressed by a predefined CI action thresholds; all while satisfying the least possible budget: all represent the tools of the optimization module to meet the objective function. Another constraint includes the addition of PI's to the structures to determine the more critical structures necessitating a priority treatment with regards to the intervention policies. A further constraint was also considered; the maximum number of locations per year where work can physically take place. The optimization technique is GA's using the MS Excel 2013 Evolver™ optimization tool. The optimization scenarios are discussed in

further detail in Chapter IV. The total LCC formulation developed by the author for this research's LCC Optimization Module is denoted by Equation 3-7, where the objective is to minimize this sum.

$$\sum_{i=1}^n \sum_{j=0}^m [M_{Uij} (1 + I)^{(Y_j - Y_o)}] L_i$$

Equation 3-7: Total LCC formulation for the study area.

Where:

- " M_{Uij} " is the intervention policy unit cost for structure " i " at age " j ";
- " I " is the inflation rate;
- " Y_j " is the current year;
- " Y_o " is the starting year of the optimization run,;
- " L_i " is the length of structure " i ";
- " n " is the total number of structures within the scope of the optimization;
- and
- " m " is the total number of years under the optimization scope.

While the objective function of the LCC is the total LCC minimization, the decision variables are the intervention policies 0, 1, 2, 3 as explained earlier in Table 3-12. The module's constraints are listed as follows:

1. Only 1 replacement per structure;
2. Maximum of number of interventions per structure over the study period;
3. Maximum number of interventions per year in the entire study area; and
4. Maximum PI threshold for each structure.

Numerical examples of these constraints are provided in Chapter IV, under the LCC and Risk Optimization Scenarios; namely in Tables 4-4 and 4-5. It is to be noted that Equation 3-8 from a mathematical point of view represents a classical assignment problem; however, choosing of the solution technique between linear and non-linear optimization had to take into account the amount of variables and solutions. For the case study for instance, there are 43 structures, with a forecast period of 35 years, and 4 possible intervention policies for each structure at each year. This meant that a global search technique was required to solve this equation

within reasonable time. GA's presented the most suitable solving technique in view of the vast population of solutions, which reached approximately 1.5×10^{16} solutions.

3-7.7. Risk Optimization Module

The objective function of the Risk Optimization Module is the minimization of the total risk, i.e. the total PI value for the entire study area. The module formulation is denoted by Equation 3-8, based upon Equation 3-9 as follows:

$$PI_{Wi} = PI_{MAXi} * L_i$$

Equation 3-8: weighted PI formulation for individual structures.

Where:

- “ PI_{Wi} ” is the weighted PI for structure “ i ”;
- “ PI_{MAXi} ” is the maximum PI for structure “ i ” over the course of the study period; and
- “ L_i ” is the length of structure “ i ”.

$$PI_T = \sum_i^n [PI_{Wi} / L_i]$$

Equation 3-9: Total PI formulation for the study area.

Where:

- “ PI_T ” is the total PI for the entire study area for all years.

The constraints on the Risk Optimization Module are identical to those of the LCC Optimization Module, however, the only two differences is that there is no PI threshold, and that there is a pre-defined budget constraint. It is to be noted that Equations 3-9 and 3-10 are developed by the author to represent the weighted and the total PI values for the study area.

CHAPTER IV – CASE STUDY, DISCUSSION, AND ANALYSIS OF RESULTS

4-1. General Overview of the Case Study

The coastal protection structures of the city of Alexandria, Egypt, shall constitute the case study of this research. Alexandria is located on the northern coast of Egypt, overlooking the Mediterranean Sea, between 31°04'02 and 31°19'55 north of the Equator, and between 29°44'32 and 30°05'09 east of the Greenwich Meridian, as shown in Figure 4-1.

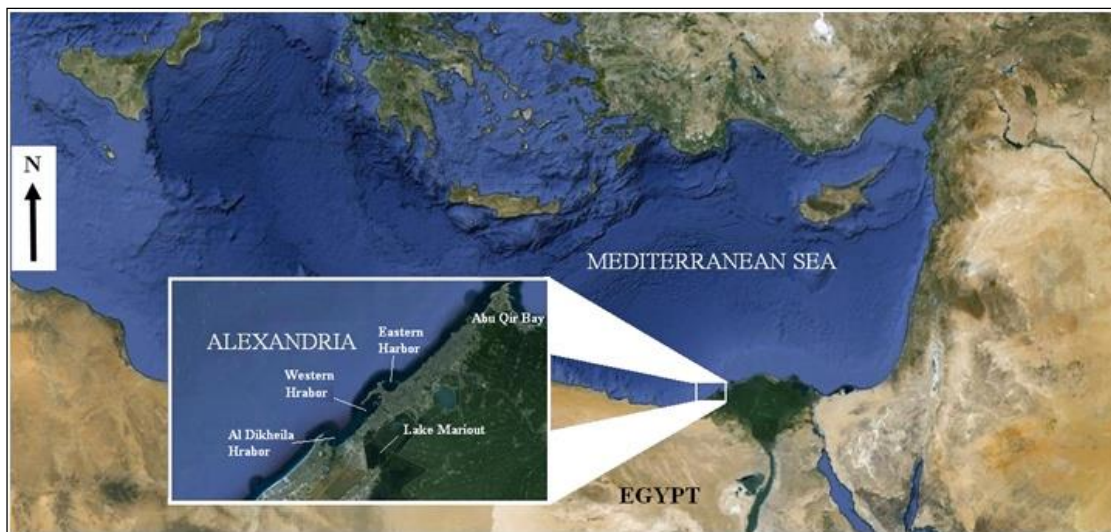


Figure 4-1: Geographic location of Alexandria (El Hakea et al., 2014).

The geographic location of the case study is shown in Figure 4-2 (Map modified by author from Google Earth Pro 2013) and extends over an approximate distance of 18.5 km, from the Pharos headland to the west all along to Al-Montaza beach to the east. It is divided into 7 distinct zones, with the AID summary provided under Appendix 2. Alexandria is renowned as being Egypt's top summer tourist destination, by virtue of its sandy beaches attracting almost 2.5 million tourists annually during summer seasons (El-Raey et al., 1995). While seasonal tourism constitutes a major income source to the Alexandria, the governorate provides nearly 40% of Egypt's industrial output, and is considered as Egypt's main port and second largest city, with a winter population of 4 million and a summer population of about 5 million people (UNESCO, 2003).



Figure 4-2: Scope of the case study area and its zoning layout.

Alexandria's waterfront extends over a distance of approximately 43 km, from Abu Qir headland eastwards to Sidi Krir westwards. Furthermore, Alexandria houses five ports; serving commercial, passenger transport, naval, and fishing sectors: the Western Harbor, the Eastern Harbor, Al-Dikheila Harbor, in addition to two other harbors in Abu Qir (Iskander, 2000). Land and real estate prices in the Alexandria in general, and within the study area in particular are among the highest in Egypt, with the most expensive lying within very close range from the shoreline. The city's main traffic and infrastructure network artery, the Cornice Road, lies directly on the city's waterfront, with elevation ranging between 2.00 m and 12.50 m above MSL, and is protected by a rubble-mound revetment parallel to the shoreline in most of its course.

Alexandria has been historically regarded as Egypt's cultural gateway, with its unique historical and cultural heritage. Historical evidence indicates that portions of the ancient city of Alexandria were inundated by the Mediterranean Sea, as demonstrated by the archeological discoveries in the Abu Qir Bay and the Eastern Harbor, in addition to the submerged remnants of the Hellenistic city of Canopus (UNESCO, 2003). The city's main archeological attractions are situated in the Eastern Harbor, located in the western portion of the study area shown in Figure 4-3. The figure's legend is explained as follows: (a) Location of Alexandria in the Eastern Mediterranean basin along with its geological features; and (b) Area defining the scope of study of this research.

Thus, recreational beaches, ancient monuments, hotels, clubs, facilities, and other assets and infrastructure that are the building blocks of Alexandria's socioeconomic life are directly dependent upon coastal protection works. This factor shows the criticality of maintaining a reliable coastal protection infrastructure, especially in light of the natural and anthropogenic factors that are imposing further risks on the reliability of coastal structures in Alexandria, which were briefly discussed in Chapter I. However, describing the risks faced by Alexandria requires as a first step a general understanding of the geomorphology, wave characteristics, climatic conditions, and sediment transport patterns along the city's waterfront, in addition to a discussion on the history of Alexandria's coastal protection works and marine construction. This is provided in detail under Appendix 5 entitled, "*Historical Overview of Alexandria's Marine Protection Works*".

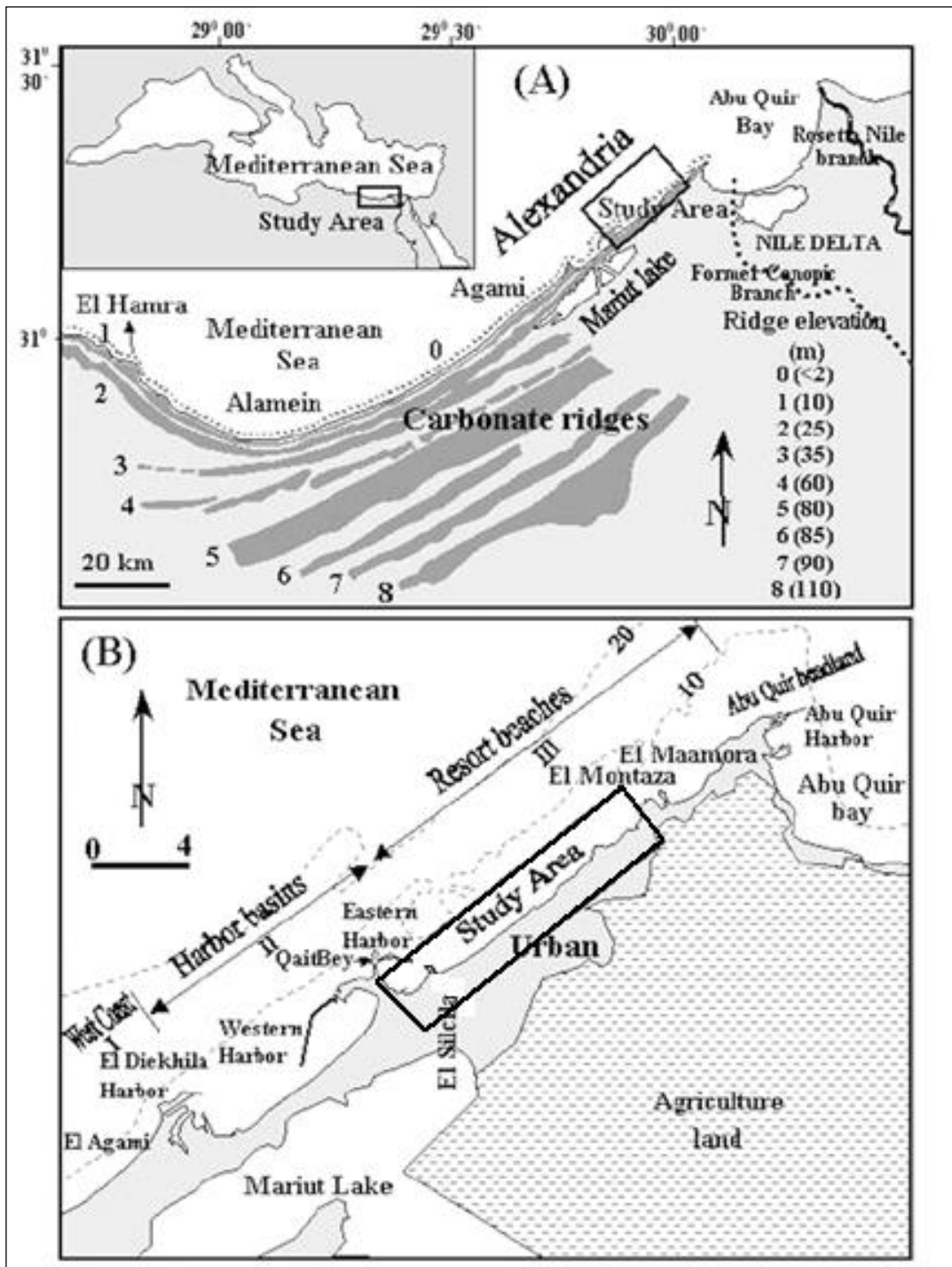


Figure 4-3: Map modified by author after Frihy et al. (2004) for the study area.

In light of these risks, summarized in Table 4-1, which are further addressed in Appendix 5, rises the need to develop an integrated infrastructure management module for Alexandria's coastal structures, that includes a mechanism of condition assessment of such existing structures, followed by the prediction of their future deterioration patterns, prior to formulating a framework for their asset management needs.

Table 4-1: Summary of threats surrounding the study area.

Threat	Threat Description
Climate Change	Climate Change affects the long-term SLR and hence increases the significant incident wave height (Hs) on coastal structures. Climate change is also responsible for reducing the return periods of intermediate and design storms, which accelerates the deterioration of coastal structures.
Seismic subsidence	Seismic subsidence of the northern Nile Delta region relative to MSL increases the RSLR, which compounds the effect of Climate Change on coastal structures.
Low-lying risk areas	Some areas along Alexandria's waterfront are extremely close in altitude to MSL, which puts life and property in such areas under continuous flooding threat during storms.

Henceforth, Alexandria is taken as the case study of this research, given its demographic and cultural significance. The impact of accelerated SLR on Alexandria was addressed in El-Raey, et al. (1995), Frihy (2003), and Frihy et al. (2010). A study by Hassaan & Abdrabo (2012) shows that natural sand dunes and manmade structures, such as the embankments of the International Coastal Highway running parallel to the shoreline between Rosetta and Port Said, actually provide unintended protection to some of the risk areas. Furthermore, the collective impact of SLR on coastal structures in the Nile Delta region and Alexandria was also discussed in Iskander (2013), and suggests that most of the existing structures are indispensable, but at the same time over-designed.

4-2. AID Analysis

As discussed previously, the study area comprises 43 different structures, totaling a length of 18,509.00 m, and including various types of coastal structures that may be either classified by their structure type, design concept, relationship with still-water level, connection to the shore, seaside armor type and weight, and construction materials. If the total length of all structures is divided onto the seven zones, the share of each zone shall be as shown in Figure 4-4. Of the total length of all assets combined within the study area, 47% is occupied by breakwaters and groins, 41% by revetments, and 13% by seawalls and quaywalls; as shown in Figure 4-5. The figure

shows reach lengths occupied by the various types of coastal structures in each of the seven zones of the study area. The pie chart on the top-right represents the total share of each of the three major types of structures of the total length of the study area. Data correspond to year 2013.

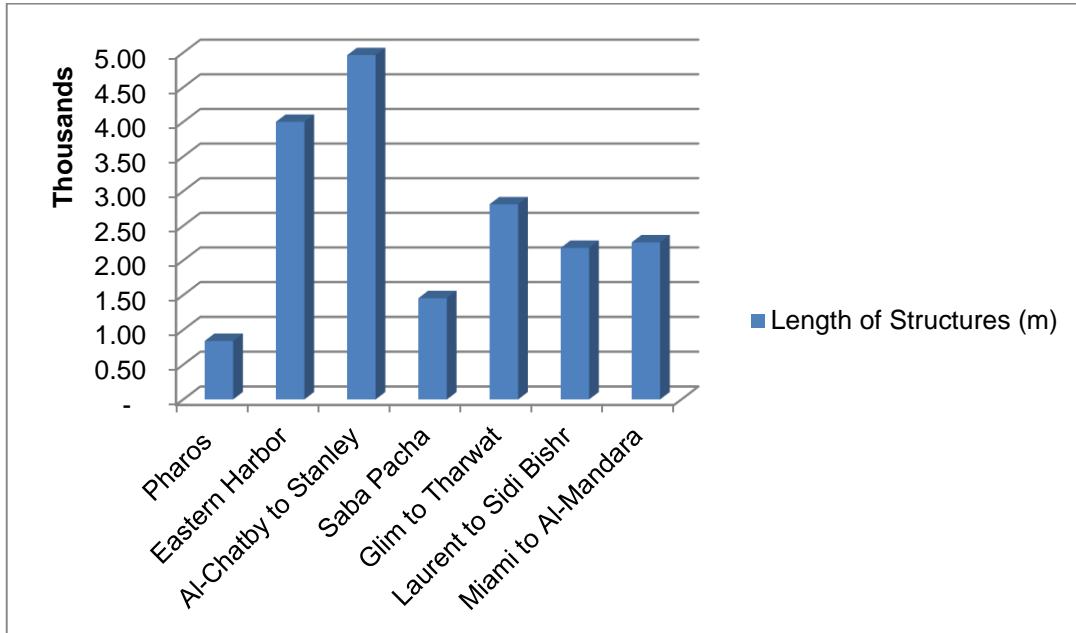


Figure 4-4: Structure’s length per zone in the study area in year 2013.

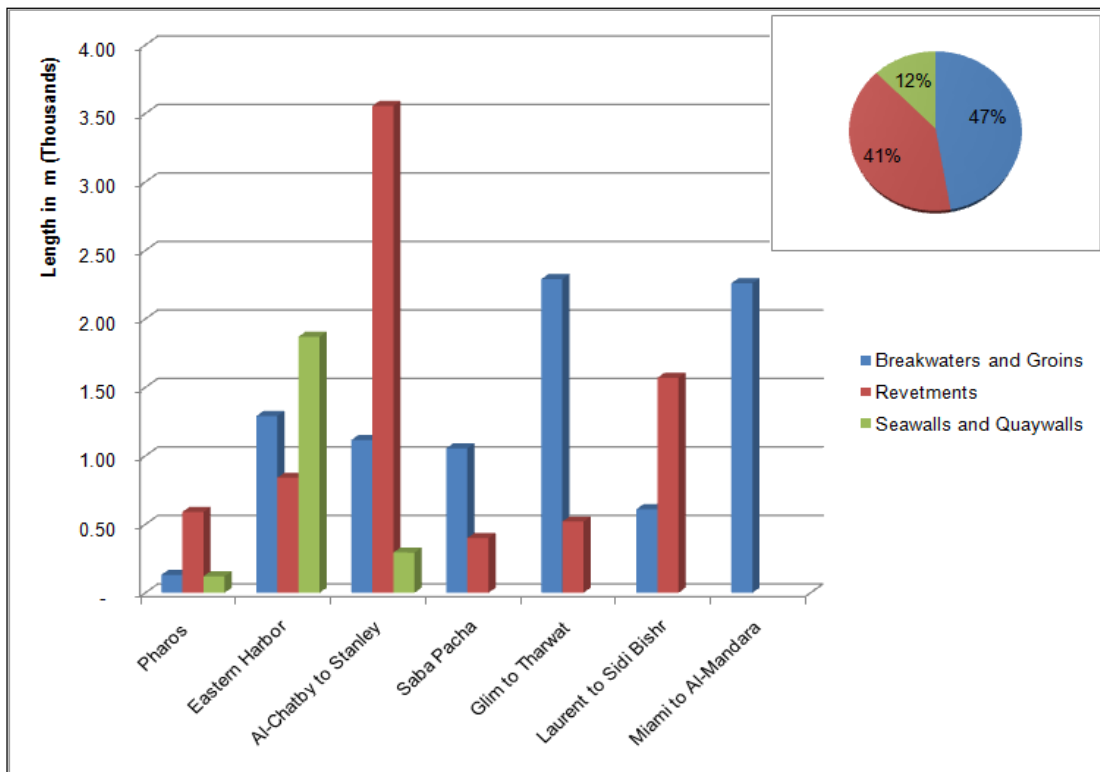


Figure 4-5: Length of each structure type per zone in year 2013.

Moreover, Figure 4-6 shows the distribution of such lengths occupied by these three categories of structures over the seven zones that together make up the entire study area. The pie chart on the top-right indicates the length share of three categories of structures.

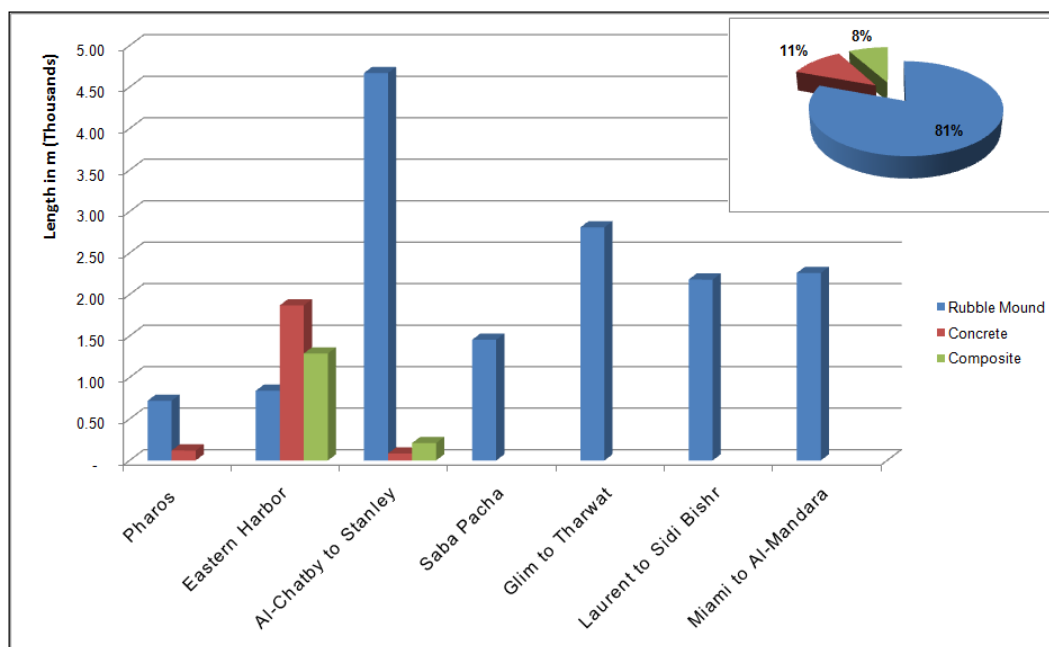


Figure 4-6: Length of each structural design concept per zone in year 2013.

Nevertheless, Figure 4-7 shows the predominant seaside armor stone types for all zones in the study area, 2013. Distributions of predominant seaside armor stone types distributed over reach lengths in each zone of the study area. The pie chart on the top RHS indicates the overall share of all armor stone types over the entire length of the study area. The figure reveals that 81% of the total length of coastal structures within the study area is represented by rubble-mound structures, 11% are concrete structures; namely seawalls and quaywalls, and 8% are composite structures. The chart also shows the way these three distinct types of structure materials are distributed among the seven zones of the AID. In addition, Figure 4-8 shows the length of structures protected by the various types of armor stone, distributed amongst all seven zones.

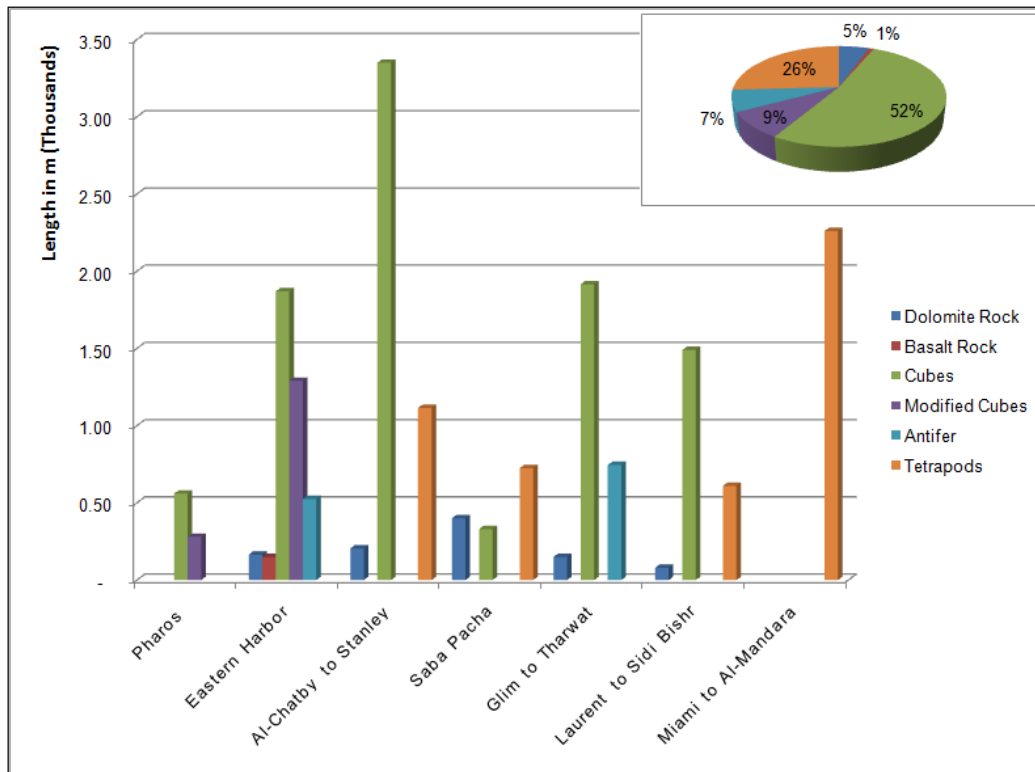


Figure 4-7: Length occupied by each type of armor per zone in year 2013.

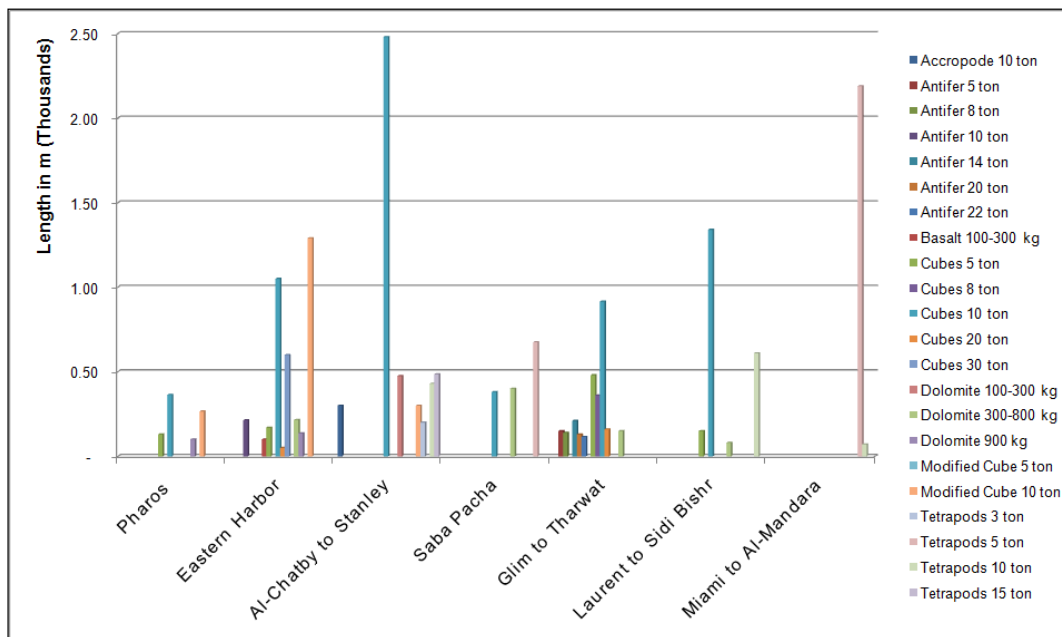


Figure 4-8: Length occupied by armor types and weights per zone in year 2013.

Figures 4-9 to 4-11 show the same distribution but this time classified according to the characteristic armor stone weights. Appendix 1 includes a schedule of the common armor stone shapes and their historical background. Figure 4-11, reveals that

57% of coastal structures possess 10 ton armor stone, while 22% possess 5 ton armor stone, 2013.

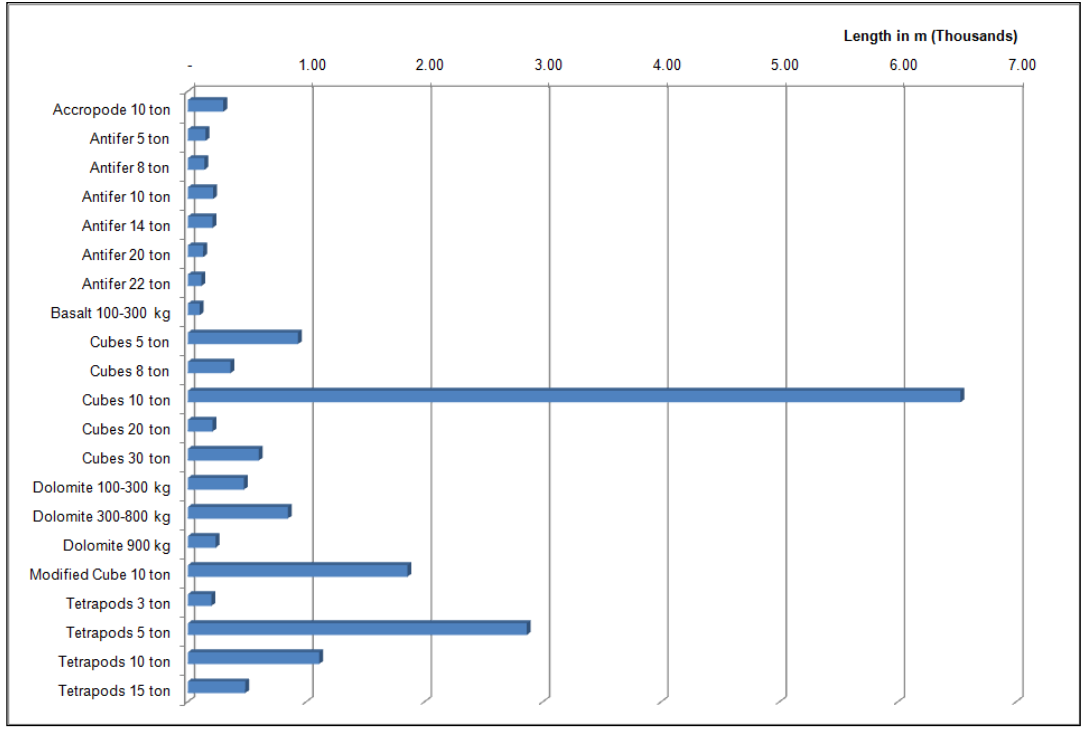


Figure 4-9: Armor shapes and weights length distribution in year 2013.

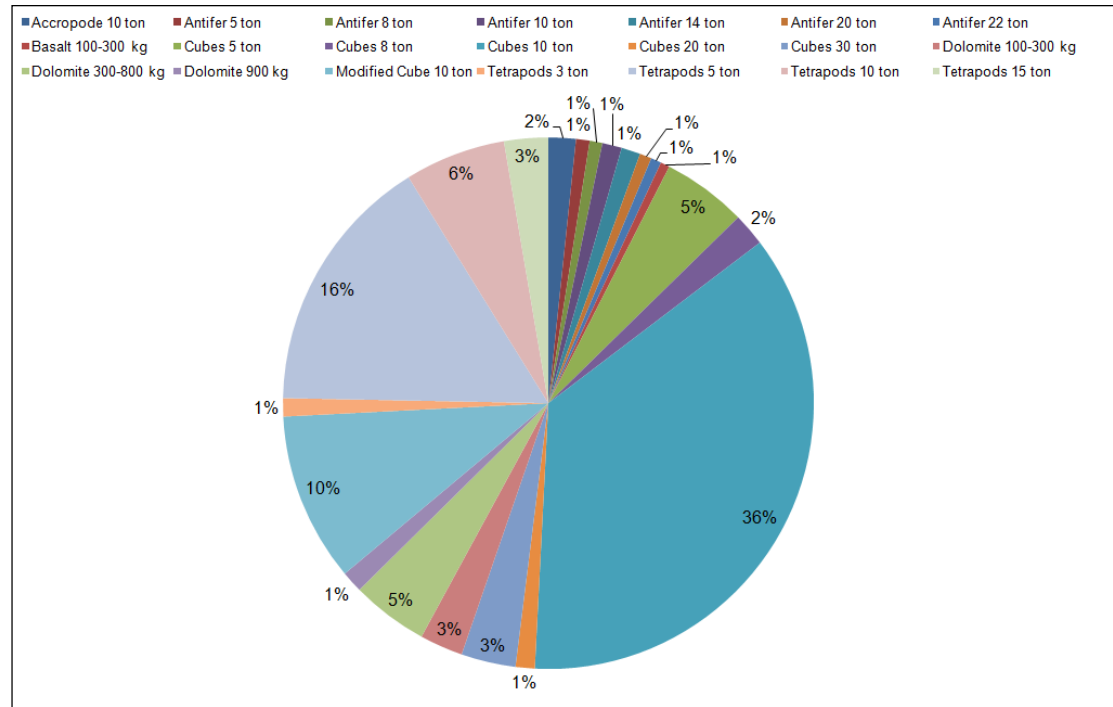


Figure 4-10: Armor shapes and weights distribution in the study area in year 2013

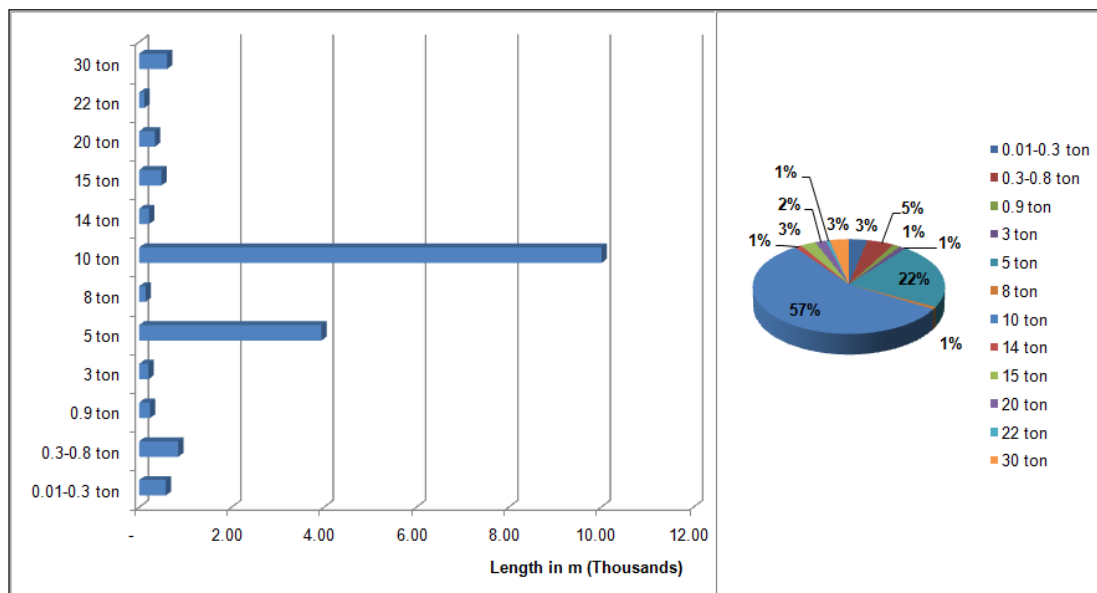


Figure 4-11: Armor stone weight distribution over the total length of the study area.

4-3. Visual Inspection and Condition Rating

4-3.1. Inspection Records

More than 6000 photographs were taken by the author to document the visual inspection for all of the various structures within the study area, using the structural and functional inspection sheets provided for the purpose of illustration in Appendices 3 and 4. Figure 4-12 and 4-13 display a collection of photographs and their corresponding observation for rubble-mound and non-rubble structures, respectively. The alphabetical legend for Figure 4-12 is explained as follows:

- a) The San Stefano North Breakwater photographed from the Glim Bay East Groin;
- b) Armor damage and displacement at the Glim Bay East Groin;
- c) Damaged crest since the December 2010 Kassem Storm at the Laurent Revetment;
- d) Head of the Teachers Club breakwater showing the utilized re-used tetrapod armor units;
- e) Crest of the Engineers Club West Breakwater located in Al-Khirban Bay;
- f) Basalt revetment at the Marine Scouts Club, Eastern Harbor;
- g) Dolomite revetment in Al-Manshiya area;
- h) View of the marine protection revetment in Sporting area; and
- i) Modified Cube armor stones of the North Qaytbey Revetment.

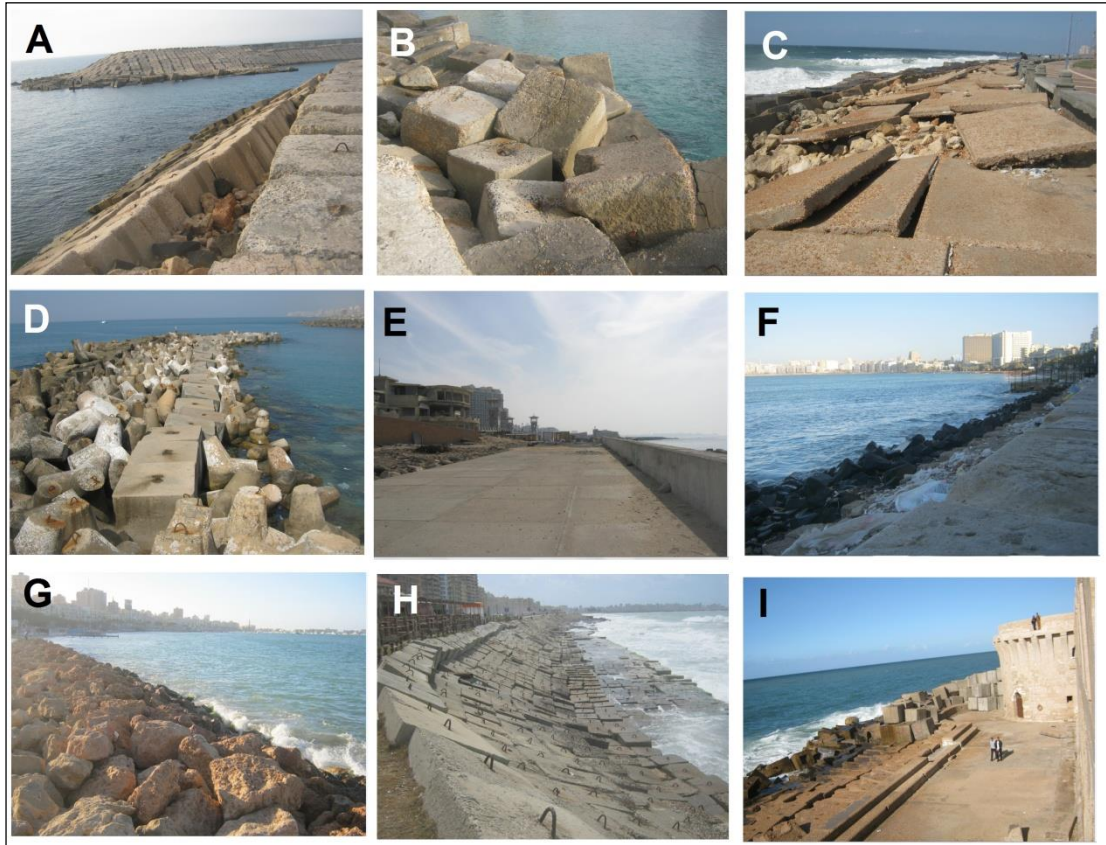


Figure 4-12: Structural inspection for rubble-mound structures in year 2013.

Furthermore, the alphabetical index for Figure 4-13 is explained as follows:

- a) Pell-mell 10-ton Modified Cube seaside armor of the Eastern Harbor West Breakwater;
- b) Crest of the Eastern Harbor composite West Breakwater;
- c) Marine Scouts Quaywall;
- d) Old Eastern Harbor Seawall with damage shown to its concrete crest;
- e) Stanley Bay composite Seawall; and
- f) East Qaytbey concrete Seawall protected with 10-ton pell-mell Modified Cube armor stones.



Figure 4-13: Structural inspection of non-rubble and composite structures in year 2013.

4-3.2. Structural Condition Rating

The results of the structural condition rating carried out in 2013 by the author and verified by expert review, are discussed in this section. The structures within the study area are divided into four categories:

1. Rubble-mound breakwaters and groins;
2. Non-rubble and composite breakwaters;
3. Rubble-mound revetments; and
4. Non-rubble seawalls and quaywalls.

By applying the same concept of aggregating the SI values for reach to calculate the SI value for the entire structure, as discussed in Chapter II; the overall SI ranges for each of the four categories of structures were calculated and plotted reflecting the length occupied by each category as shown in Figure 4-14. The figure indicates the as-inspected SI ranges in 2013 for the four main types of structures within the study area distributed on the lengths of the entire structures. The SI range distribution for each category separately is shown in Figure 4-15, and the SI value for each category is shown in Figure 4-16.

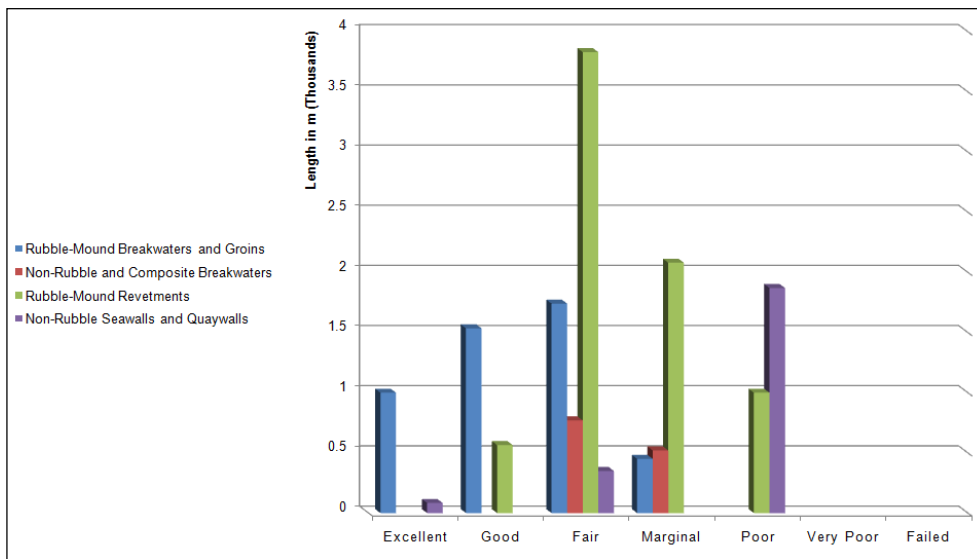


Figure 4-14: SI values for the study area's structures in year 2013.

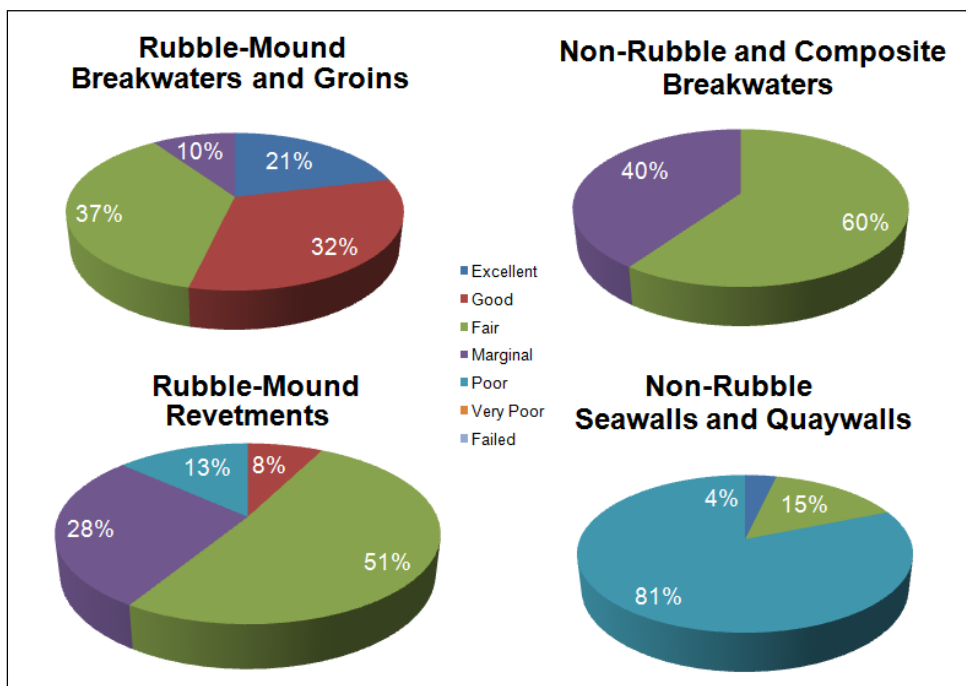


Figure 4-15: SI results by type of structure in year 2013.

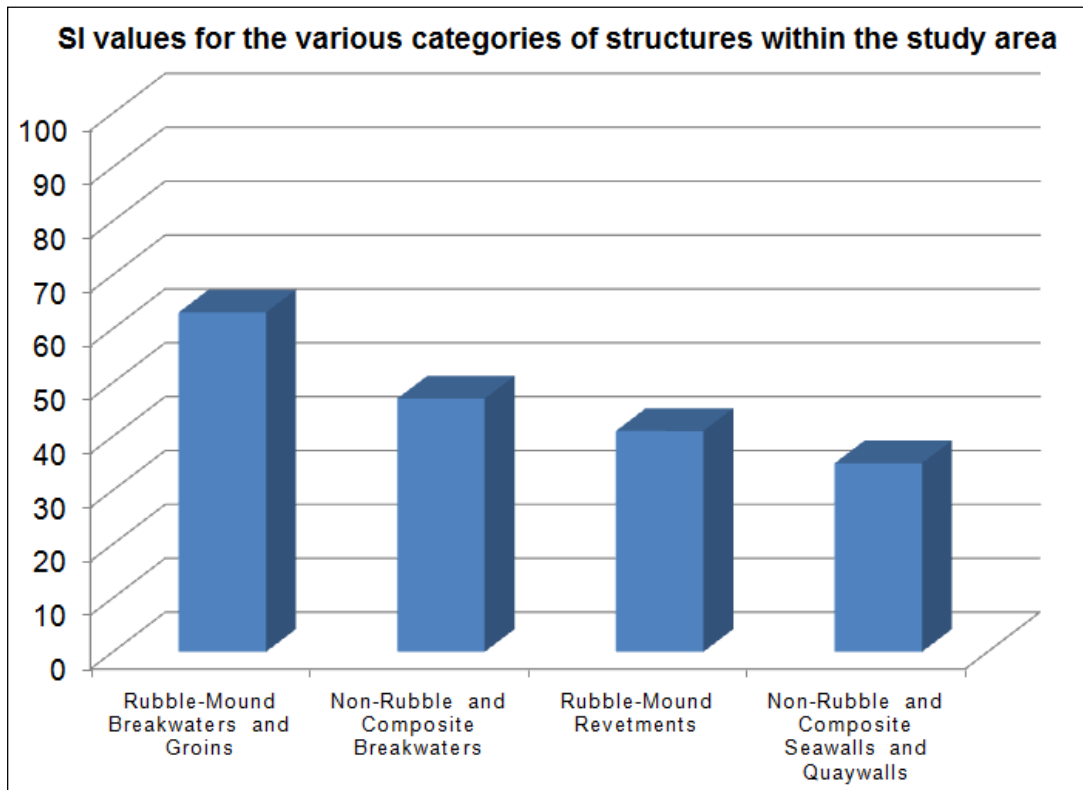


Figure 4-16: Overall SI values per each type of structures in 2013.

Alternatively, SI values for each of the seven zones in the study area were calculated based upon the inspection condition rating, and the overall SI for the entire study area was estimated to be within the "Fair" range, as shown in Table 4-2. Equally important were the obtained SI ranges for all structure reaches listed as opposed to the type and weight of seaside armor stones and units, as presented in Figure 4-17. The figure shows the calculated SI ranges for all structures within the study area based upon the visual inspection carried out in 2013; and expressed in terms of reach lengths, while showing the corresponding seaside armor types and weights. It is to be noted that as the submerged structures within the study area were not visually inspected, their corresponding FI values were assumed to be equivalent to their SI values only for the sake of demonstrating the functionality of the model with respect to SI calculation. In this work, SI's are taken as equivalent to CI's.

Table 4-2: SI values for the study area and its zones in year 2013.

Zone	Length (m)	Percentage of total length	Zone SI
Pharos	840.00	5%	39
Eastern Harbor	4,000.00	22%	31
Al-Chatby to Stanley	4,964.00	27%	62
Saba Pacha	1,455.00	8%	73
Glim to Tharwat	2,810.00	15%	62
Laurent to Sidi Bishr	2,180.00	12%	50
Miami to Al-Mandara	2,260.00	12%	92
Totals	18,509.00	100%	58

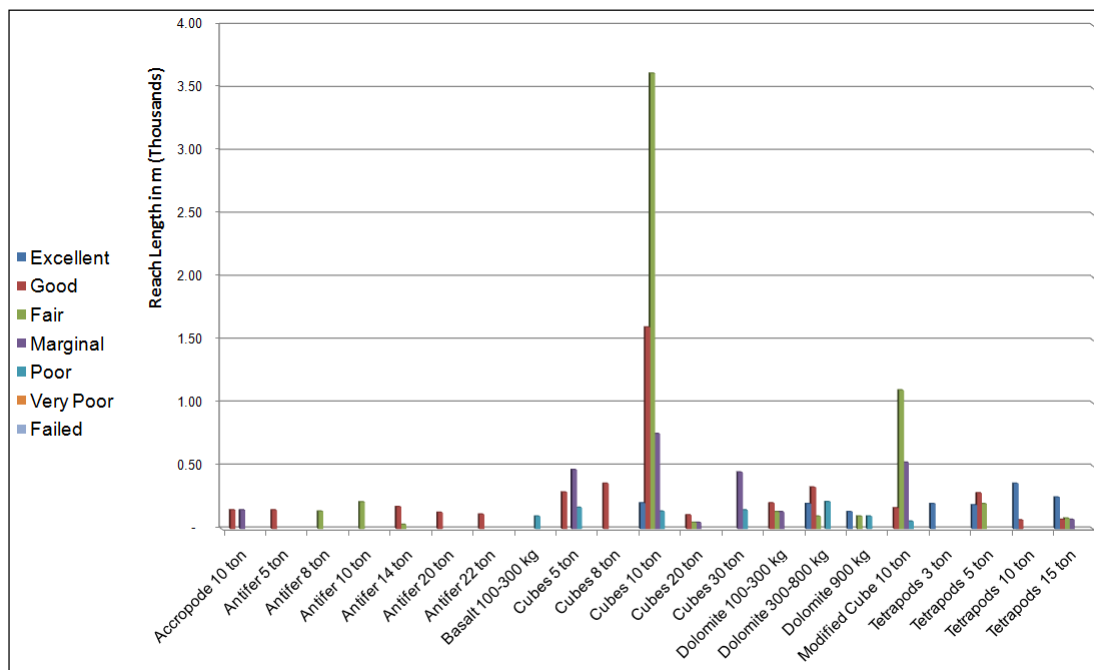


Figure 4-17: SI distribution against armor stone shapes and weights in year 2013.

4-3.3. Functional Condition Rating

The FI ranges for all structure reaches classified into one of the four categories illustrated in Figure 4-18, where the FI ranges for each category separately are shown in Figure 4-19. Also, While FI values for each category of structures is shown in Figure 4-20; FI values for each of the seven zones of the AID are shown in Table 4-3, reflecting an overall FI within the "Poor" condition range for the entire study area.

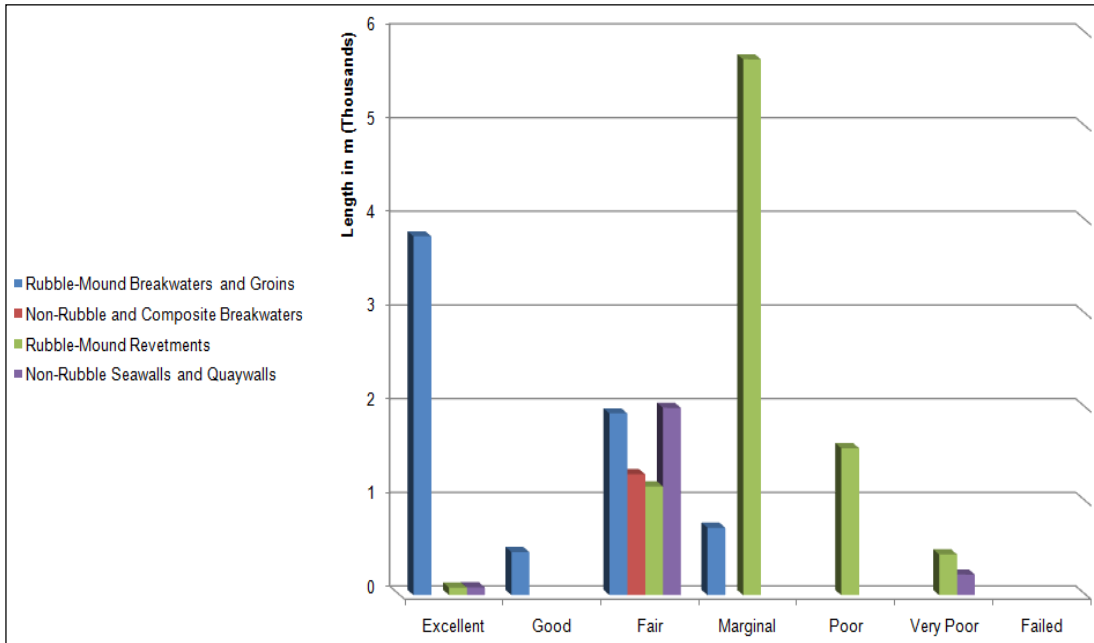


Figure 4-18: Length distribution of FI ranges in year 2013 per type of structure.

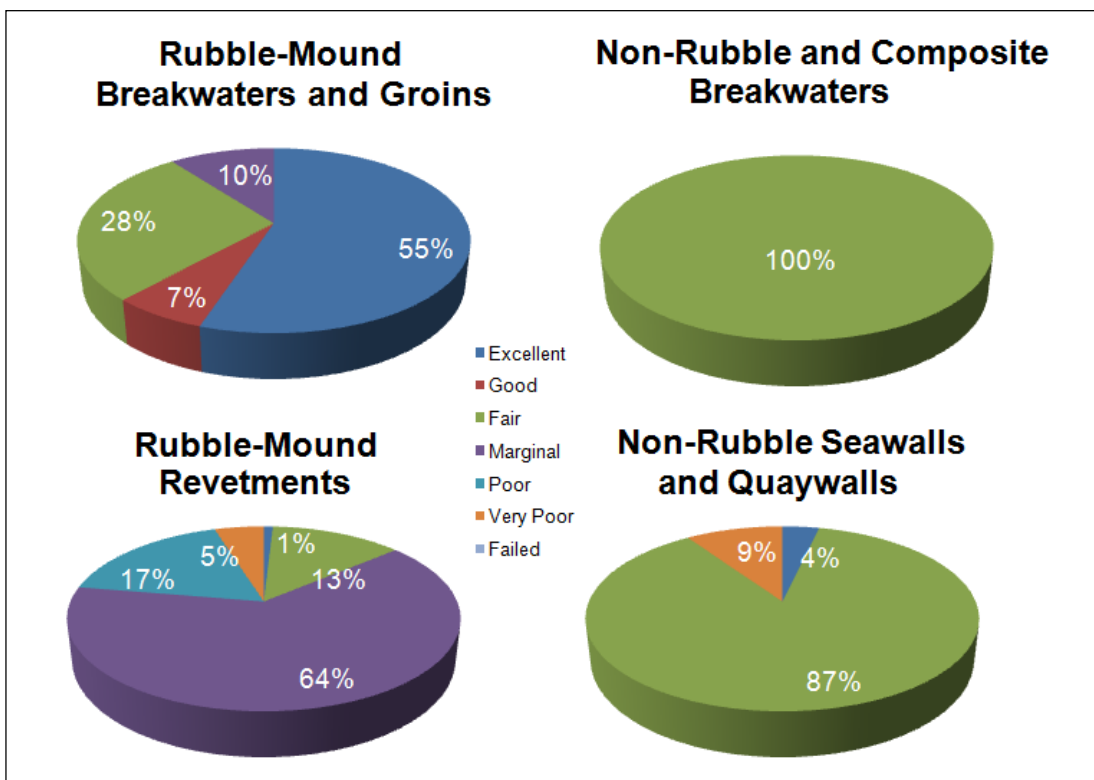


Figure 4-19: FI percentage distribution per structure type in year 2013.

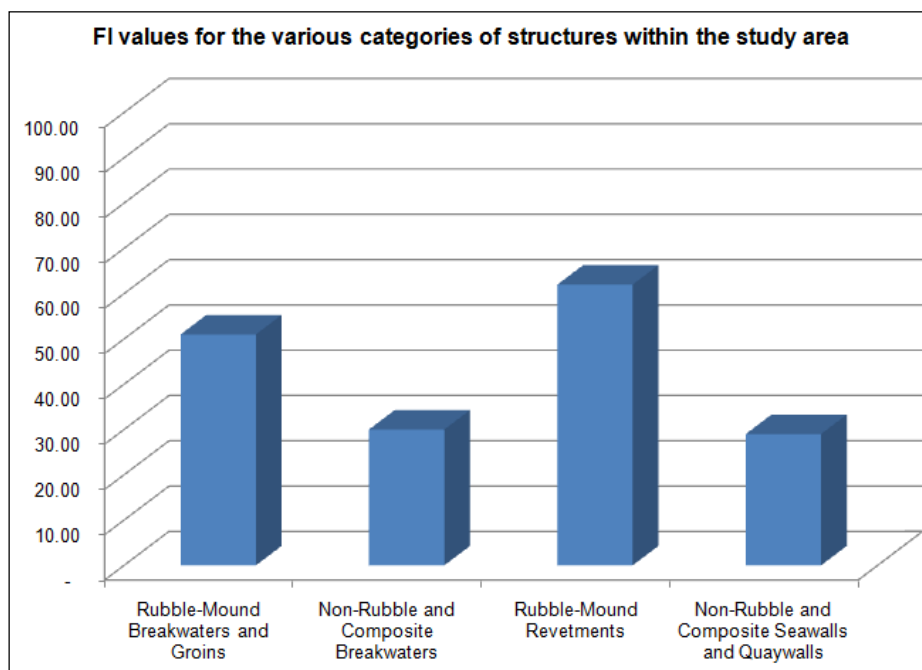


Figure 4-20: FI values per structure type in year 2013.

Table 4-3: FI's of the study area and its zones in year 2013.

Zone	Length (m)	Percentage of total length	Zone FI
Pharos	840.00	5%	44
Eastern Harbor	4,000.00	22%	25
Al-Chatby to Stanley	4,964.00	27%	32
Saba Pacha	1,455.00	8%	46
Glim to Tharwat	2,810.00	15%	46
Laurent to Sidi Bishr	2,180.00	12%	37
Miami to Al-Mandara	2,260.00	12%	91
Totals	18,509.00	100%	43

4-4. Deterioration Module

The deterioration modeling for all structures featured the Backward MC Module, followed by the Forward MC Module. For the purpose of illustration, the sudden deterioration effect of intermediate and design storms is shown for Al-Chatby to Sidi Gaber Revetment in Figure 4-21. The figure shows the MC-based timely decline and the storm-induced sudden decline in the overall CI of the structure, considering 2 scenarios of design and intermediate storms. For ease of optimization using GA's, these MC deterioration patterns for each structure were translated into best-fit

regression formulae. In the figure, Scenario 1 corresponds to the occurrence of a design storm in year 2016, followed by two intermediate storms in years 2018 and 2030. In addition, Scenario 2 features an intermediate storm occurrence in 2016, followed by a design storm in 2035 and an intermediate storm in 2041. The instant drops in CI's upon the occurrence of storms is shown in the figure for both scenarios for the purpose of illustrations, such that the regular deterioration pattern is further resumed following the same trend after storm occurrence.

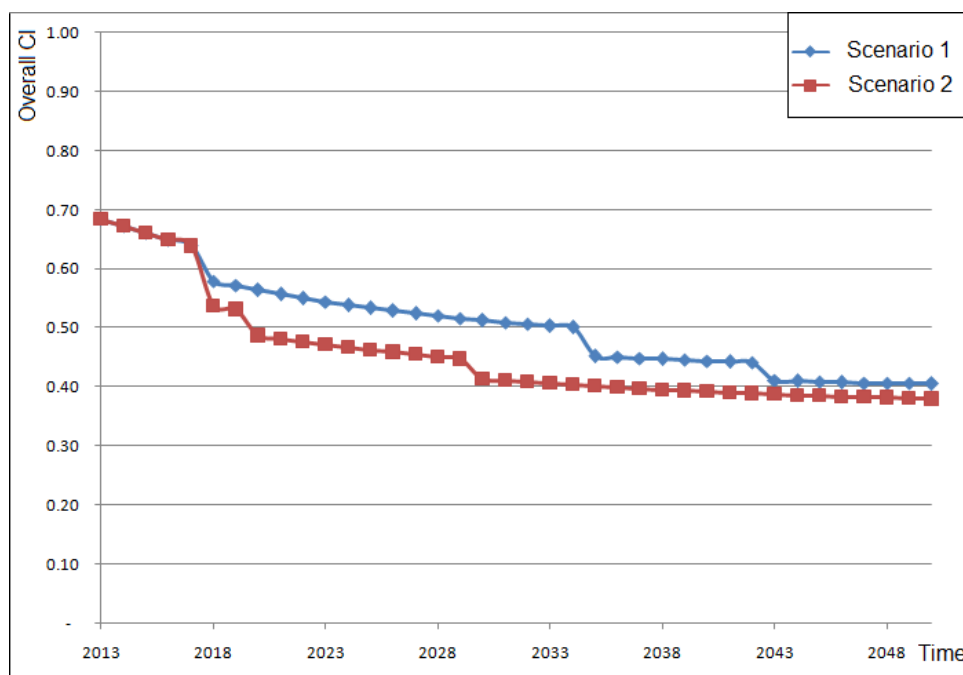


Figure 4-21: Storm simulator demonstration on Al-Chatby to Sidi Gaber Revetment.

4-5. LCC Optimization Scenarios and Results

The LCC optimization scenarios were considered for the entire study area, as shown in Table 4-4. The first running attempts were made directly on the Forward MC Module and integrated with the storm simulator, but significant runtime was consumed when running was made for the entire 198 sub-reaches belonging to the 43 structures within the study area. The PI threshold is the lower limit of the high-risk range as per Table 3-13. As such, the decision was taken to express the complicated forward MC results in terms of mathematical functions using best-fit regression, in order to eliminate the runtime issue and to reduce the model complexity. Furthermore, Figure 4-22 displays the LCC Optimization Module spreadsheet model output formulation. The inflation rate used was 12% annually.

Table 4-4: LCC Optimization Module scenarios.

Scenario	Design Storm	Intermediate Storm	Objective Function	Optimization Variables	Budget Constraint	Intervention Policy Constraint	PI Constraint
1	2018	2016, 2041	Minimize total LCC	Intervention Policies for every structure for each year between 2014 and 2050 (Integer values 0, 1, 2, 3)	2% of initial total construction cost per year for all structures	<ul style="list-style-type: none"> • Maximum of 1 replacement per structure • Maximum of 10 interventions per structure • Maximum of 10 interventions per year for the entire study area 	Maximum PI threshold of 2.00
2	2018, 2048	2016, 2031, 2046					

Annual and Cumulative Cost Matrix					
Structure	2048	2049	2050	Total Structure Cost	Total Budget Constraint Per Structure
West Breakwater	0.00	586,304,975.93	0.00	586,304,975.93	40,525,113.28
Middle Breakwater	0.00	952,189,053.59	0.00	952,189,053.59	73,516,952.42
Qaytbey East Seawall	0.00	0.00	0.00	0.00	1,963,086,455.85
Marine Scouts Quaywall	0.00	0.00	0.00	0.00	867,340,034.15
Rami Station to Al-Silsila Seawall	0.00	73,667,880.00	0.00	73,667,880.00	80,150,665.54
Police Club Quaywall	0.00	0.00	0.00	0.00	257,161,319.72
Stanley Beach Seawall	0.00	0.00	0.00	0.00	74,492,258.07
Pharos Promenade Breakwater	0.00	0.00	0.00	0.00	56,558,936.68
Teachers Club Breakwater	0.00	0.00	0.00	0.00	104,840,955.80
Police Club West Breakwater	0.00	0.00	0.00	0.00	22,071,780.17
Police Club Middle Breakwater	0.00	0.00	0.00	0.00	45,523,046.60
Police Club East Breakwater	0.00	0.00	0.00	0.00	402,226,679.57
Engineers Club West Breakwater	0.00	0.00	0.00	0.00	96,564,038.24
Professional Clubs Breakwater	0.00	0.00	0.00	0.00	211,357,017.79
Glim West Groin	0.00	0.00	0.00	0.00	174,369,539.68
Glim East Groin	0.00	0.00	0.00	0.00	218,965,849.28
San Stefano South Pier	0.00	0.00	0.00	0.00	88,287,120.67
San Stefano North Breakwater	0.00	0.00	0.00	0.00	41,384,587.82
San Stefano Quay	0.00	0.00	0.00	0.00	239,493,897.65
San Stefano East Breakwater / Headland	0.00	0.00	0.00	0.00	13,794,862.61
26 of July Club Submerged Breakwater	0.00	0.00	0.00	0.00	376,976,357.19
26 of July Club East Breakwater	0.00	0.00	0.00	0.00	22,031,814.86
Bir Masoud Breakwater	0.00	0.00	0.00	0.00	41,384,587.82
Miami Breakwater	0.00	35,555,919.54	0.00	35,555,919.54	145,065,359.84
Al-Mandara Breakwater	0.00	212,587,210.34	0.00	212,587,210.34	3,884,859,904.53
Al-Montaza Breakwater	0.00	63,030,948.27	0.00	63,030,948.27	35,866,642.77
Pharos Promenade West Revetment	0.00	20,286,903.28	0.00	20,286,903.28	35,866,642.77
Pharos Promenade East Revetment	0.00	8,790,991.42	0.00	8,790,991.42	82,769,175.63
Qaytbey North Revetment	0.00	0.00	0.00	0.00	195,505,241.46
Bahari Revetment	0.00	0.00	0.00	0.00	44,913,366.28
Marine Scouts Revetment	0.00	0.00	0.00	0.00	8,412,147.49
Al-Manshiya Revetment	0.00	19,645,148.93	0.00	19,645,148.93	105,678,508.90
Al-Silsila to Al-Chatby Casino West Revetment	0.00	0.00	0.00	0.00	383,084,594.75
Al-Silsila to Al-Chatby Casino East Revetment	0.00	0.00	0.00	0.00	25,502,011.31
Al-Chatby to Sidi Gaber Revetment	0.00	0.00	0.00	0.00	59,505,750.58
Armed Forces Club Revetment	0.00	0.00	0.00	0.00	300,559,419.03
Engineers Club Revetment	0.00	0.00	0.00	0.00	557,674,736.78
Glim West Revetment	0.00	0.00	0.00	0.00	1,222,753,496.95
Glim Middle Revetment	0.00	0.00	0.00	0.00	52,875,826.90
Glim East Revetment	0.00	0.00	0.00	0.00	246,336,580.44
Laurent Revetment	0.00	0.00	0.00	0.00	38,253,016.97
Automobile Club Revetment	0.00	0.00	0.00	0.00	243,060,570.46
Bir Masoud Revetment	0.00	0.00	0.00	0.00	2,392,080,641.52
Total Annual Costs	0.00	0.00	0.00	1,972,059,031.30	
Constraint on the Annual Cost	1,045,081,586.70	1,128,688,113.64	1,218,983,162.73	15,572,727,506.80	15,572,727,506.80
	895,989,014.66	967,668,135.83	1,045,081,586.70	13,225,056,230.44	
	1,941,070,601.36	2,096,356,249.47	2,264,064,749.43	28,797,783,737.24	

Total Budget Constraint per Structure

Cost of Decision Variables

Total Budget Constraint for Study Area

List of Structures

Annual Costs and Budget Constraints

Total LCC between 2013 and 2050

Figure 4-22: LCC Optimization Module's output formulation.

Running of Scenarios 1 and 2 was conducted using the MS Excel Evolver™ add-in, featuring a GA-based optimization engine. The population used was 200, with a crossover rate of 80% and a mutation rate of 20%. With a total number of variable possibilities equal to 15.3×10^{16} , hence the stoppage criteria was 24 hours with a total number of trials exceeding 300,000. Crossover rate was decreased and mutation rate was increased in the same proportion when results were shown to be trapped in local minima. Converging results started to show after 35,000 trials approximately for all scenarios. As expected the total LCC for Scenario 2, where double of the number of design and intermediate storms are included as opposed to Scenario 1, was estimated to be 3,144,668,150 EGP. This figure is 62% larger than the total LCC spent on intervention policies in case of Scenario 1. All constraints were successfully met by the LCC Optimization Module for both running scenarios. The cumulative LCC versus time for both scenarios is shown in Figure 4-23. Further, the maximum yearly PI values for the entire study area between 2013 and 2050 for both scenarios are plotted against the PI threshold as shown in Figure 4-24.

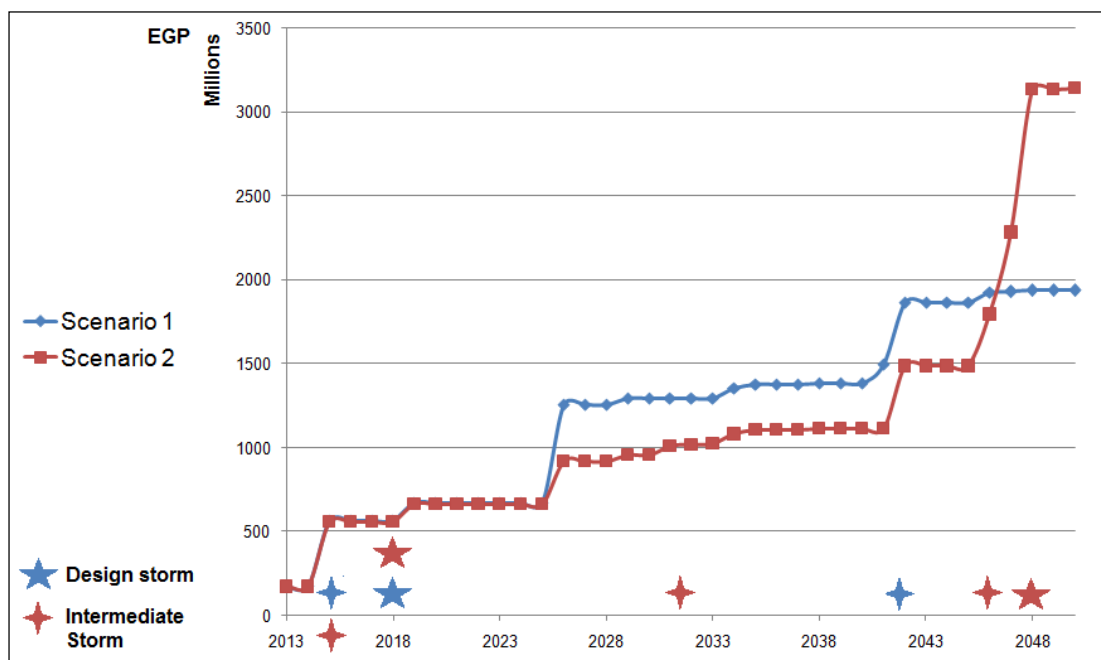


Figure 4-23: Cumulative LCC for all coastal structures within the study area.

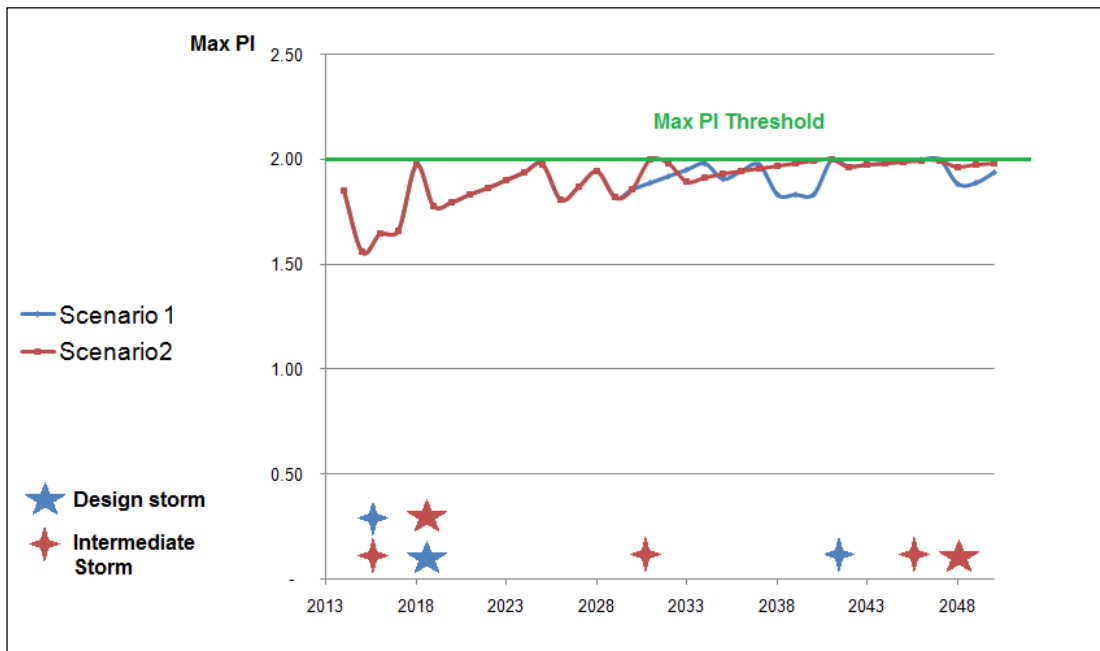


Figure 4-24: PI versus time for the study area against the PI threshold.

Both Figures 4-23 and 4-24 need to be analyzed in relation to each other. For instance, the cumulative LCC expenditures between 2013 and 2025 coincide perfectly in both scenarios, and are echoed by superposed maximum PI values for both scenarios. Starting year 2031, Scenario 2 maximum PI value approaches to the PI threshold at a faster rate than Scenario 2 due to the intermediate storm taking place in Scenario 2 in 2031. Between 2031 and 2050, the cost required to keep the maximum PI values below the threshold of 2.00 was significantly larger in Scenario 2 compared to Scenario 1, given the more frequent storm occurrences in the former scenario. Furthermore, while less LCC, Scenario 1 was able to achieve less PI values between 2046 and 2050.

The total LCC spent in the period between 2013 and 2050 on each of the four categories of coastal structures is shown in Figure 4-25. The data were obtained from actual bills of quantities from the study area, provided after taking the permission of a list of local contracting and design firms. Some other replacement cost data for specific structures were available in the literature for the study area as in Tetra Tech (1985:1986). It is evident that while rubble-mound breakwaters and groins, rubble-mound revetments, and non-rubble seawalls and quaywalls exhibited very minor LCC variance per meter run between Scenarios 1 and 2; the LCC of composite breakwaters exceeded 1,600,000 EGP per meter run between 2014 and 2050 in

Scenario 2. Moreover, in most of the years between 2025 and 2048, Scenario 1 achieved better PI performance but with more LCC expenditures than Scenario 2.

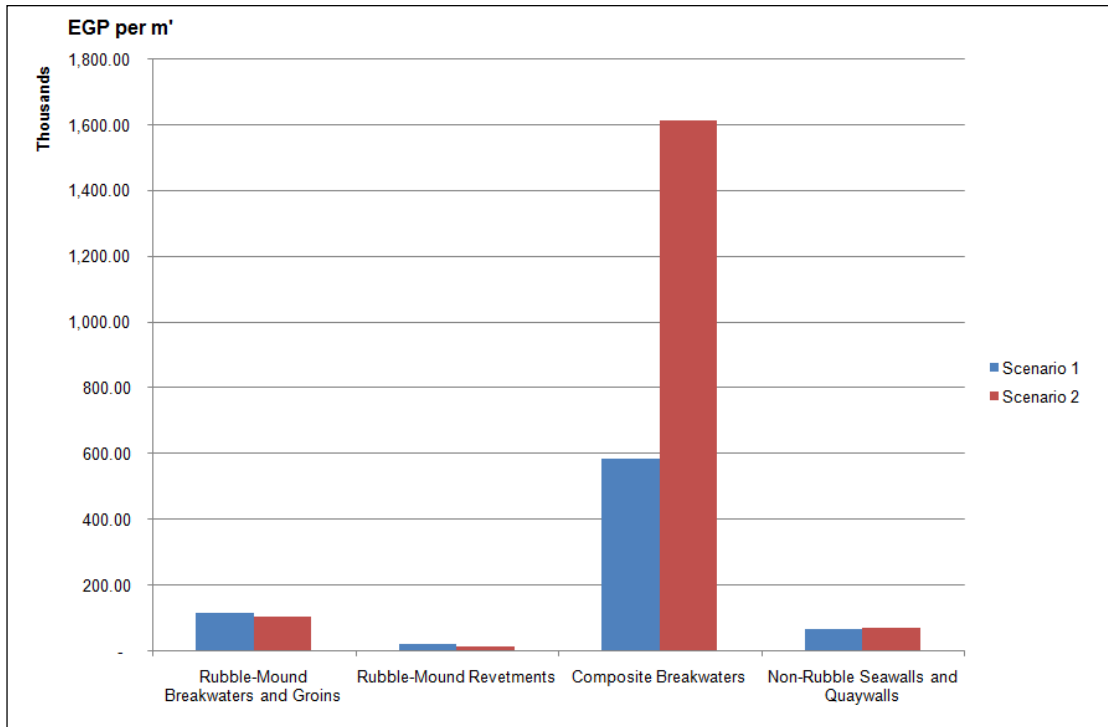


Figure 4-25: LCC per meter run per structure type between year 2013 and 2050.

Prior to performing the categorization of LCC per type of structure, it could have been premature to attribute the significant variance in the total LCC between both scenarios to the costs allocated for routine maintenance, rehabilitation, and replacement, following the more frequent storm occurrences in Scenario 2. While this assumption does not in fact prove to be the case for rubble-mound structures in general, it is evident in the case of non-rubble seawalls and quaywalls, and extremely evident in the case of composite breakwaters. Composite breakwaters in Alexandria are the West and Middle Breakwaters protecting Alexandria’s Eastern Harbor basin. Those massive structures were constructed in 1929, and were subject to a major rehabilitation in 1986, as explained in Tetra Tech (1985:1986). Those structures rest on a stone pad and toes, with concrete blocks weighing 10, 35, and 70 tons, as shown in Figure 4-26. In 1986, the seaside 35-tons then-damaged blocks were compensated by pell-mell 15-ton modified cubes.

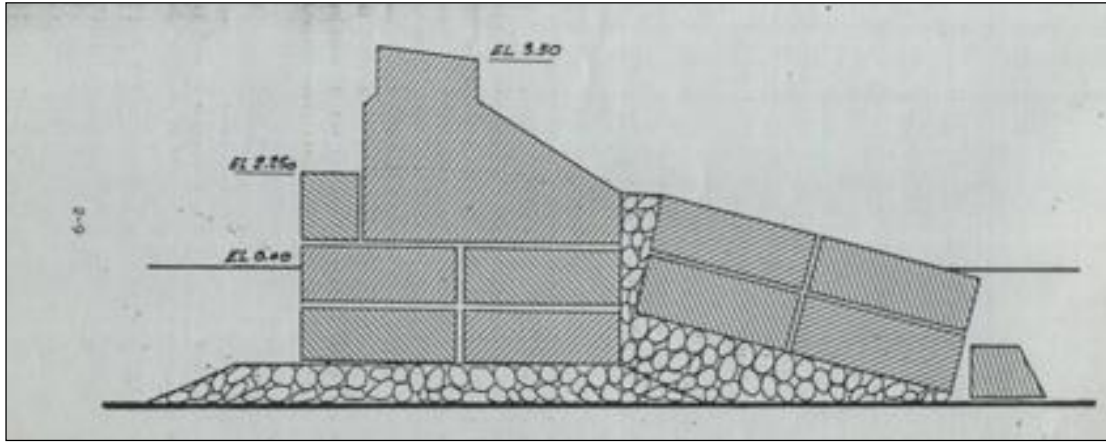


Figure 4-26: Cross-section of the Eastern Harbor Breakwaters, (Tetra Tech, 1986).

Amongst all of the 43 structures included in the scope of this research, those particular two breakwaters stand out in terms of the magnitude of seaside still-water depth at their toe, exceeding 13.00 m (El-Geziry et al., 2007). Rubble-mound revetments and non-rubble seawalls and quaywalls are all located directly on the shoreline, with water depths at toe varying between 1.00 m and 3.00 m. Rubble-mound breakwaters and groins are either shore-connected elevated structures, or shore-parallel submerged structures, in either cases the maximum water depth at the toe varies between 1.00 m and 10.00 m. Given the above, the justification as to the reason behind the dramatic increase in LCC for the Eastern Harbor composite breakwaters in Scenario 2 could be summarized as follows:

1. High risk factor attributed to both structures, prompting more frequent interventions as opposed to other structures.
2. Both structures possess the deepest still-water level at the toe of the structure amongst the entire study area, hence are the most prone to increased hydrodynamic wave impact in storm events.
3. Both structures require waterborne construction methods, taking into account that the middle breakwater is the most distant structure from the shoreline in the entire study area.
4. The costs associated with the maintenance, rehabilitation, and replacement of such composite structures and their 10, 35, and 70-ton

concrete blocks are significantly higher than ordinary rubble-mound structures. This cost is even greater taking into account the inflation rate.

5. Rubble-mound revetments were not significantly affected by decreased storm return periods being the closest to the shoreline, such that the maximum H_s would be equivalent to 78% of the maximum still-water depth at toe, and could hardly be affected by deep-water waves and hydrodynamic conditions during storms. This appeared through the less cost spent per unit length over the study period as opposed to composite breakwaters for instance.
6. Rubble-mound breakwaters and groins are shore-connected except the submerged breakwaters in Miami and Al-Mandara areas. This means they are less prone to increased wave heights due to climate change effects. The cost spent per linear meter for these structures was significantly larger than rubble-mound revetments due to the involvement of waterborne construction. However, the cost spent per meter run for rubble-mound breakwaters and groins was significantly less than composite breakwaters due to the less armor layer weight, and to the more shallow underwater profile depths.
7. The vast majority of non-rubble structures are located inside the Eastern Harbor basin, and already protected by the primary protection structures: the Eastern Harbor West and Middle Breakwaters. Which means the more cost allocated to the primary protection structures, the more the secondary structures would be maintained, even if this occurs unintentionally.

It could be also observed from the above findings that the effect of climate change impacted those structures that are farthest from the shoreline the most. In addition, the LCC results obtained for 41 out of 43 structures in the study area, and occupying almost 60% of the total length of the study area, echo the findings suggested in Iskander (2013), whereby the coastal protection structures in Alexandria were found to be over-designed and hence were estimated not to be significantly affected by increased hydrodynamic loading resulting from global climate change.

4-6. Risk Optimization Scenarios and Results

The Risk Optimization Module's objective function is to minimize PI_T . Table 4-5 illustrates the running scenarios for the optimization, along with the years of intermediate and design storm occurrence, and the optimization constraints. The aim behind these scenarios is to provide an assessment platform for the risk performance of all the structures in the study area against the combination of LCC constraints with climatic conditions. The same GA running and stoppage strategy followed for the LCC Optimization Module were followed in the Risk Optimization runs.

As shown in Figure 4-27, the total LCC is plotted against PI_T , the results of Scenarios 1 to 6 show that risk level reflected by the value of PI_T , is inversely proportional to the total LCC. Furthermore, it is observed that as the budget constraint is gradually lifted, the rate of decrease in risk, reflected by the decreased PI_T value, for the normal climate conditions tends to be asymptotic; while the rate of decrease in PI_T for the stringent climate condition is exponential. This result that was actually expected, and constitutes in itself a validation of the consistency of the Risk Optimization Module outcomes

Table 4-5: Risk Optimization Module scenarios.

Scenario	Design Storm	Intermediate Storm	Objective Function	Optimization Variables	Budget Constraint (Yearly % of initial construction cost)	Intervention Policy Constraint
1	2018	2016, 2041	Minimize PI_T	Intervention Policies for every structure for each year between 2014 and 2050 (Integer values 0, 1, 2, 3)	2 %	<ul style="list-style-type: none"> • Maximum of 1 replacement per structure. • Maximum of 10 interventions per structure • Maximum of 10 interventions per year for the entire study area
2	2018	2016, 2041			4 %	
3	2018	2016, 2041			6 %	
4	2018, 2048	2016, 2031, 2046			2 %	
5	2018, 2048	2016, 2031, 2046			4 %	
6	2018, 2048	2016, 2031, 2046			6 %	

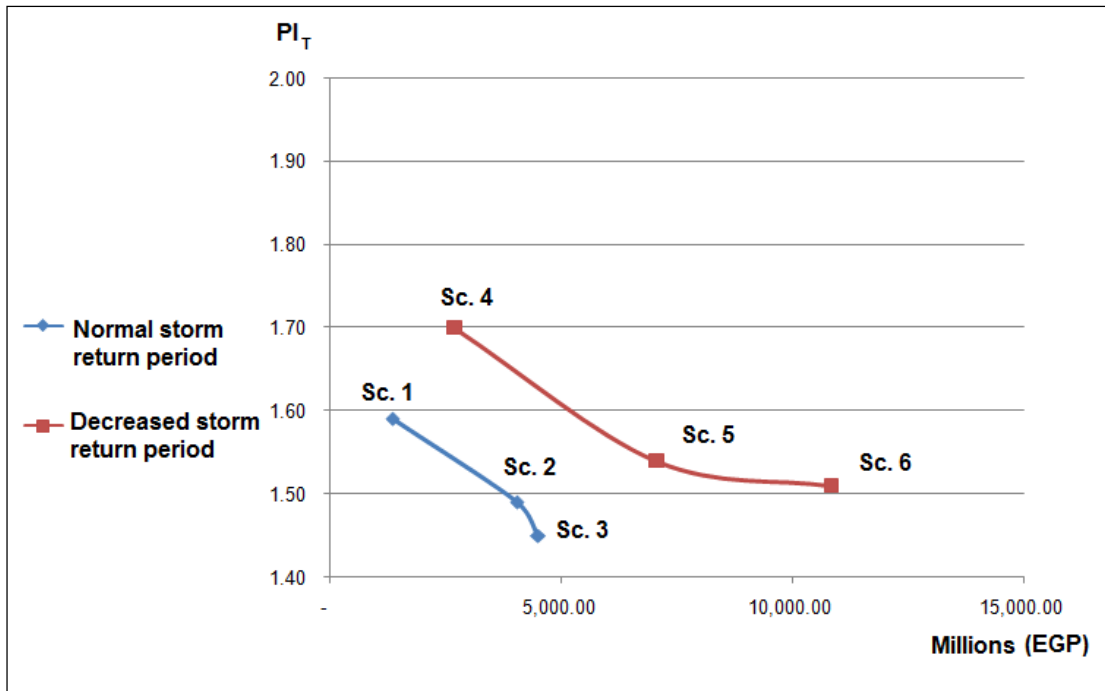


Figure 4-27: Risk Optimization Module results for the six scenarios.

Nevertheless, the results show that for the same budget ranges, but in case of low storm return periods, the risk exposure level expressed by PI_T becomes on average 8% higher as opposed to the scenarios featuring normal storm return periods. The budget ranges in all 6 scenarios were sufficient in terms of keeping the PI_T values well below the High Risk threshold of $PI_T = 2.00$. In view of the results of the Risk Optimization Module, the following observations could be deduced:

1. For the same climatic conditions but for different budget expenditures, the risk level decreases the more budget is allocated for maintenance, repair, and replacement.
2. For the same budget range but for different climatic conditions, the risk level increases with the decrease in design and intermediate storm return periods.
3. The cost of minimizing the value of PI_T increased by 200%, 175% and 241% in case of stringent storm conditions compared to the normal storm conditions, in the scenarios featuring low, medium, and high budget constraints, respectively.

4-7. Verification and Validation

4-7.1. Verification of AID Data Sufficiency and Accuracy

Due to the lack of any records of inspection and condition rating of coastal structures in Alexandria, the author conducted his own field survey and visual inspection of the study area between March and July 2013. The author visually inspected a total length of approximately 19 km, and documented the inspection with approximately 6000 photographs of the surveyed structures. The visual inspection and condition rating procedures were according to the REMR procedures of the US Navy Corps of Engineers. Furthermore, the verification of the outcomes of the inspection and condition rating was conducted through the advice of the experts of the matter.

Extreme care was taken to verify that the gathered raw data correspond to the existing structures at the time of the inspection. This could be further explained in light of the various stages of coastal protection and Cornice Road widening projects in Alexandria. Some acquired bathymetric maps, for instance, were obsolete as they pre-date the Cornice Widening works. An example of this is illustrated in the Glim Bay groins, which were initially four groins, before extending one of these groins and transforming the other into a maintenance embankment leading to the shore-parallel San Stefano breakwater. As such, the verification was first carried out by comparing the raw data received from contractors, design offices, and governmental agencies with the data found in literature, and then checking the findings with field surveys. Field survey findings were also verified against literature data. For instance, the bathymetry of the Eastern Harbor basin was discussed in El-Geziry et al. (2007), who produced a survey of the harbor's seafloor. For the seaside of the Eastern Harbor breakwaters, and the rest of the Pharos peninsula surrounding the Qaytbey Fort, Albrecht et al. (1997) produced another detailed bathymetric survey.

The next step involved verifying the accuracy and sufficiency of the data and field work through expert interviews. This was crucial in order to segregate obsolete from valid data. The verification of historical data was further ascertained by checking the satellite imagery using Google Earth Pro 2013 chronological imagery feature for the study area between 2000 and 2013. In parallel, other reports by Albrecht et al. (1997) and UNESCO (2003) also provide an ascertainment of the data available in AF Co. photographic construction progress report dated 1994, regarding the incomplete marine protection works at the northeastern corner of the fort, due to

the presence of the ancient submerged ruins of the Lighthouse of Alexandria. In addition, a further report by AF Co. in 2010 documents the course of constructing the 26 July Club breakwaters and the Automobile Club protection rip-rap. It includes design cross-sections, bills of quantities, and progress reports showing the impact of the *Kassem* storm that hit Alexandria in December 2010 on the course of construction.

The second part of the required data was surrounding the cost of repair, maintenance and replacement of coastal structures within the study area. This cost is taken as percentages from the construction cost by applying the inflation rate over the studied time period. Most of the previously-mentioned data sources included bills of quantities of the construction costs, however, further guidance as to the best construction and repair methods and their associated cost elements required expert interviews.

Nevertheless, modeling the long-term deterioration of coastal structures also required expert guidance. All of the experts included in Tables 4-6 and 4-7 were interviewed by the author considering the issue of cost data as well as the issue of the effect of single-time events (i.e. intermediate and design storms) on the condition of coastal structures. Among the interviewed experts were contractors, consultants, and engineers working in the field of marine construction.

4-7.2. Condition Rating Procedures and Results

The adopted condition rating approach was first verified during the field survey stage against the procedures and guidelines of REMR, whether in accordance with Oliver et al. (1998) for rubble-mound structures, or Pirie et al. (2005) for non-rubble structures. Prior to the conduction of the field survey, a thorough review of the previous literature addressing shoreline problems, beach erosion, problems in coastal protection works, coastal risk areas, water quality issues, and responses of coastal structures to storms was conducted. For instance, Tetra Tech (1985:1986) discussed structural issues with the Eastern Harbor Middle Breakwater, in addition to functional issues regarding Al-Manshiya Seawall. El-Raey et al. (1995:1999) explained the progression of sand beach erosion and accretion in Alexandria. Meanwhile, Iskander (2000) examined the effect of marine construction activities on sediment transport patterns in the beaches of Alexandria. In addition, as stated in the previous section, the reports by AF Co. (1994), Albrecht et al. (1997), and UNESCO (2003) document the issues with the Qaytbey Fort marine protection works. Furthermore, El Dakkak

(2004) and Hassaan & Abd rabo (2012) observed that the increased wave run-up on the Cornice revetments is a direct result of not using the random pell-mell placement for armor stones. Another study by Sharaki (2007) contained an evaluation of the water quality post the construction of Al-Mandara breakwater, while the response of the same breakwater to the December 2010 storm was examined by El-Sharnouby & Soliman (2011). Last, El Hakea et al. (2014) performed a complete inspection and condition rating of the Eastern Harbor coastal protection structures.

Summing this up, the Inspection and Condition Rating Module procedures and functionality were verified both against the REMR manuals, previous work by others, and through expert consultation. Next, the output of Inspection and Condition Rating Module was further validated by experts of the matter, in the form of interviews conducted with specialized personnel as indicated in Tables 4-6 and 4-7.

4-7.3. Deterioration Modules

Using of the MC-based backward deterioration was the initial step in developing the regression deterioration model. The MC module was carried out by establishing the link between the condition at the year of construction, or at the year of the last major repair, and the condition as rated in 2013. The verification of the MC backward and forward modules was performed in comparison with the procedures outlined in Yokota & Komure (2003) and El Hakea et al. (2014), while the module general functionality was verified by experts of the matter. When consulting experts of the subject matter, this idea was accepted in light of the multitude of uncertainties surrounding the deterioration process, but all while respecting the indicative ranges of the transition probabilities between each of the successive condition state categories. For that purpose, expert feedback was sought by the author as to the indicative limits of the transition probabilities for the DTM's.

On the other hand, the MC-based model's optimization objective function was to match both conditions at the start and ending points of the forecast, as explained in Chapter II, which was carried out with a 2% error margin. Furthermore, the obtained MC deterioration patterns were tested against ANN patterns for the Eastern Harbor coastal structures in El Hakea et al. (2014); where the outcomes of the comparison between ANN and MC deterioration patterns were in favor of the Markovian model. This was a further verification justifying the use of MC modeling.

Regarding the intermediate and design storm simulator, the idea itself was one of the main recommendations for future work suggested by El Hakea et al. (2014) after applying MC modeling of the deterioration of Alexandria's Eastern Harbor coastal structures. The reason behind this recommendation was primarily expert feedback, induced by the importance to consider single-time storm events causing sudden decrease in the CI value of the structure. Expert feedback was essential in estimating the range of CI decrease for each combination of design and environmental attributes within the study area, which constituted the major input in the storm simulator module. As such, the regression-based deterioration model for each structure was based upon data stemming from the MC-based model not only for individual structures, but also for every single reach. Henceforth, the effect of storms on CI's was verified through expert consultation, while the model results in terms of sudden CI drop due to storms were also validated by the same experts listed in Tables 4-6 and 4-7.

4-7.4. LCC and Risk Optimization Modules

The objective of the optimization module is to provide the near optimum set of solutions meeting cost constraints and at the same time keeping the minimum condition state and priority indices thresholds unattained. In the part concerning the cost, the data regarding construction and repair costs were not only gathered from construction companies that carried out the majority of coastal protection works in Alexandria, but also they were verified by experts belonging to these companies. Nevertheless, expert opinion was also of extreme importance in relation of the selection of the maintenance and repair strategies associated with coastal structures, and calculating their cost for the various structures as a percentage of the initial construction cost. The chosen annual inflation rate in the optimization for calculations involving time value of money were taken in line of the CAPMAS average inflation rates for Egypt. Equally important was expert opinion with regards to the identification of risk exposure levels for each structure within the scope of this research, and the expression of such risk levels numerically in order to provide an overall ranking of structures according to their risk level and accounting for their consequences of failure. The major risk areas identified by experts coincided with the risk areas that were found in the literature, which constitutes a further validation of the expert consensus. The formulation of the Optimization module and its functionality were both verified using expert opinion, and the results of the modules

were validated also using expert consultation. Section 4-7.5 provides a summary of expert involvement in the verification and validation of the thesis formulation and outputs.

4-7.5. Summary of Consulted and Interviewed Experts

Table 4-6 lists the various experts consulted in relation to the of the thesis framework, along with their positions and years of experience in coastal engineering and management. In addition, Table 4-7 lists the experts of the matters involved in the validation of the results of the various modules featured in this work.

Table 4-6: List of experts consulted for the data and framework verification.

Position	Company / Agency	Years of Experience	Verification Field
Ex-Chief Engineer	Egyptian Naval Forces	48	Design data; Deterioration Module; Storm Simulator; Risk
Chairman	AF Co.	40	Design, environmental, and historical data; Cost Database
Head of Execution Department	Suez Canal Co. for Marine Works and Mega Projects	30	Cost Database for the LCC and Risk Optimization Modules
Head of Technical Department	Arab Contractors Co., Alexandria Branch	25	Design and historical data; Cost Database; and Storm Simulator
Head of Engineering Department	Alexandria Co. for Construction (Talaat Mostafa)	25	Design and environmental data; Risk
Research Professor	HRI, Alexandria	24	Environmental and historical data; Risk
Head of Technical Department	FZ Consulting Office	23	Design data; Deterioration Module; and Storm Simulator
Head of Engineering Division, PhD	Alexandria Port Authority	20	Design, environmental; and historical data; Risk
Head of Hydrodynamics Department, PhD	Coastal Research Institute	20	Design and environmental data, and Deterioration Module; Risk

Table 4-7: List of experts consulted for the validation of the module outputs.

Position	Company / Agency	Years of Experience	Validation Field
Ex-Chief Engineer	Egyptian Naval Forces	48	Inspection and Condition Rating Module Output
Chairman	AF Co.	40	Deterioration Module output
Head of Technical Department	Arab Contractors Co., Alexandria Branch	25	LCC Optimization Module output
Head of Technical Department	FZ Consulting Office	23	Deterioration Module and Storm Simulator output
Head of Engineering Division, PhD	Alexandria Port Authority	20	Inspection and Condition Rating Module Output
Head of Hydrodynamics Department, PhD	Coastal Research Institute	20	Inspection and Condition Rating Module Output; Deterioration Module including Storm Simulator output, and LCC and Risk Optimization Modules output

CHAPTER V – CONCLUSION AND RECOMMENDATIONS FOR FUTURE WORK

5-1. Research Summary

The stages of this research could be summarized as follows:

1. An AID containing the design, environmental, and historical records of maintenance and repair for coastal structures was first presented. Next, established methods for inspection and condition assessment and rating were discussed. After that, structural and functional inspections were carried out for coastal structures within the study area, followed by condition rating; all in conformity with the REMR guidelines both for rubble-mound and non-rubble structures.
2. The findings of the structural condition rating were considered as a single-inspection point, based upon which a backward MC-based model was established. Such model simulates the structural; deterioration pattern connecting the condition at the year of the construction with the rated condition in 2013. The following step was to utilize the pattern obtained for each structure using the Backward MC Module and project it to the time period spanning the years between 2013 and 2050 to simulate future deterioration; this is the Forward MC Deterioration Module. Based upon expert opinion, in order for the deterioration to be accurate, it needed to account for the sudden drop in CI due to intermediate and design storms. As such, the effects to intermediate and design storms were obtained for each structure based upon expert opinion, where design and environmental data were provided, followed by expert estimation of the decrease that both types of storms inflict on the structure's CI. These data were used to construct the storm simulator and integrate it with the Forward MC Deterioration Module.
3. Afterwards, the Forward MC Module was expressed using best-fit regression for ease of use. The GA-based LCC Optimization Module for maintenance,

repair, and replacement was run for different scenarios of seasonal storm occurrence, within given budget, PI threshold, maximum number of projects per year, and minimum CI constraints. The objective function was to minimize LCC, maximize budget savings, and adhere to the model constraints.

4. Next, the Risk Optimization Module was developed with the objective function of minimizing the total PI of the study area with the same constraints as in the LCC Optimization Module, but without the PI threshold. Finally, a comparison was made between the findings of the running of both modules under various storm occurrence scenarios to account for climate change effect on LCC and risk levels.

5-2. Research Findings

- The primary finding of this research through the field survey of both the functional and the structural conditions of coastal structures within the study area is that there is a pressing need for establishing a robust timely plan for inspection, condition rating, maintenance, rehabilitation, and replacement. This comes given the lack of effective coordinated efforts between the various governmental and private owners of coastal assets as to the establishment and the implementation of an asset management plan encompassing the entire study area. Nevertheless, as shown in Scenarios 1 and 2, the impact of design and intermediate storm frequencies of occurrence on the deterioration of coastal structures, and the associated consequential LCC cost implications varied significantly between both Scenarios. This represents a new tool that is not currently considered in practice by managing authorities and bodies, while being of paramount importance as to future investment needs.
- Another major finding of this work is that unlike the current practice, where coastal structures are being annually maintained with 2% to 6% of their initial construction cost, the LCC Optimization module suggests that introducing distant replacements of armor layer while not stringently following the annual or bi-annual routine maintenance can generate sizable savings on the long run, while meeting budget, CI, and risk constraints. The LCC Optimization

Module running showed that 66% of the estimated annual cost currently being spent on the maintenance and rehabilitation of coastal structures could be saved while maintaining the safe range of the PI threshold.

- The main finding of the LCC Optimization Module runs is that the total LCC is directly proportional to the frequency of storm occurrence for the entire study area. However, this increased LCC was majorly attributed to the Eastern Harbor composite breakwaters, which are in addition to being critical protection structures, are significantly old, distant from the shore, and are the most exposed to hydrodynamic loading and impact. On the other hand, the Risk Optimization Module showed that the risk level is inversely proportional to the maintenance, repair and rehabilitation LCC. In addition, it was demonstrated that for the same budget ranges, but in case of decreased storm return periods, the risk level increases by almost 8%.
- Considering the study area, while various individual attempts were made to study the structural and functional response of certain individual structures within the study area to seasonal storms; this research offers one of the earliest attempts to conduct an overall structural and functional rating of all structures within the study area, using the same inspection and condition assessment criteria. Ratings are based upon visual inspection, REMR procedures, interviews with concerned parties, and expert consultations.
- While most of the structures within the study area are over-designed, which enables them to overcome excessive deterioration due to increased storm intensity in light of global climate change; some structures still have weak sections and reaches where works are either on hold or incomplete. This directly reflects on the calculated SI and FI values. The REMR condition rating equations followed throughout this research are designed in such a way as to approach the overall rating of the structure to the lowest reach rating, given the hydraulic nature of coastal structure. As of 2013-2014; the primary areas of concern are the Qaytbey North Revetment, Al-Manshiya Revetment, and Laurent Revetment in terms of SI value. Regarding the FI values, the primary areas of concern were Al-Chatby to Sidi-Gaber Revetment and Laurent Revetment. Moreover, as suggested by the literature review and the

expert consultations, Alexandria is expected to withstand the impacts of eustatic RSLR in the period between 2014 and 2050, due to the over-design of armor layers in its coastal structures.

5-3. Contribution to the Body of Knowledge

This work offers for the first time an effort to establish future deterioration forecasts for coastal structures based upon a single-inspection point. This is extremely useful in case of the lack of past historical records of condition rating and assessment. Such single-inspection point was the basis for the establishment of the Backward MC Module; another innovation proposed by this research, whose pattern was then projected onto the future to forecast future deterioration of coastal structures using the Forward MC Module.

A major contribution to the body of knowledge in this research is the ability to integrate the impact single-time event on the long-term deterioration of coastal structures due to regular loading, with a MC-based deterioration pattern running in the background. While the MC modules were not used in the LCC and Risk Optimization Modules, since the deterioration patterns were expressed using best-fit regression curves, MC-based deterioration patterns using single-time storm impact were obtained. The integration between condition rating, deterioration, LCC, risk exposure, and climate change effect is yet the major contribution of this work to the body of knowledge with regards to IAM in general, and coastal structures in particular.

5-4. Research Limitations

When running the LCC and Risk Optimization Modules directly on the Forward MC Deterioration Module, significant amount of computer memory and runtime were consumed; this directed the research towards establishing deterministic best-fit regression curves to represent the deterioration patterns obtained using the stochastic Markovian approach. This represented the overcoming mechanism as to the difficulty in running the GA-based optimization on the MC modules.

In addition, while it was practically difficult to accurately validate the findings of the LCC Optimization Module in view of the fact that coastal structures in the study areas are in fact owned by more than a dozen of public and private

institutions; the choice of the suggested repair, maintenance and rehabilitation policies was actually based upon the consensus of the majority of these owning bodies. The model nevertheless is capable of optimizing the annual intervention costs within a predefined budget spanning the entire horizon of the study.

5-5. Recommendations for Future Work

The quality of inspections may be further enhanced using modern inspection tools and technologies, especially for under-water portions of coastal structures, and more important, for submerged breakwaters. It is understood that the costs associated with underwater inspections are significant, but will provide more reliable figures for actual condition indices, and hence increasing the accuracy of the deterioration forecast. Radar sonography and air photogrammetry are two suggested inspection technologies in addition to inspections using divers, as discussed in Chapter II.

As discussed in Section 5-4 of this Chapter, a future area of work is envisioned in the conduction of another round of visual inspection and condition rating of the study area to refine and retune the findings of the Backward MC Module, obtained using a single-inspection point. The Backward MC Module shall be then applied between two exactly known data points, where actual inspections and condition ratings would have been carried out. By the same token, the MC deterioration forecast model can be systematically upgraded with every new inspection and condition assessment.

A new window for future research is suggested whereby various runs for the optimization module are carried out but using different sets of storm return periods. This is viewed as an essential need for sensitivity analysis and long-term management planning for coastal assets, especially in light of the ever-increasing environmental impacts of global climate change. Another suggested area of study is the examination of the deterioration rate of coastal structures after the n^{th} intervention. In IAM, most types of infrastructure assets, the rate of deterioration after a certain number of interventions increases when compared to the rate of deterioration immediately after earlier intervention during the asset lifetime. Hence, another suggested refinement to the model is the provision for the increased deterioration patterns both after the n^{th} intervention, and after the n^{th} storm.

Through the various attempts for running the Optimization Module, it is highly recommended not to run such module directly on the MC-based deterioration modules using the MS Excel Evolver™ evolutionary algorithm add-in; unless the specifications of the computer can support at least 16GB of Random Access Memory (RAM); which is quite uncommon even in advanced university computer labs. For this reasons, it is also recommended to explore new fields and new tools of deterioration prediction other than the MC technique; such as Fuzzy Logic, in order to avoid data oversize and eliminate runtime issues while running a GA-based Optimization Module.

REFERENCES

- Adger, W. N., Hughes, T. P., Folke, C., Carpenter, S. R., & Rockstrom, J. (2005). Social-Ecological Resilience to Coastal Disasters. *Science*, 507 (5737), 1036-1039.
- AF Co. 26 July Armed Forces Club Marine Works. Alexandria, 2010: Unpublished.
- AF Co. *Qaytbey Fort Marine Protection Works*. Abdel-Salam El-Fiky for Marine Construction. Alexandria, 1994: Unpublished.
- Aguirre, R., & Plotkin, D. (1998). *REMR Management Systems - BREAKWATER Computer Program User Manual (Version 1.0)*. US Army Corps of Engineers.
- Ahrens, J. P. (1975). *Large wave tank tests of riprap stability. Technical Memorandum 51*. Vicksburg, MS: US Army Engineer Waterways Experiment Station, Coastal Engineering Research Center.
- Ahrens, J. P., & McCartney, B. L. (1975). Wave period effect on the stability of riprap. *Proceedings of the Conference on Civil Engineering and Oceans III* (pp. 1019-1034). Reston, VA: ASCE.
- Albrecht, D., Menon, J.-M., Peltier, E., & Allam, Y. (1997). *Wave propagation and sedimentation at the Pharos site*. Retrieved April 12, 2013, from Environment and Development in Coastal Regions and in Small Islands: <http://www.unesco.org/csi/pub/source/alex9.htm>
- Arab Contractors. *Marine Protection Works and Renovation of the Corniche*. Alexandria and the Delta Sector, Alexandria Branch. Alexandria: Information Center of the Arab Contractors - Alexandria Branch, 2007: Unpublished.
- Breakwaters (2000). In *Fishing Harbor Planning, Construction and Management* (pp. 87-106).
- Broderick, L. L. (1983). Riprap stability, a progress report. *Proceeding of the Coastal Structures 83'* (pp. 320-330). ASCE.
- Bucharth, H. F. (1984). Fatigue in breakwater armour units. *Proceedings of the 19th International Conference on Coastal Engineering* (pp. 2592-2607). Reston, VA: ASCE.
- Bucharth, H. F. (1991). Introduction of partial coefficients in the design of rubble-mound breakwaters. *Proceedings of the Coastal Structures and Breakwaters Conf.* (pp. 543-566). London: ICE, UK.

- Bucharth, H. F. (1997). Reliability based design of coastal structures. *Advances in Coastal and Ocean Engineering* , 3, 145-214.
- Bucharth, H. F. (2000). Reliability based design of coastal structures. In *Coastal Engineering Manual (CEM)* (pp. VI.6.1 - VI.6.47). Vicksburg, MS: Coastal Engineering Research Center.
- Bucharth, H. F. (1994). Reliability evaluation of a structure at sea. *Proceedings of the International Workshop on Wave Barriers in Deep Water*. Yokosuka, Japan: Port and Harbour Research Institute.
- Bucharth, H. F., & Sorensen, J. D. (1998). Design of vertical wall caisson breakwaters using partial safety factors. *Proceedings of the 25th International Coastal Engineering 2*, pp. 2138-2151. Reston, VA: ASCE.
- Carver, R. D., & Wright, B. L. (1991). *An investigation of random variations in the stability response of stone armored, rubble-mound breakwaters*. Technical Report CERC-91-17. Vicksburg, MS: US Army Engineer Waterways Experiment Station.
- Castillo, C., Castillo, E., Fernandez-Canteli, A., Molina, R., & Gomez, R. (2012). Stochastic model for damage accumulation in rubble-mound breakwaters based on compatibility conditions and the central limit theorem. *Journal of Waterway, Port, Coastal, and Ocean Engineering*, 451-463.
- Castillo, C., Minguez, R., Castillo, E., & Losada, M. (2006). An optimal engineering design method with failure rate constraints and sensitivity analysis: Example application to composite breakwaters. *Coastal Engineering*, 53 (3), 1-25.
- Castillo, E., Iglesias, A., & Ruiz-Cobo, R. (2004). Functional equations in applied sciences. *Mathematics in Science and Engineering* .
- CIRIA. (2007). Chapter 9 - Construction. In CIRIA, *Rock Manual. The Use of Rock in Hydraulic Engineering* (2 ed., pp. 1067-1176). London, UK: CIRIA.
- CIRIA. (1991). *Manual on the use of rock in coastal and shoreline engineering*. Construction Industry Research and Information Association. London: CIRIA.
- Davies, M. H., Mansard, E. D., & Cornett, A. M. (1994). Damage analysis for rubble mound breakwaters. *Proceedings of the 24th Coastal Engineering Conference 1*, pp. 1001-1015. Reston, VA: ASCE.
- El Dakkak, M. A. *Alexandria's Corniche and Beaches: A Status Assessment*. Alexandria: TELConsult, 2004: Unpublished.
- El Hakea, A., Abu-Samra, S., Hosny, O., & Osman, H. (2014). Structural Deterioration Prediction Modeling for Alexandria City Coastal Structures using

- Markov Chains and Artificial Neural Networks. *Proceedings of the Construction Research Congress 2014*. Atlanta, GA: ASCE.
- El-Geziry, T. M., Abdellah, R. G., & Maiyza, I. A. (2007). Bathymetric Chart of Alexandria Eastern Harbor. *Egyptian Journal of Aquatic Research*, 33 (1), 15-21.
- El-Nahry, A. H., & Doluschitz, R. (2010). Climate change and its impacts on the coastal zone of the Nile Delta, Egypt. *Environment, Earth and Science* (59), 1497-1506.
- El-Raey, M., Dewidar, K., & El Hattab, M. (1999). Adaptation to the impacts of sea level rise in Egypt. *Climate Research* , 12, 117-128.
- El-Raey, M., Nasr, O., Frihy, O. E., Desouki, S., & Dewidar, K. M. (1995). Potential Impacts of Accelerated Sea-Level Rise on Alexandria Governorate, Egypt. *Journal of Coastal Research* (14), 190-204.
- El-Sharnouby, B., & Soliman, A. (2011). Behaviour of shore protection structures at Alexandria, Egypt, during the storm of 2010. *Coastal Engineering Practice* , 780-792.
- El-Sharnouby, B., El Dakkak, M., & Soliman, A. (2010). Integrated Overview for the Egyptian Delta Coasts Problems. *8th International Conference on Role of Engineering Towards a Better Environment*. Alexandria, Egypt: Alexandria University.
- Fanos, A. M., & Sharaf El Din, S. H. (2008). The impact of sea level rise and how it will effect in the Nile Delta Coast. *IEEE* .
- Farouk, A.-A. (1985). Erosion of the Nile Delta coast. *Coastal Zone* , 1601-1611.
- Font, J. B. (1968). The effect of storm duration on rubble mound breakwater stability. *Proc. 11th Coast. Eng. Conf. 1*, pp. 779-786. Reston, VA: ASCE.
- Frihy, O. E. (2001). The necessity of environmental impact assessment (EIA) in implementing coastal projects: lessons learned from the Egyptian Mediterranean Coast. *Ocean & Coastal Management* (44), 489-516.
- Frihy, O. E. (2003). The Nile Delta-Alexandria Coast: Vulnerability to sea-level rise, consequences and adaptation. *Mitigation and Adaptation Strategies for Global Change* (8), 115-138.
- Frihy, O. E., & Dewidar, K. M. (2003). Patterns of erosion/sedimentation, heavy mineral concentration and grain size to interpret boundaries of littoral sub-cells of the Nile Delta, Egypt. *International Journal of Marine Geology, Geochemistry and Geophysics* (199), 27-43.

- Frihy, O. E., Deabes, E. A., Shereet, S. M., & Abdalla, F. A. (2010). Alexandria-Nile Delta coast, Egypt: update and future projection of relative sea-level rise. *Environment, Earth and Science* (61), 253-273.
- Hassaan, M. A., & Abdrabo, M. A. (2012). Vulnerability of the Nile Delta coastal areas to inundation by sea level rise. *Environmental Monitoring and Assessment*.
- Hudson, R. Y. (1958). *Design of quarry-stone cover layers for rubble-mound breakwaters*. Vicksburg, MS: US Army Engineer Water-ways Experiment Station.
- Hudson, R. Y. (1959). Laboratory investigation of rubble-mound breakwaters. *Journal of Waterway, Harbor Div. , 85* (WW3), 93-121.
- Hughes, S. A. (2003). Monitoring, Maintenance, and Repair of Coastal Projects. In *Coastal Engineering Manual* (Vol. VI, pp. VI.8.1-VI.8.68). US Army Corps of Engineers, Department of the Army.
- Iribarren, R. (1938). Una formula para el calculo de los discos en escollera [A formula for the calculation of rock-fill dikes]. *Revista de Obras Publicas , 116-295*.
- Iskander, M. M. (2000). Sediment Transport Along Alexandria Coast. *Thesis Dissertation . Alexandria, Egypt: Alexandria University*.
- Iskander, M. M. (2013). Wave Climate and Coastal Structures in the Nile Delta Coast of Egypt. *Emirates Journal for Engineering Research , 18* (1), 43-57.
- Jensen, T., Andersen, H., Gronbeck, J., Mansard, E. D., & Davies, M. H. (1996). Breakwater stability under regular and irregular wave attack. *Proceedings of the 25th Coastal Engineering Conference 2*, pp. 1679-1692. Reston, VA: ASCE.
- Kamali, B., & Hashim, R. (2009). Recent advances in stability formulae and damage description of breakwater armour layer. *Australian Journal of Basic and Applied Sciences, 3* (3), 2817-2827.
- Losada, M. A., & Gimenez-Curto, L. (1982). Mound breakwaters under oblique wave attack. *Coastal Engineering , 6* (1), 83-92.
- Mase, H., Sakamoto, M., & Sakai, T. (1995). Neural network for stability analysis of rubble mound breakwaters. *Journal of Waterway, Port, Coastal and Ocean Engineering, 6* (121), 294-299.
- Medina, J. M., & McDougal, W. G. (1990). Discusion on deterministic and probabilistic design of breakwater armor layers. *Journal of Waterway, Port, Coastal and Ocean Engineering, 116* (4), 508-510.






















- Medina, J. R. (1996). Wave climate simulation and breakwater stability. *Proc. 25th Coast. Eng. Conf.* (pp. 1789-1802). Reston, VA: ASCE.
- Medina, J. R., Garrido, J., Gomez-Martin, M. E., & Vidal, C. (2003). Armor damage analysis using neural networks. *Proc. Coast. Struct.* (pp. 236-248). Reston, VA: ASCE.
- Melby, J. A. (1999). *Damage progression on rubble-mound breakwaters. Technical Report CHL-99-17*. Vicksburg, MS: US Army Corps of Engineers, Waterways Experiment Station.
- Melby, J. A., & Kobayashi, N. (1998). Progression and variability of damage on rubble mound breakwaters. *Journal of Waterway, Port, Coastal and Ocean Engineering*, 286-294.
- Minguez, R., Castillo, E., Castillo, C., & Losada, M. (2006). Optimal cost design with sensitivity analysis using decomposition techniques: Application to composite breakwaters. *Structure Safety*, 28 (4), 321-340.
- Nafaa, M. G., Fanos, A. M., & Elganainy, M. A. (1991). Characteristics of Waves off the Mediterranean Coast of Egypt. *Journal of Coastal Research*, 7 (3), 665-676.
- Nguyen, D. V., Van Gelder, P. A., Verhagen, H. J., & Vrijling, J. K. (2010). Optimal inspection strategy for rubble-mound breakwaters with time-dependent reliability analysis. (Ale, Papazoglou, & Zio, Eds.) *Reliability, Risk and Safety*, 1409-1415.
- Oliver, J., Plotkin, D., Lesnik, J., & Pirie, D. (1998, November). *Condition and Performance Rating Procedures for Rubble Breakwaters and Jetties*. Retrieved August 30, 2013, from US Army Corps of Engineers Water Resources Infrastructure:
http://wri.usace.army.mil/remr/technical_reports/operations/REMR-OM-24.pdf
- Oliver, J., Plotkin, D., Lesnik, J., & Pirie, D. (1997). Condition and performance rating system for breakwaters and jetties. *Proceedings of the Annual International Conference of Coastal Engineering*. 2, pp. 1852-1861. New York: ASCE.
- Pfeffer, W. T., Harper, J. T., & O'Neel, S. (2008). Kinematic constraints on glacier contributions to 21st-century sea-level rise. *Science* (321), 1340-1343.
- Pfeiffer, H. L. (1991). *Comparison of four rubble-mound stability equations with prototype data from burns harbor breakwater. MS Thesis, Civil Eng. Dept.* College Station, TX: Texas A&M University.

- Pilarczyk, K. W., & Den Boer, K. (1983). Stability and profile development of coarse materials and their application in coastal engineering. *Proceedings of the International Conference on Coastal and Port Engineering in Developing Countries* (pp. 43-61). Brussels, Belgium: World Association for waterborne Transport Infrastructure (PIANC).
- Pirie, D., Plotkin, D., Kubinski, J., Foltz, S., & McKay, D. (2005). *Condition and Performance Rating Procedures for Nonrubble Breakwaters and Jetties*. Construction Research Laboratory. US Army Corps of Engineers.
- Plotkin, D., Davidson, D. D., & Pope, J. (1991). *REMR Management Systems - Coastal/Shore Protection Structures: Condition Rating Procedures for Rubble Breakwaters and Jetties*. Department of the Army. Champaign, Illinois: US Army Corps of Engineers.
- Prickett, T. (1998). *Coastal Structure Inspection Technologies: Investigation of Multibeam Sonars for Coastal Surveys*. Waterways Experiment Station. US Army Corps of Engineers.
- Quinn, A. D. (1971). *Design and construction of ports and marine structures*. McGraw-Hill.
- Rahmstorf, S. (2007). A semi-empirical approach to projecting future sea-level rise. *Science* (325), 268-370.
- Reson Inc. (2009). *Underwater Inspection using Multibeam Seabat 8125*. Retrieved April 2, 2014, from Youtube:
<https://www.youtube.com/watch?v=GT3Ig0bDG6U>
- Sharaki, M. (2007, October 25). *Evaluation of El-Mandara Breakwater*. Retrieved 2013, from www.coastalconference.com:
http://www.coastalconference.org/h20_2007/pdf_07/2007-10-25-Thursday/Session_8B-Shoreline_Protection/Sharaki-Evaluation_of_Elmandra_Breakwater_-_Alexandria-Egypt.pdf
- Small, C., & Nichols, R. J. (2003). A global analysis of human settlement in coastal zones. *Journal of Coastal Research* , 19 (3), 584-599.
- Sorensen, J. D., & Burcharth, H. F. (2004). *Risk-based optimisation and reliability levels of coastal structures*. Allborg, Denmark: Allborg University.
- SPM. (1984). *Shore protection manual*. Washington DC: US Army Engineer Waterways Experiment Station, US Government Printing Office.

- Teledyne Reson. (2010, November 4). *RESON SeaBat 7125 quay side inspection*. Retrieved April 2, 2014, from Youtube: <https://www.youtube.com/watch?v=kai3wr024p0>
- Tetra Tech. (1985). *Progress Report No. 2: Shore Protection Master Plan for the Nile Delta Coast*. Cairo: Shore Protection Authority.
- Tetra Tech. (1986). *Shore protection master plan for the Nile Delta*. Shore Protection Authority. Cairo: Ministry of Irrigation.
- Thompson, D. M., & Shuttler, R. M. (1975). *Riprap design for wind wave attack. A laboratory study in random waves*. Wallingford, UK: H.R. Walligford.
- Torum, A., Mathiesen, B., & Escutia, R. (1979). Reliability of breakwater model tests. *Proc. Coast. Struct.* (pp. 454-469). Reston, VA: ASCE.
- UNESCO. (2003). *Towards integrated management of Alexandria's coastal heritage*. Coastal region and small island papers 14. Paris: UNESCO.
- US Army Corps of Engineers. (2008). *Coastal Structures Condition Assessment and Standardized Reporting Application*. Retrieved from operations.usace.army.mil: <http://operations.usace.army.mil>
- Van der Meer, J. W. (1988). *Rock slopes and gravel beaches under wave attack. PhD dissertation*. Emmeloord, Netherlands: Delft Hydraulics Laboratory.
- Vidal, C., Losada, M. A., & Mansard, E. D. (1995). Suitable wave-height parameter for characterizing breakwater stability. *Journal of Waterway, Port, Coastal and Ocean Engineering*, 121 (2), 88-97.
- Vidal, C., Losada, M. A., & Medina, R. (1991). Stability of mound breakwater's head and trunk. *Journal of Waterway, Port, Coastal and Ocean Engineering*, 117 (6), 570-587.
- Vidal, C., Martin, F. L., & Migoya, L. (2003). Parametros de oleaje para la descripcion de la evolucion del dano en diques rompeolas. *Actas de las VII Jornadas Espanolas de Coasta y Puertos* (pp. 1-10). Rotterdam, Netherlands: Balkema.
- Vidal, C., Medina, R., & Lomonaco, P. (2006). Wave height parameter for damage description of rubble-mound breakwaters. *Coastal Engineering*, 53 (9), 711-722.
- Vidal, C., Medina, R., Martin, F. L., & Migoya, L. (2004). Wave height and period parameters for damage description on rubble-mound breakwaters. In J. McKee-Smith (Ed.), *Proc. 29th Intl. Conf. Coast. Eng. 4*, pp. 3688-3700. Hackensack, NJ: World Scientific.

- Vrijling, J. K. (2001). Probabilistic design of water defense systems in the Netherlands. *Reliability Engineering and System Safety*, 74 (2001), 337-344.
- Yagci, O., Mercan, D. E., Cigizoglu, H. K., & Kadbasli, M. S. (2005). Artificial intelligence methods in breakwater damage ratio estimation. *Ocean Engineering*, 32, 2088-2106.
- Yokota, H., & Komure, K. (2003). Estimation of Structural Deterioration Process by Markov-Chain and Costs for Rehabilitation. In ASCE, D. M. Frangopol, E. Bruhwiler, M. H. Faber, & B. Adey (Eds.), *Life-Cycle Performance of Deteriorating Structures: Assessment, Design, and Management* (pp. 424-431). ASCE.

APPENDIX 1 – Common Coastal Structure Concrete Armor Units

	Name armour unit	Year of Introduction	Country
	Cube	-	-
	Tetrapode	1950	France
	Tribar	1958	USA
	Modified cube	1959	USA
	Stabit	1961	United Kingdom
	Akmon	1962	Netherlands
	Tripod	1962	Netherlands
	Dolos	1963	South Africa
	Cob	1969	United Kingdom
	Antifer Cube	1973	France
	Seabee	1978	Australia
	Accropode®	1980	France
	Shed	1982	United Kingdom
	Haro	1984	Belgium
	Core-loc®	1995	USA
	A-Jack®	1996	USA
	Diahitis	1998	Ireland
	Ecopode®	2000	France
	Xbloc®	2003	Netherlands
	Accropode II®	2004	France
	Core-loc II®	2006	USA

Note: Accropode® and Ecopode® are registered trademarks of Sogreah; Core-loc® is a registered trademark of the US government

Table courtesy of Delta Marine Consultants.

APPENDIX 2 – AID Summary

No	Zone	Sub-Zone	Structure Name and Type	Material	Design Concept	Seaside Armor Type and Weight	Structure Length (m)
1	Pharos	Pharos Promenade	West Revetment	Rubble-Mound	Sloped	Cubes, 10 tons	300.00
			East Revetment	Rubble-Mound	Sloped	Cubes, 5 tons	130.00
			Pharos Breakwater	Rubble-Mound	Semi-detached	Cubes, 10 tons	130.00
		Qaytbey North	Qaytbey Revetment	Rubble-Mound	Sloped	Modified Cubes, 10 tons	160.00
		Qaytbey East	Qaytbey Seawall	Concrete	Vertical	Modified Cubes, 10 tons	120.00

No	Zone	Sub-Zone	Structure Name and Type	Material	Design Concept	Seaside Armor Type and Weight	Structure Length (m)
2	Eastern Harbor	West Breakwater	West Breakwater	Composite	Semi-detached	Modified Cubes, 10 tons	520.00
		Middle Breakwater	Middle Breakwater	Composite	Detached	Modified Cubes, 10 tons	770.00
		Bahari	Bahari Revetment	Rubble-Mound	Rip-rap	Dolomite rock, 500 kg	165.00
		Marine Scouts Club	Marine Scouts Quaywall	Concrete	Vertical	Cubes, 5 tons	220.00
			West Revetment	Rubble-Mound	Rip-rap	Basalt rock, 10 - 300 kg	150.00
		Al-Manshiya	Al-Manshiya Revetment	Rubble-Mound	Sloped	Antifer, 10 tons	525.00
		Raml Station to Al-Silsila	Eastern Harbor Seawall	Concrete	Vertical	Cubes, 10, 20, and 30 tons	1,650.00

No	Zone	Sub-Zone	Structure Name and Type	Material	Design Concept	Seaside Armor Type and Weight	Structure Length (m)
3	Al-Chatby to Stanley	Al-Silsila to Al-Chatby Casino	West Revetment	Rubble-Mound	Sloped	Dolomite rock, 10 – 300 kg	205.00
			East Revetment	Rubble-Mound	Sloped	Dolomite rock, 10 – 300 kg	270.00
		Al-Chatby to Sidi Gaber	Al-Chatby to Sidi Gaber Revetment	Rubble-Mound	Sloped	Cubes, 10 tons	2,700.00
		Armed Forces Club	Armed Forces Club Revetment	Rubble-Mound	Sloped	Cubes, 10 tons	380.00
		Teachers Club	Teachers Club Breakwater	Rubble-Mound	Semi-detached, elevated	Tetrapods, 3, 10, and 15 tons	460.00

No	Zone	Sub-Zone	Structure Name and Type	Material	Design Concept	Seaside Armor Type and Weight	Structure Length (m)
3	Al-Chatby to Stanley (Cont'd)	Police Club	West Breakwater	Rubble-Mound	Semi-detached, elevated	Tetrapods, 10 tons	200.00
			Middle Breakwater	Rubble-Mound	Semi-detached, elevated	Tetrapods, 15 tons	85.00
			East Breakwater	Rubble-Mound	Semi-detached, elevated	Tetrapods, 15 tons	370.00
			Police Club Quaywall	Concrete	Vertical	None	84.00
		Stanley	Stanley Seawall	Composite	Vertical	None	210.00

No	Zone	Sub-Zone	Structure Name and Type	Material	Design Concept	Seaside Armor Type and Weight	Structure Length (m)
4	Saba Pacha	Engineers Club	West Breakwater	Rubble-Mound	Semi-detached, elevated	Cubes, 10 tons	330.00
			Engineers Club Revetment	Rubble-Mound	Sloped	Dolomite rock, 10 – 300 kg	400.00
			Professional Clubs Breakwater	Rubble-Mound	Semi-detached, elevated	Tetrapods, 5 tons	725.00
5	Glim to Tharwat	Glim Bay	West Groin	Rubble-Mound	Semi-detached, elevated	Cubes, 5, 10, and 20 tons	350.00
			East Groin	Rubble-Mound	Semi-detached, elevated	Cubes, 5, 10, and 20 tons	320.00

No	Zone	Sub-Zone	Structure Name and Type	Material	Design Concept	Seaside Armor Type and Weight	Structure Length (m)		
5	Glim to Tharwat (Cont'd)	Glim Bay (Cont'd)	West Revetment	Rubble-Mound	Sloped	Cubes, 10 tons	50.00		
			Middle Revetment	Rubble-Mound	Sloped	Dolomite rock, 300 – 800 kg	150.00		
			East Revetment	Rubble-Mound	Sloped	Cubes, 5 tons	320.00		
				San Stefano	San Stefano Pier	Rubble-Mound	Semi-detached, elevated	Cubes, 8 tons	360.00
					North Breakwater	Rubble-Mound	Shore-parallel, elevated	Antifer, 14, 20, and 22 tons	370.00
					San Stefano Quay	Rubble-Mound	Shore-parallel, elevated	Cubes, 10 tons	120.00
					East Breakwater (Headland)	Rubble-Mound	Semi-detached, elevated	Antifer, 5, 8, 14, and 20 tons	375.00

No	Zone	Sub-Zone	Structure Name and Type	Material	Design Concept	Seaside Armor Type and Weight	Structure Length (m)	
5	Glim to Tharwat (Cont'd)	26 July Club	East Breakwater	Rubble-Mound	Semi-detached, elevated	Cubes, 10 tons	190.00	
			West Breakwater	Rubble-Mound	Semi-detached, low-crest	Cubes, 10 tons	205.00	
6	Laurent to Sidi Bishr	Laurent	Revetment	Rubble-Mound	Sloped	Cubes, 10 tons	1,140.00	
			Automobile Club	Revetment	Rubble-Mound	Rip-rap	Dolomite rock, 300 – 800 kg	80.00
			Bir Masoud	Bir Masoud Revetment	Rubble-Mound	Sloped	Cubes, 5 and 10 tons	350.00
				Bir Masoud Breakwater	Rubble-Mound	Semi-detached, submerged	Tetrapods, 10 tons	610.00

No	Zone	Sub-Zone	Structure Name and Type	Material	Design Concept	Seaside Armor Type and Weight	Structure Length (m)
7	Miami to Al-Mandara	Miami	Miami Breakwater	Rubble-Mound	Semi-detached, submerged	Tetrapods, 5 and 10 tons	220.00
		Al-Mandara	Al-Mandara Breakwater	Rubble-Mound	Semi-detached, submerged	Tetrapods, 5 tons	1,650.00
		Al-Montaza	Al-Montaza Breakwater	Rubble-Mound	Semi-detached, submerged	Tetrapods, 5 tons	390.00
						Total	18,509.00

APPENDIX 3 – Sample Structural Inspection Sheet

Structural Rating for Rubble-Mound Coastal Structures

Zone Pharos
Sub-Zone: Pharos Promenade **Page** 1 **of** 3
Description of Structure: Rubble-Mound Breakwater **Reach:** 3 (Head)
Asset ID: PH-PP-BW-01 **STA:** 100+00 **to** 130+00
Inspected by: Ayman H. El Hakea **Date:** 16-Mar-13 **Time:** 16:30
Weather: Mild, 18C

Wave Conditions (Water level, wave height, etc.): A. Overtopping B. Non overtopping

Inspection Procedure (walking, boating, other): Walking

Rating Table

Rating Categories	Deficiencies	Cap / Crest		Seaside (or Head)		Leeside	
		Rating (0-100)	Comment No.	Rating (0-100)	Comment No.	Rating (0-100)	Comment No.
Breach		95					
Core-Exposure		95		68	1		
Armor Loss				80	2		
Loss of Armor Contact and Interlock				80	2		
Armor Quality Defetcs				65	3		
Slope Defects				90	4		

Key to Deficiencies

Breach: a) Displaced cap/armor ; b) Settling cap/armor; c) Other
 Core Exposure / Loss: %
 Armor Loss: a) Displaced; b) Settling; c) Bridging; d) Other
 Loss of Armor Contact and Interlock: %
 Armor Quality defects: a) Rounding; b) Cracking; c) Spalling; d) Fracturing
 Slope defetcs: a) Steepening; b) Settling; c) Slipping ; d) Other

Comment Number

Foundation Fault Suspected in: A) Armor Displacement, B) Slope Steepening, C) Slope Sliding
 Caused by: (a) Scour (b) Settlement (c) Shear (d) Liquefaction
 4 Item (A) (B) (C) (a) (b) (c) (d) STA 120+00 to 130+00
 _____ Item (A) (B) (C) (a) (b) (c) (d) STA _____
 _____ Warning signs / gates
 _____ Auxiliary structures (walkways, stairs, navigation lights, etc..)
 _____ Amount of debris in armor (rubble, trash, logs, etc..)

Comments / Recommended Actions

Action Key: IA = Immediate Action; A = Action; M = Monitor; I = Investigate; N = No Action

Comment Number	Action	Location (Stations)	Comments and Sketches
1	IA	All	The underlayer of the breakwater is left exposed between the crest and the armor layer on purpose in the design. Strangely, some of the felucca owners have displaced some armor stones from the leeside exposed portions to create leveled surfaces in order to place their feluccas. Some undelrayer stones can be seen dispersed on top of the leeside armor stones.
2	M	90+00 to 100+00	2 no armor stones on the leeside have been completely displaced down-slope and shifted > 1 full width of the armor stone. This is causing adjacent armor stones to lose interlock.
3	M	All	Some armor units have deep cracks, while the rest all have spalls, exposed gravel, and visible cracks along lifting hooks with stain marks. Damage level on the seaside is slightly higher.
4	M	All	The first row of armor stones adjacent to the crest is tilting at a very steep angle, however, old construction photographs show the steepness angle unchanged. Investigation needs to confirm if this is a design feature.



Photographic Record

Page

3

of

3

Photo Number	Photo	Notes
1		See comment no 2
2		See comment no 3

APPENDIX 4 – Sample Functional Inspection Sheet

Functional Rating for Rubble-Mound Coastal Structures

Zone: Pharos
 Sub-Zone: Pharos Promenade
 Description of Structure: Rubble-Mound Breakwater
 Asset ID: PH-PP-BW-01
 Rater: Ayman H. El Hakea
 Weather: Mild, 18C
 Wave Conditions (Water level, wave height, etc.):

Page: 1 of 2
 Reach: 3 (Head)
 STA: 100+00 to 130+00
 Date: 17-Mar-13 Time: 15:30

A. Overtopping

B. Non-Overtopping

Inspection Procedure (walking, boating, other): Walking

Has structural inspection been recently completed?

YES NO

Rating Table

Function	Rating (0-100)	Comment No.
Harbor Area	Harbor Navigation	95
	Harbor Use	95
	a. Moored Vessles	
	b. Harbor Structures	
	c. Other Facilities	
Navigation Channel	Entrance Use	90
	Channel	2
Sediment Management	Ebb Shoal	3
	Flood Shoal	
	Harbor Shoal	
	Shoreline Impacts	
Structure Protection	Nearby Structures	69
	Toe Erosion	90
	Trunk Protection	4
Other Functions	Public Access	5
	Recreational Use	5
	Environmental Effects	6, 7
	Aids to Navigation	8

Comment No

Are there functional deficiencies which are NOT related to structural defects?

YES NO

7

Is there risk of loss of function within the next budget cycle?

YES NO

Comments / Recommended Actions

Action Key: IA = Immediate Action; A = Action; M = Monitor; I = Investigate; N = No Action

Comment Number	Action	Location (Stations)	Comments and Sketches
1	N	All	No Harbor Use rating is included apart from the Moored Vessels section since the purpose of the breakwater is the provision of a recreational walkway at its crest, and the provision of a micro-harbor at its leeside for small recreational feluccas. The water is generally safe for feluccas at the micro-harbor zone, however, the problem is that due to the lack of mooring accessories, the boat owners places the feluccas on top of the groin's slope. This practice has been consistent ever since the groin was constructed as demonstrated by historic satellite imaging of the area.
2	N	All	No Channel rating is included given that there is no design channel for large boats; the entrance of the micro-harbor only serves small feluccas. The entrance is adequate for safe exit and entrance of these small feluccas but not during storms.
3	N	All	Sediment management not included as the seabed is rocky.
4	M	00+00 to 100+00	Damage on the seaside of the breakwater cannot be attributable to the inadequacy of the head protection given the groin's orientation relative to the prevailing North-Westerly prevailing winds/storm waves.
5	N	All	The Pharos Promenade is a national tourist attraction in Alexandria, and attracts heavy pedestrian traffic as well as street sellers pushing manual chariots. The breakwater at the sub-reach makes pedestrian access safe within the parapet's limits, but there is oversplash during intermediate and heavy storms.
6	A	All	Cleanup of food and plastic waste disposed on top of the filter layer is required. Amount of debris is substantial.
7	M	All	Significant amount of marine algae and floating trash observed on the leeside armor, indicating inadequacy of water quality inside the micro-harbor.
8	N	All	N/A

APPENDIX 5 – Historical Overview of Alexandria’s Marine Protection Works

A5-1. Introduction

The purpose of this Appendix is to provide a literature overview of the case study zone, namely Alexandria, Egypt. This review briefly covers the following sub-topics:

- Site Characteristics of Alexandria;
- Historical Summary of Major Coastal Works in the Study Area; and
- Socioeconomic Impacts of Coastal Risks on the City of Alexandria.

A5-2. Site Characteristics of Alexandria

A5-2.1. Geology, Morphology, and Nature of Beaches

From a geological perspective, Alexandria is located on an elevated rocky Pleistocene carbonate ridge separating the Mediterranean Sea from the Lake Mariout, making it generally considered one of the best naturally-protected zones relative of the northern Nile Delta region; this is illustrated in Figure A5-1.

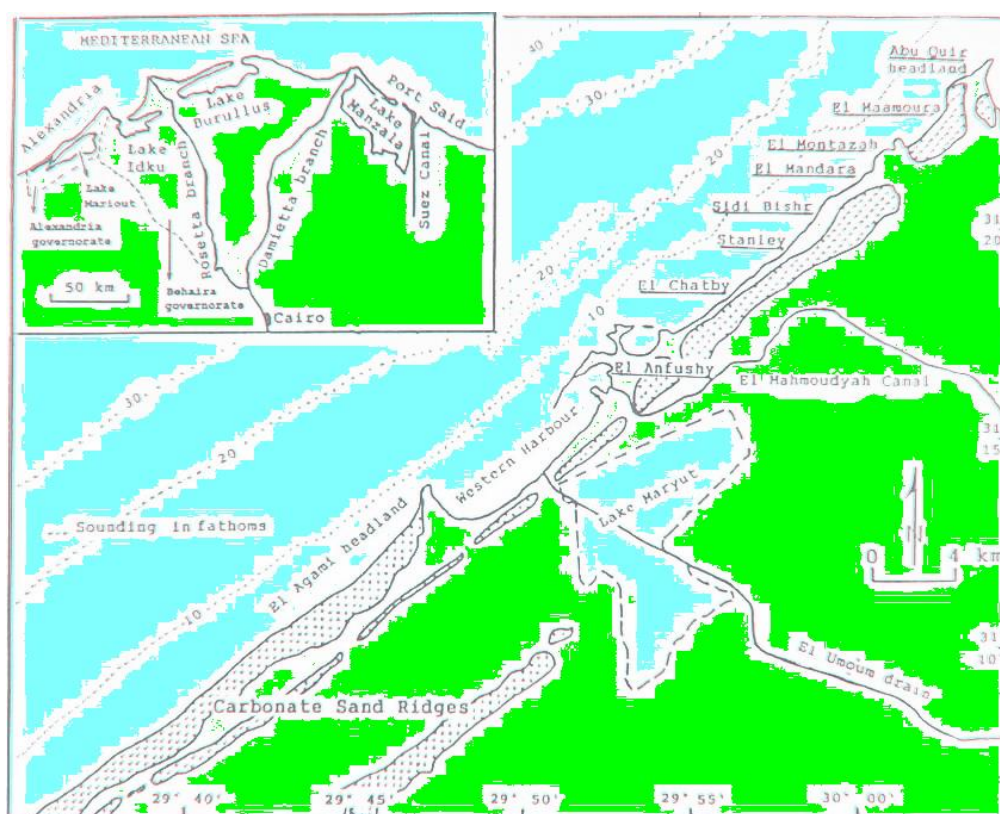


Figure A5-1: Geomorphology of Alexandria¹.

¹ El-Raey, M., Dewidar, K., & El Hattab, M. (1999). Adaptation to the impacts of sea level rise in Egypt. *Climate Research*, 12, 117-128.

The middle parts of Alexandria stretch over a length of approximately 13 km starting from Al-Montaza rocky headland in the east, up to the Eastern Harbor in the west. The coastline and the seabed are predominantly characterized by a rocky nature, featuring a complex bathymetry and topography. The coastline includes a multitude of rocky headlands and outcrops that run almost parallel to the shoreline, which at some locations form islets or reefs. Sandy beaches are either in the form of pocket or perched beaches, or are protected by virtue of natural islets in the same way salient is accumulated at the leeside of a shore-parallel breakwater. Alexandria's beaches have been exposed to noticeable levels of beach erosion amounting to the level of sediment deprivation since the mid 1980's at least. This has been partly due to the lack of sediment sources and to the global eustatic sea level rise, and has been also compounded by the steep offshore seabed slopes off the coast of Alexandria, which are relatively much steeper as opposed to the rest of the northern Nile Delta coasts².

A5-2.2. Winds, Tides, and Waves

The prevailing wind in Alexandria is northerly and north westerly, i.e. between 270° and 360° measured from the north direction, and concentrated in the range between 300° and 330°. The sustained extreme wind speed is approximately between 40 and 60 knots, with return periods of 20 and 30 years respectively. The characteristics of deep water waves in open sea are similar across the northern Egyptian coasts². One of the main features of waves along the northern Egyptian coasts in their high seasonality, such that the highest occurring waves coincide with the winter season, in the period between the beginning of November and the beginning of April. The highest waves come from the west and the North West, during the seasonal storms, which are interrupted by short calm-state periods. Table A5-1 shows the approximate schedule of storms conventionally occurring in Alexandria between October and March every year. This schedule, locally known as *Jadwal Al-Nawwat*, is regarded with high level of attention by whomever involved with port administration and vessel navigation in Alexandria. During the summer season, which starts from mid June up to the beginning of September, the prevailing

² El Dakkak, M. A. *Alexandria's Corniche and Beaches: A Status Assessment*. Alexandria: TELConsult, 2014: Unpublished.

waves are non-stormy and are generated in deep water from the North West and the North directions.

Table A5-1: *Jadwal Al-Nawwat* in Arabic, or the approximate schedule of occurrence of conventional storms in Alexandria³.

Date	Month	Storm Name	Prevailing Wind	Duration (Days)	Description
1	October	Riyah Al-Saliba	W	3	Windy
21	October	Riyah Al-Saliba	W	3	Windy
17	November	Al-Muknisa	NW	4	Heavy rain
5	December	Kassem	SW	5	Stormy
20	December	Al-Fayda Al-Sughra	NW	5	Rainy
29	December	Eid Al-Milad	W	2	Heavy rain
2	January	Ras Al-Sana	W	4	Rainy
12	January	Al-Fayda Al-Kubra	SW	6	Heavy rain
19	January	Al-Ghatas	W	3	Rainy
28	January	Al-Karam	W	7	Heavy rain
18	February	Al-Shams Al-Soghra	NW	3	Rainy
1	March	Al-Saloum	SW	2	Rainy
10	March	Al-Hosoum	SW	7	Rainy
19	March	Al-Shams Al-Kubra	E	2	Windy
24	March	‘Awwa	E	6	Windy

As for spring and autumn seasons wave energy along the Egyptian northern coasts is limited². The seasonality of wave characteristics of Alexandria's waters were discussed in a great level of detail in various previous studies^{2 3 4 5}. Figure A5-2

³ Nafaa, M. G., Fanos, A. M., & Elganainy, M. A. (1991). Characteristics of Waves off the Mediterranean Coast of Egypt. *Journal of Coastal Research*, 7 (3), 665-676.

⁴ Frihy, O. E., Iskander, M. M., & Badr, A. E. (2004). Effects of shoreline and bedrock irregularities on the morphodynamics of the Alexandria coast littoral cell, Egypt. *Geo-Mar Lett.* , 195-211.

provides seasonal wave height distributions in Alexandria's Abu Qir Bay between 1971 and 1977. Field measurements were carried out in Abu Qir bay between 1971 and 1977 using an Offshore Pressure-Operated Suspended Wave Recorder (OSPOS), and then again between 1981 and 1987 using a more advanced and accurate Cassette Acquisition System (CAS). Figure A5-3 shows a schematic of the OSPOS and the CAS wave height measurement devices. The measurements were represented with the wave roses shown in Figure A5-4. The results indicate that the calm condition reaches its maximum during winter and spring, while the stormy condition reaches its peak also during spring and winter.

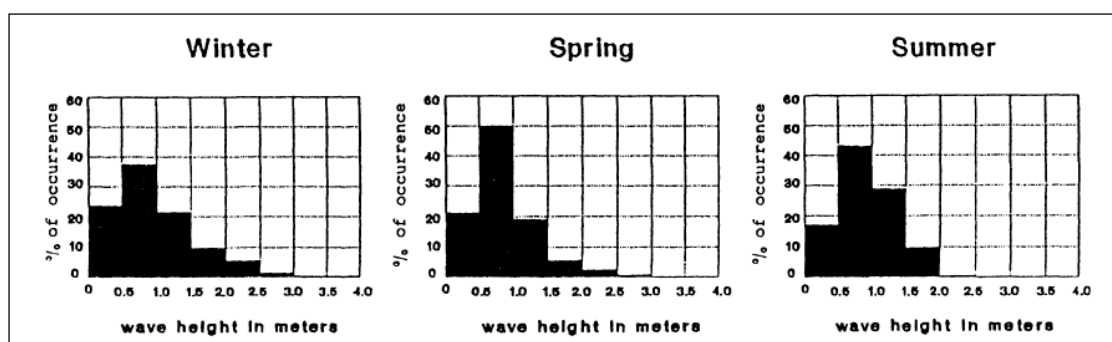


Figure A5-2: Seasonal wave heights measured in Abu Qir Bay (1971-1977)³.

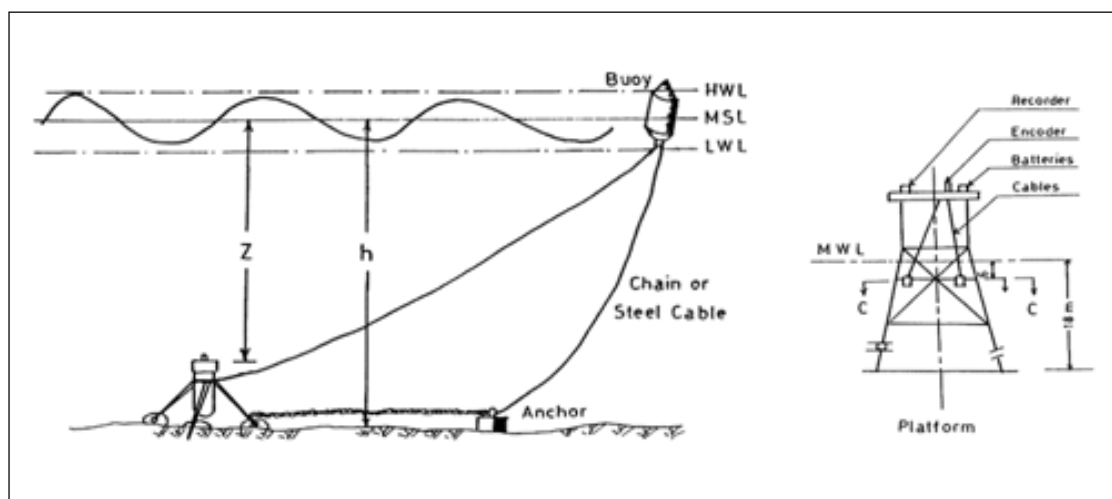


Figure A5-3: OSPOS and the CAS wave recording systems³.

⁵ Frihy, O. E., & Dewidar, K. M. (2008). Pre- and Post-Beach Response to Engineering Hard Structures Using Landsat Time-Series at. *Journal of Coastal Conservation*, 11 (2), 133-142.

The coast of Alexandria is subject to semi-diurnal astronomical tides, which result in MSL fluctuations, which is in its turn further affected by wind and wave set-up. MSL readings in Alexandria are shown in Table A5-2².

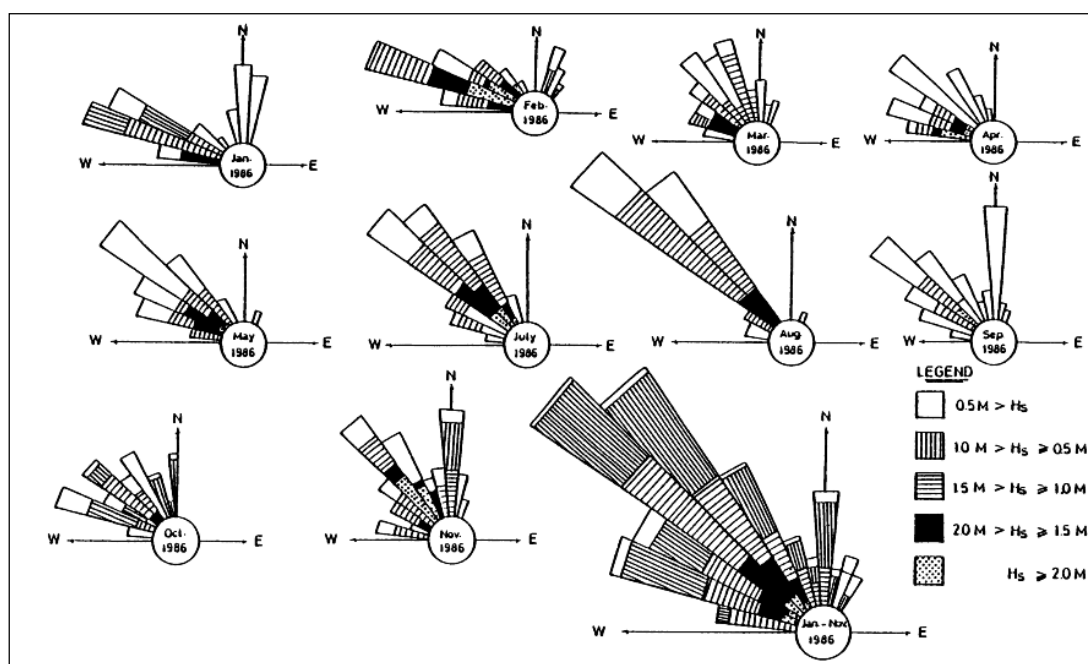


Figure A5-4: Wave roses in Abu Qir Bay in 1986³.

Table A5-2: Effect of tides on sea level fluctuations in Alexandria².

Parameter	Abbreviation	Level relative to Still-Water Level
Highest High Water Level	HHWL	+0.66 m
Mean High Water Level	MHWL	+0.13 m
Still Water Level	SWL	+0.00 m
Mean Low Water Level	MLWL	-0.13 m
Lowest Low Water Level	LLWL	-0.51 m
Admiralty Chart Datum at the Port of Alexandria	ACD	-0.43 m
Survey Datum	SD	-0.29 m

A5-2.3. Currents, Littoral Drift, and Sediment Transport

Nearshore water currents off the shoreline of Alexandria possess small to moderate velocities. Surface current velocities range between 0.25 and 0.50 knots, which is equivalent to approximately 12 to 25 cm/sec, with the prevailing direction being from west to east. As for littoral currents located within wave-breaking zones, their velocities depend upon height, direction, and frequency of waves in addition to the seabed bathymetry. The speeds of such currents may reach 1 m/sec and even more during high wave occurrence. The direction of such littoral currents depends on the direction of incident waves relative to the shoreline orientation. Littoral currents play the essential role in sediment transport to and from beaches, which follows the direction of the currents. This phenomenon is called littoral drift, and results in the evolution of the shoreline and the seabed². Littoral currents and coastal structures have also influenced beach erosion and accretion patterns in the mid-1990s¹.

Previous literature examined the combined effect of longshore and cross-shore sediment transport patterns and coastal structures on the evolution of Alexandria's beaches throughout the 20th century; it was concluded that Alexandria represents a closed sediment transport cell with a distinct nature as opposed to the northwestern Egyptian coast and the Nile Delta⁶. His field work showed that the three sets of submerged carbonate ridges parallel to Alexandria's shoreline, along with Al-Dikheila and Abu Qir headlands allow no sediment input or output. It could be hence stated that as far as sediment transport is concerned, Alexandria's shoreline is in a state of dynamic stability⁶. Furthermore, two master plans of coastal protection works of Alexandria were initiated in 1986 and 1995 by Tetra Tech Inc. and Sogréah, respectively; where the exact scope that was implemented and the consequences of such works on the status of Alexandria's shoreline prior to the Cornice widening works between 1998 and 2002 were discussed⁶. Other works compared the status of Alexandria's coastal structures between Al-Silsila eastwards to Al-Montaza westwards, before and after the widening of the Cornice Road between 1998 and 2002, revealing that most of Alexandria's beaches between Al-Silsila and Al-Montaza disappeared³.

⁶ Iskander, M. M. (2000). Sediment Transport Along Alexandria Coast. *Thesis Dissertation* . Alexandria, Egypt: Alexandria University.

A5-3. Historical Summary of Major Coastal Works in the Study Area

A5-3.1. Greco-Roman Era

Upon being founded by Alexander the Great in 331 BC, Alexandria witnessed its first coastal works by the connection of the Pharos Island to the port town of Rhacotis through the Heptastadion earth dike, the oldest coastal structure ever recorded, to form the Eastern and Western Harbors, as shown in Figure A5-5. The pattern of the shoreline did not remain uniform, as demonstrated by the submerged archeological findings in the Eastern Harbor, the Abu Qir Bay, and the disappeared city of Canopus which was located on the promontory of the Canopic Branch of the Nile, and which extended 8 km to the north of Abu Qir Bay⁷.

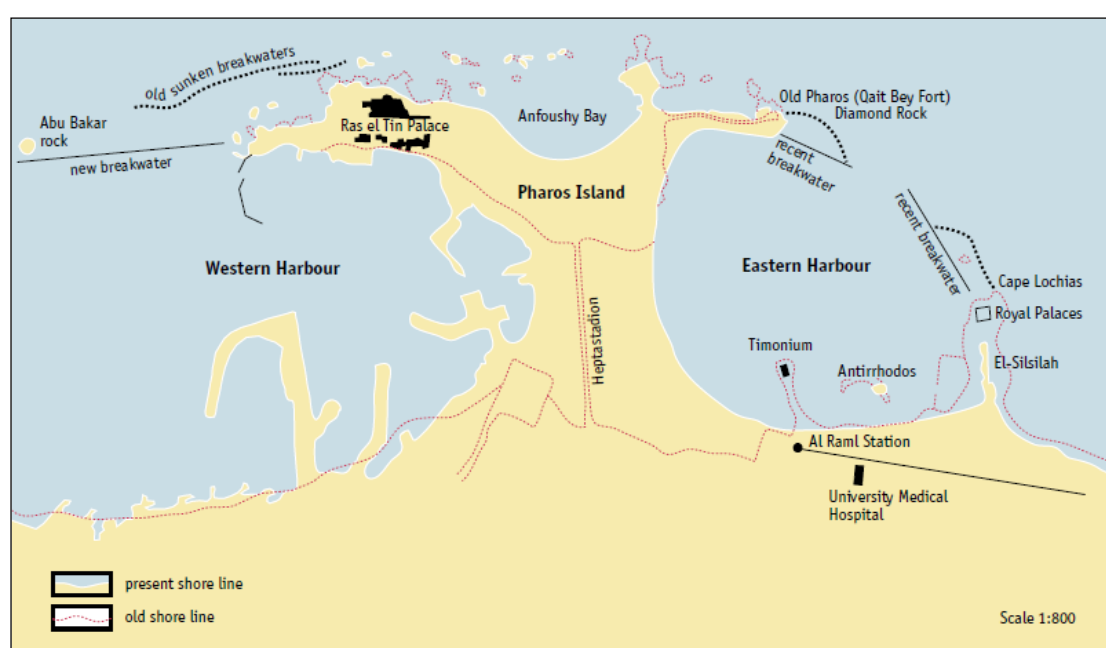


Figure A5-5: Greco-Roman Alexandria and its coastal structures⁷.

A-5.3.2. Modern Era

In the late 17th century, the French constructed a naval wharf in Al-Dikheila during Napoleon Bonaparte's campaign between 1798 and 1799. The area is still known as the French Harbor or *Al-Mina Al-Faransawy* until today. In the early 19th century, Egypt's Governor Muhammad Ali decided to dig Al-Mahmudiya Canal with the aim to deliver potable water from the Rosetta Branch of the Nile to the city of

⁷ UNESCO. (2003). *Towards integrated management of Alexandria's coastal heritage*. Coastal region and small island papers 14. Paris: UNESCO.

Alexandria⁸. This could not be possible given that the Rosetta Branch was separated at that time from the city of Alexandria by the former Abu Qir Lagoon and Mareotis Lake, which consisted of shallow marshlands connected to the Mediterranean Sea in the Abu Qir Bay. Muhammad Ali was capable of drying the Mareotis Lake and Abu Qir Lagoon, and protecting the resulting lowlands which became known by Al-Beheira from the Mediterranean Sea by a seawall along the Abu Qir Bay. Muhammad Ali's Al-Tarh Seawall is still performing its role until today, and has undergone various cycles of failures and subsequent restoration and strengthening throughout its lifetime.

A-5.3.3. Twentieth and Twenty-First Century

In 1929, the current middle and western Eastern Harbor breakwaters were constructed, providing a harbored area for vessels and medium-size ships, and soon followed the construction of the Cornice Road along the city's waterfront in 1934⁹. This construction of the Cornice Road is considered significant, since it provided researchers with a fixed datum line parallel to the shoreline against which sea regression and transgression could be monitored and evaluated. In 1984, the SPA assigned Tetra Tech Inc. of Pasadena, California to develop the Master Plan for Coastal Protection of the Nile Delta Shores up to the year 2005. The Master Plan included all coastal areas bounded between 30 km west of Alexandria and 30 km west of Port Said, and thus included the city of Alexandria⁹. The recommendations of the Master Plan regarding Alexandria were centered on the definition of a set of short-term primary projects that included periodic beach nourishment and monitoring of sediment transport patterns in Al-Mandara area, along with the construction of three rubble-mound shore-parallel breakwaters. For Al-Asafra beach, the Tetra Tech plan recommended the construction of a 60.00 m-long pier to the east, as well as a 40.00 m-long rubble-mound groin to the west of the beach. The plan also suggested periodic beach nourishment for Stanley Beach and the area extending from Al-Ibrahimiya to Al-Chatby, where a 75.00 m-long groin was recommended to be built at the eastern end of Al-Ibrahimiya beach².

⁸ Frihy, O. E., Deabes, E. A., Shereet, S. M., & Abdalla, F. A. (2010). Alexandria-Nile Delta coast, Egypt: update and future projection of relative sea-level rise. *Environ Earth Sci* (61), 253-273.

⁹ Tetra Tech. (1985). *Progress Report No. 2: Shore Protection Master Plan for the Nile Delta Coast*. Cairo: Shore Protection Authority.

In the early 1990's, and through a grant from the French Government, the French house of expertise "Sogréah" produced a detailed design of coastal protection structures designed particularly for Alexandria's beaches. Two pilot projects for the development and protection of Alexandria's sandy beaches were launched in 1997. The first scheme suggested four shore-parallel detached low-crest breakwaters at Cleopatra area, in addition to a rubble-mound groin at the eastern part of Cleopatra beach. The project was awarded by the SPA to the Suez Canal Company for Port Works in 1999. Two of the four breakwaters were constructed between August 1999 and October 2000, but were subjected to severe damage following a winter storm in December 2001. In the report issued by Sogréah on tested prototypes of the breakwaters, it was recommended to increase the weight of armor stone and to transform the structures into elevated breakwaters². While previous works conclude that the detached breakwaters of Cleopatra area represent a case of design failure, the detached breakwaters at Cleopatra area were not completed due to funding issues as advised by the Technical Office Manager of Suez Canal Company.

The second project suggested by Sogréah was the protection of the beach between Al-Chatby and Al-Ibrahimiya with an 800.00 m-long low-crest shore-parallel near-shore breakwater. The SPA awarded the project to the Egyptian Dredging Company, but again, the project did not materialize and was overridden by the Cornice Widening Project. The recommendations of Sogréah's beach protection scheme were only achieved partially in Alexandria, partly due to funding limitations, and partly due to other plans set out by the Alexandria Governorate to widen the Cornice Road as a measure to ease the pressure on the city's main traffic arteries. Both the Tetra Tech and the Sogréah scheme did not take into account the Cornice widening plans. Still during the 1990's, the SCA launched a plan for the protection of the historic Qaytbey Fort located in the Eastern Harbor. However, as will be discussed in the Asset Inventory Database section, the protection was not completely achieved due to the presence of sunken remnants of the ancient lighthouse of Alexandria at the area where the protection works were to be executed.

It was observed through the Google Earth Pro 2013 satellite imagery and also based upon previous literature that some other projects were executed before the Cornice widening works². Such projects include the coastal protection works for clubs and other facilities directly located on the shore, such as the Beaurivage Casino

pier in Miami Beach, and the clubs area extending between Glim and Stanley areas. Marine protection works for numerous other clubs were either constructed or extended after the Cornice widening works, these include the coastal protection works for Mustapha Kamel Armed Forces Club, Teachers Club, Police Club, Engineers Club, Doctors Club, Lawyers Club, Judges Club, Dar Misr, San Stefano Hotel, and 26th of July Club. Periodic beach nourishment projects were also conducted by the SPA during the period between 1986 and 1995, prior to the Cornice widening project. Previous studies provided some details on Alexandria's sandy beaches, along with their sediment change features and the annual periodic sand nourishment costs of eroding beaches as of 1995¹⁰.

The six-phase program for the widening of the Alexandria Cornice started in 1998 and ended in late 2007. The design of the widened Cornice Road featured a retaining wall at elevations ranging between 0 and 6.00 m above still-water level, from field survey. In some areas where there is a beach that is wide enough to protect the Cornice, such beach has been kept as the only type of protection. In other areas where beaches disappeared as a result of the Cornice widening works, a revetment seawall typical cross-section was used for protecting the Cornice. The cross-section consists mainly of a small toe, a slope ranging between 1:2 and 1:3, and two layers of 10-ton plain concrete cube armor stones (1.70 x 1.70 x 1.70 m), laid on top of a stone filter layer, while protecting the underside of the section with geotextile membrane². The armor layer is laid in an orderly way and not pell-mell, creating a smooth impermeable slope. This has led to decreased wave energy dissipation when comparing the current design with placing the armor stone randomly. Furthermore, a plain concrete promenade was built at the crest of the revetment. During the course of the Cornice Widening project phases, several works have been carried out, such as the construction of groins in Al-Mandara and Glim areas².

After the completion of the Cornice widening project in the eastern part of the study area, namely the area between Bir Masoud and Al-Mandara, a series of submerged rubble-mound breakwaters were constructed between 2005 and 2007 in Miami, Al-Mandara and Al-Montaza areas, as a means to protect the low-lying risk

¹⁰ El-Raey, M., Nasr, O., Frihy, O. E., Desouki, S., & Dewidar, K. M. (1995). Potential Impacts of Accelerated Sea-Level Rise on Alexandria Governorate, Egypt. *Journal of Coastal Research* (14), 190-204.

area of Al-Mandara Cornice, protect the sandy beaches in the area, and provide a safe swimming zone for summer tourists. These works have further extended in 2013 to Bir Masoud area for the same reasons and are currently in progress.

A-5.4. Socioeconomic Impacts of Coastal Risks on the City of Alexandria

Given the previously explained risks and their consequential effects on Alexandria's population, properties, and infrastructure, it is essential to consider an effective IAM for Alexandria's coastal protection structures. Such plan is the focus of this study, and shall feature the establishment of condition rating methods for various types of existing coastal infrastructure, followed by modeling the expected deterioration patterns for such structures, according to which the prioritization and optimization of repair and maintenance investments shall be decided.

The necessity behind a sound IAM Plan for coastal protection structures in the city of Alexandria is best advocated in view of the possible estimates of social and economic impact caused by RSLR. Limited number of studies has tackled this issue¹. Figure A5-6 shows an image produced by the LANDSAT program for Alexandria's coastal environs and its land use patterns in 1999. This map was used to estimate the socioeconomic impacts of RSLR on the city of Alexandria, based upon the contour maps of Alexandria, and based upon the net estimated coastal erosion resulting from RSLR in the event of no intervention¹.

However, the predicated shoreline retreat due to RSLR is only a rough estimate given that the basis of estimating the extent of coastal erosion was the two-dimensional Bruun formula, which is in itself considered a global theoretical estimation mechanism and not a case-specific equation that can accommodate the actual site geomorphologic and hydrodynamic features¹¹: The formula is denoted as follows:

$$R = S L (h^* + B)$$

Where:

- "R" is the rate of shoreline retreat;
- "S" is the SLR;

¹¹ Bruun, P. (1962). Sea level rise as a cause of shore erosion. *Journal Waterways and Harbors Division*, 88, 117-130.

- " L " is the active profile length perpendicular to the shoreline;
- " h^* " is the active profile depth; and
- " B " is the berm elevation.

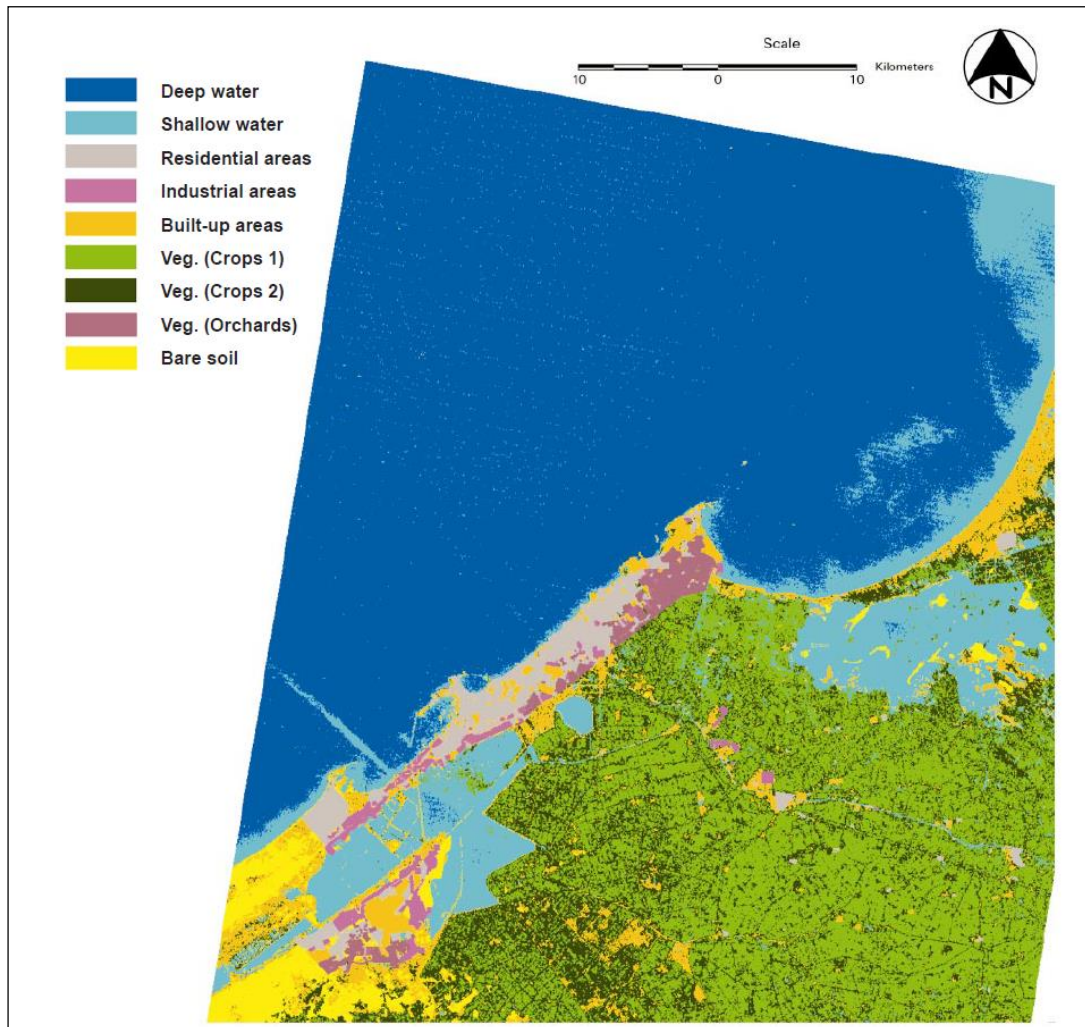


Figure A5-6: Satellite image of Alexandria showing land use features.¹

In addition to the reasons previously stated that limit the reliability of using Bruun's rule in estimating the exact extent of shoreline retreat, the active profile depth is very difficult to obtain¹⁰. In later studies, percentages of population and other land use features that would be endangered due to various scenarios of RSLR in Alexandria were estimated¹. This is further illustrated in Figure A5-7. The figure shows the percentages of population and various types of public and private properties existing in Alexandria at MSL, and percentages of such items that are expected to be lost to the sea under various RSLR scenarios. Further, Table A5-3 displays the estimated displaced population and job losses in tourism and industry in Alexandria Governorate in 2025 and 2050, for RSLR of 0.30 m and 0.50 m¹. The

table shows the predicted area losses and loss of employment in various economic sectors in Alexandria as a result of RSLR in 2025 and 2050, using the two-dimensional Bruun's rule for shoreline retreat.

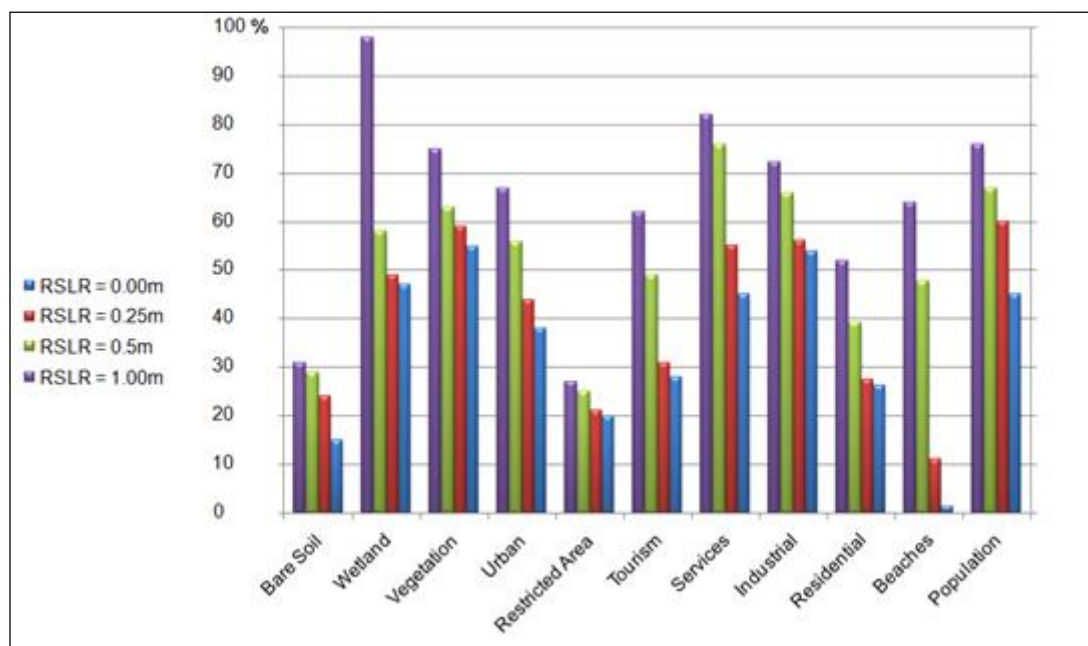


Figure A5-7: Risk to population and property posed by RSLR in Alexandria¹.

Table A5-3: Expected population and area losses due to RSLR in Alexandria¹.

Description of Loss	RSLR 30 cm (2025)	RSLR 50 cm (2050)
Area loss (sq. km)	19.00	31.70
Population displaced	545,000	1,512,000
Loss of employment in Agriculture	3,205	8,812
Loss of employment in Tourism	12,323	33,919
Loss of employment in Industry	54,936	151,200
Total loss of employment	70,465	195,443

A tabular representation of the distributions of Alexandria's population, as well as land use sectors, versus altitudes relative to MSL, is presented in Figure A5-8. The figure shows the distribution of population against areas according to their use relative to MSL in Alexandria, excluding Lake Mariout area¹⁰.

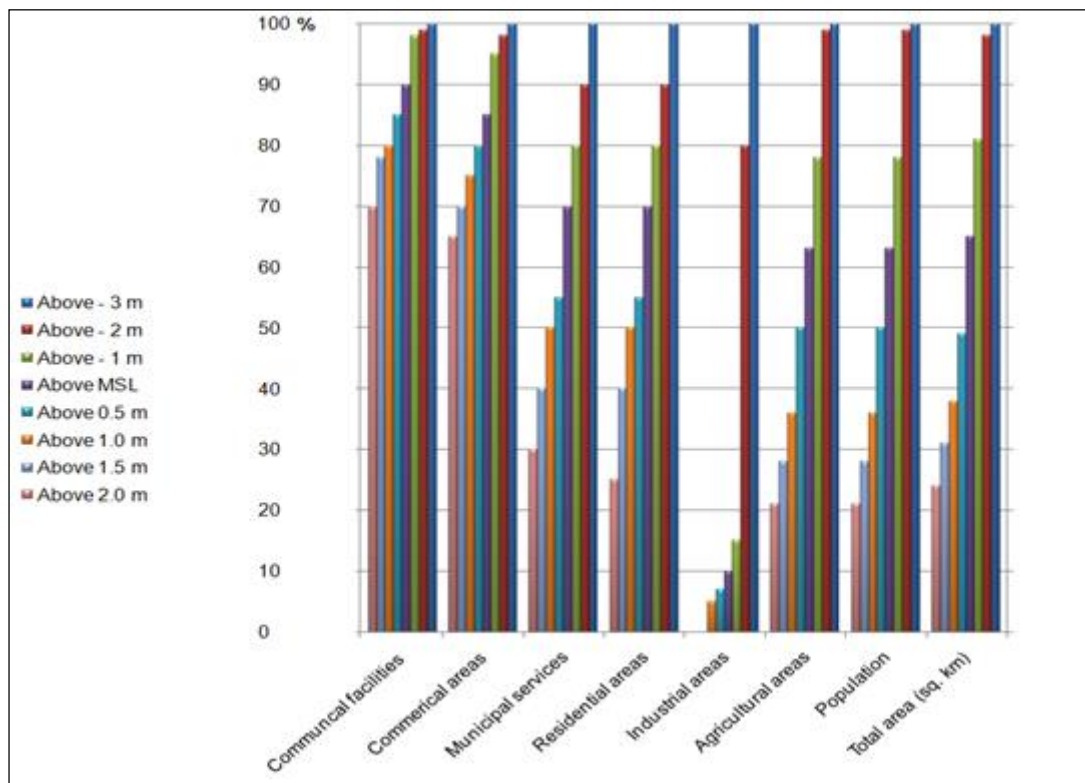


Figure A5-8: Risk to land use patterns in Alexandria for different RSLR scenarios¹⁰.

The total estimated economic loss as a consequence of the predicted shoreline retreat using Bruun's rule was estimated for Alexandria's beaches¹. The total economic loss corresponded to 1990, and included loss of beach sand volume, job losses, and beach protection through periodic sand nourishment. The same study also predicted the economic losses in lands and properties under different sets of RLSR scenarios for year 1990. In addition to the limitations of the Bruun's rule, a recent study provided an alternative analysis from a hydrodynamic perspective on the readiness of current coastal protection structures in Alexandria to sustain any possible RSLR scenario, including its consequential effect in increasing significant wave heights during winter storms. The study suggests that the weight of the armor layer for nearly most of Alexandria's coastal structures is overdesigned, making them to present an effective protection of Alexandria's shoreline, provided that adequate maintenance and monitoring is maintained¹².

¹² Iskander, M. M. (2013). Wave Climate and Coastal Structures in the Nile Delta Coast of Egypt. *Emirates Journal for Engineering Research*, 18 (1), 43-57.

APPENDIX 6 – Summary of Intervention Policy Unit Cost Database for the Study Area in 2013

SN	Structure	Routine Maintenance Unit Cost (EGP/m')	Rehabilitation Unit Cost (EGP/m')	Replacement Unit Cost (EGP/m')
1	26 of July Club East Breakwater	1,248.86	2,904.32	48,405.39
2	26 of July Club Submerged Breakwater	2,099.80	4,883.25	81,387.48
3	Al-Chatby to Sidi Gaber Revetment	4,257.16	9,900.36	165,006.04
4	Al-Mandara Breakwater	3,077.86	7,157.82	119,296.98
5	Al-Manshiya Revetment	893.91	2,078.85	34,647.53
6	Al-Montaza Breakwater	3,860.87	8,978.77	149,646.13
7	Al-Silsila to Al-Chatby Casino East Revetment	1,615.44	3,756.83	62,613.90
8	Al-Silsila to Al-Chatby Casino West Revetment	1,615.44	3,756.83	62,613.90
9	Armed Forces Club Revetment	1,615.44	3,756.83	62,613.90
10	Automobile Club Revetment	1,615.44	3,756.83	62,613.90
11	Bahari Revetment	1,615.44	3,756.83	62,613.90
12	Bir Masoud Breakwater	3,860.87	8,978.77	149,646.13
13	Bir Masoud Revetment	1,615.44	3,756.83	62,613.90
14	Engineers Club Revetment	3,093.86	7,195.02	119,916.92
15	Engineers Club West Breakwater	3,093.86	7,195.02	119,916.92
16	Glim East Groin	4,006.54	9,317.54	155,292.41
17	Glim East Revetment	1,615.44	3,756.83	62,613.90
18	Glim Middle Revetment	1,615.44	3,756.83	62,613.90
19	Glim West Groin	4,006.54	9,317.54	155,292.41
20	Glim West Revetment	1,615.44	3,756.83	62,613.90
21	Laurent Revetment	1,936.21	4,502.81	75,046.82

SN	Structure	Routine Maintenance Unit Cost (EGP/m')	Rehabilitation Unit Cost (EGP/m')	Replacement Unit Cost (EGP/m')
22	Marine Scouts Quaywall	586.36	1,363.64	22,727.27
23	Marine Scouts Revetment	1,615.44	3,756.83	62,613.90
24	Miami Breakwater	3,860.87	8,978.77	149,646.13
25	Middle Breakwater	29,541.22	68,700.51	1,145,008.48
26	Pharos Promenade Breakwater	1,615.44	3,756.83	62,613.90
27	Pharos Promenade East Revetment	1,615.44	3,756.83	62,613.90
28	Pharos Promenade West Revetment	1,615.44	3,756.83	62,613.90
29	Police Club East Breakwater	3,093.86	7,195.02	119,916.92
30	Police Club Middle Breakwater	3,093.86	7,195.02	119,916.92
31	Police Club Quaywall	586.36	1,363.64	22,727.27
32	Police Club West Breakwater	3,093.86	7,195.02	119,916.92
33	Professional Clubs Breakwater	2,792.74	6,494.75	108,245.85
34	Qaytbey East Seawall	1,066.57	2,480.40	41,340.00
35	Qaytbey North Revetment	2,177.62	5,064.24	84,404.00
36	Raml Station to Al-Silsila Seawall	1,066.57	2,480.40	41,340.00
37	San Stefano East Breakwater	8,707.50	20,250.00	337,500.00
38	San Stefano North Breakwater	19,350.00	45,000.00	750,000.00
39	San Stefano Quay	2,580.00	6,000.00	100,000.00
40	San Stefano South Pier	4,007	9,317.54	155,292.41
41	Stanley Beach Seawall	1,067	2,480.40	41,340.00
42	Teachers Club Breakwater	3,094	7,195.02	119,916.92
43	West Breakwater	26,935	62,639.42	1,043,990.34